Aus der Klinik für Strahlentherapie und Radioonkologie,
Universitätsklinikum des Saarlandes, Homburg/Saar

Klinische Translation der [^{89}Zr]Zr-PSMA-617-PET/CT: Biodistribution, Tracerkinetik, Dosimetrie und erste Anwendungen

Dissertation

zur Erlangung des Grades eines Doktors der Theoretischen Medizin

der Medizinischen Fakultät

der UNIVERSITÄT DES SAARLANDES

2026

vorgelegt von: Florian Rosar

geb. am: 07.02.1992 in St. Wendel

Tag der Promotion: 18. März 2026

Dekan: Univ.-Prof. Dr. med. dent. Matthias Hannig

Berichterstatter: Prof. Dr. Dr. Yvonne Dzierma

Prof. Dr. Dr. Philipp Staber

Meiner Frau Mona

„Ich habe gelernt, dass der Weg des Fortschritts weder kurz noch unbeschwerlich ist.“

Marie Curie (1867 – 1934)

Kumulative Dissertation

Inhaltsverzeichnis

I. Auflistung der Originalarbeiten

Originalarbeit 1

Rosar F, Schaefer-Schuler A, Bartholomä M, Maus S, Petto S, Burgard C, Privé BM, Franssen GM, Derks YHW, Nagarajah J, Khreish F, Ezziddin S (2022) [^{89}Zr]Zr-PSMA-617 PET/CT in biochemical recurrence of prostate cancer: first clinical experience from a pilot study including biodistribution and dose estimates. Eur J Nucl Med Mol Imaging 49:4736–4747

Originalarbeit 2

Rosar F, Khreish F, Marlowe RJ, Schaefer-Schuler A, Burgard C, Maus S, Petto S, Bartholomä M, Ezziddin S (2023) Detection efficacy of [^{89}Zr]Zr-PSMA-617 PET/CT in [^{68}Ga]Ga-PSMA-11 PET/CT-negative biochemical recurrence of prostate cancer. Eur J Nucl Med Mol Imaging 50:2899–2909

Originalarbeit 3

Rosar F, Burgard C, Larsen E, Khreish F, Marlowe RJ, Schaefer-Schuler A, Maus S, Petto S, Bartholomä M, Ezziddin S (2024) [^{89}Zr]Zr-PSMA-617 PET/CT characterization of indeterminate [^{68}Ga]Ga-PSMA-11 PET/CT findings in patients with biochemical recurrence of prostate cancer: lesion-based analysis. Cancer Imaging 24:27

II. Zusammenfassung / Summary

2.1 Zusammenfassung

Die prostataspezifische Membranantigen (PSMA)-gerichtete Positronenemissions-tomographie/Computertomographie (PET/CT) ist ein etabliertes Verfahren zur Diagnostik des Prostatakarzinoms, insbesondere für die Lokalisation eines biochemischen Rezidivs (BCR) nach Primärtherapie. Standardmäßig erfolgt die PSMA-PET/CT derzeit unter Verwendung kurzlebiger PSMA-Tracer, wie beispielsweise [^{68}Ga]Ga-PSMA-11. Trotz der insgesamt hohen diagnostischen Genauigkeit der konventionellen PSMA-PET/CT gibt es weiterhin eine relevante Zahl von Fällen, in denen sich bei bestehendem BCR keine tumorsuspekten Läsionen nachweisen lassen oder nur unklare Befunde vorliegen. Ein limitierender Faktor der etablierten konventionellen PSMA-Tracer liegt in der kurzen physikalischen Halbwertszeit der verwendeten Radionuklide (Halbwertszeit ^{68}Ga: ca. 67,7 Minuten). Diese begrenzt die Bildgebung auf wenige Stunden nach der Injektion des Tracers und verwehrt Bildakquisitionen zu späteren Zeitpunkten. Der Einsatz von PSMA-Tracern mit langlebigen Radionukliden, wie Zirkonium-89 (Halbwertszeit ^{89}Zr: ca. 78,4 Stunden) könnte die PSMA-PET/CT-Bildgebung entscheidend erweitern.

Die kumulative Dissertation umfasst drei Originalarbeiten zur klinischen Translation von [^{89}Zr]Zr-PSMA-617, einem langlebigen PSMA-Tracer für die PET/CT-Diagnostik des Prostatakarzinoms.

Originalarbeit 1 untersucht die Biodistribution und Tracerkinetik von [^{89}Zr]Zr-PSMA-617 sowie die damit verbundene Strahlenexposition bei 7 Patienten mit BCR des Prostatakarzinoms und präsentiert erste klinische Erfahrungen mit der [^{89}Zr]Zr-PSMA-617-PET/CT. Dabei zeigte [^{89}Zr]Zr-PSMA-617 eine mit konventionellen PSMA-Tracern vergleichbare Biodistribution und war mit einer akzeptablen Strahlenexposition verbunden (effektive Dosis: 10,1 mSv bei Applikation von 111 MBq). Die [^{89}Zr]Zr-PSMA-617-PET/CT erwies sich als sicheres Verfahren ohne Hinweis auf unerwünschte Nebenwirkungen. Die lange Halbwertszeit von ^{89}Zr ermöglicht im Vergleich zu konventionellen Tracern eine Bildgebung zu späteren Zeitpunkten (in dieser Studie untersucht bis zu 72 Stunden nach Injektion), was zu einer erhöhten Anreicherung des Tracers in Tumorläsionen und zeitlich zunehmendem Tumor-zu-Hintergrund-Verhältnis führt. Klinische Beobachtungen dieser Pilotstudie weisen darauf hin, dass dadurch Läsionen erkannt werden können, die in der konventionellen PSMA-PET/CT Bildgebung nicht oder nicht eindeutig sichtbar sind.

Basierend auf dieser Erkenntnis untersuchte Originalarbeit 2 daraufhin systematisch den Einsatz und die Detektionsrate der [^{89}Zr]Zr-PSMA-617-PET/CT bei Patienten mit BCR und zuvor negativer konventioneller PSMA-PET/CT. Bei 18 der untersuchten 23 Patienten mit BCR

und zuvor unauffälliger [^{68}Ga]Ga-PSMA-11-PET/CT-Bildgebung konnten mittels [^{89}Zr]Zr-PSMA-617-PET/CT insgesamt 36 eindeutig tumorsuspekte Läsionen identifiziert werden, was einer patientenbasierten Detektionsrate von 78 % entspricht. Die Befunde wurden durch biochemische Ansprechraten nach gezielter Strahlentherapie sowie im Falle einer Operation durch eine histopathologische Untersuchung validiert.

In Originalarbeit 3 wurde der Einsatz der [^{89}Zr]Zr-PSMA-617-PET/CT bei Patienten mit BCR und zuvor unklaren Befunden in der konventionellen PSMA-PET/CT evaluiert. Bei 15 untersuchten Patienten mit insgesamt 20 Läsionen, die in einer vorangegangenen [^{68}Ga]Ga-PSMA-11-PET/CT als unklar eingestuft wurden, ermöglichte die [^{89}Zr]Zr-PSMA-617-PET/CT eine präzise Einordnung (6 Läsionen tumorsuspekt, 14 nicht tumorsuspekt). Dabei zeigte sich eine unterschiedliche Tracerkinetik beider Gruppen, wobei Tumorläsionen in den ersten 24 Stunden einen steigenden Traceruptake und ein im weiteren zeitlichen Verlauf zunehmenden Kontrast gegenüber dem physiologischen Gewebe aufwiesen.

Die [^{89}Zr]Zr-PSMA-617-PET/CT erweist sich zusammenfassend als eine vielversprechende, sichere, komplementäre Bildgebungsoption mit akzeptabler Strahlenexposition für Patienten mit BCR des Prostatakarzinoms. Sie ermöglicht zum einen die Detektion von Tumorläsionen, die in der konventionellen PSMA-PET/CT nicht abgrenzbar sind und zum anderen die weitere Abklärung sowie präzise Einordnung zuvor unklarer Befunde. Die Ergebnisse der Originalarbeiten 1 – 3 liefern damit eine wissenschaftliche Grundlage und eine klare Rationale für zukünftige, idealerweise prospektive Studien mit größeren Patientenkohorten.

2.2 Summary

Clinical translation of [^{89}Zr]Zr-PSMA-617 PET/CT: biodistribution, tracer kinetics, dosimetry, and first applications

Prostate-specific membrane antigen (PSMA)-targeted PET/CT is an established imaging modality for prostate cancer, particularly for the localization of biochemical recurrence (BCR) after primary therapy. Currently, PSMA PET/CT is routinely performed using short-lived PSMA tracers, such as [^{68}Ga]Ga-PSMA-11. Despite the overall high diagnostic accuracy of conventional PSMA PET/CT, a substantial number of cases remains in which no tumor-suspicious lesions can be detected, despite presence of BCR, or in which findings remain indeterminate. A limiting factor of the established conventional PSMA tracers is the short physical half-life of the radionuclides used (half-life of ^{68}Ga: approximately 67.7 minutes). This restricts imaging to a few hours after injection and precludes image acquisition at later time points. The use of PSMA tracers labeled with long-lived radionuclides, such as zirconium-89 (half-life of ^{89}Zr: approximately 78.4 hours), could substantially improve the diagnostic performance of PSMA PET/CT imaging.

This cumulative thesis comprises three original articles focusing on the clinical translation of [^{89}Zr]Zr-PSMA-617, a long-lived PSMA tracer for PET/CT imaging in prostate cancer.

Original article 1 investigated the biodistribution and tracer kinetics of [^{89}Zr]Zr-PSMA-617, as well as the associated radiation exposure in 7 patients with BCR of prostate cancer, and presents initial clinical experience with [^{89}Zr]Zr-PSMA-617 PET/CT. [^{89}Zr]Zr-PSMA-617 demonstrated a biodistribution comparable to that of conventional PSMA tracers and was associated with an acceptable radiation exposure (effective dose: 10.1 mSv for an administered activity of 111 MBq). [^{89}Zr]Zr-PSMA-617 PET/CT proved to be safe with no evidence of adverse events. The long half-life of ^{89}Zr enables imaging at later time points compared to conventional tracers (in this study investigated up to 72 hours post injection), resulting in increased tracer uptake in tumor lesions and a progressively improving tumor-to-background ratio over time. Clinical observations from this pilot study indicate that [^{89}Zr]Zr-PSMA-617 PET/CT imaging may allow the detection of lesions that are not visible or only indeterminate on conventional PSMA PET/CT imaging.

Building on these findings, original article 2 systematically evaluated the use and detection rate of [^{89}Zr]Zr-PSMA-617 PET/CT in patients with BCR and previously negative conventional PSMA PET/CT imaging. In 18 of 23 patients with BCR and previously negative [^{68}Ga]Ga-PSMA-11 PET/CT imaging, a total of 36 tumor-suspicious lesions were identified using [^{89}Zr]Zr-PSMA-617 PET/CT, corresponding to a patient-based detection rate of 78 %. The findings were validated by biochemical response rates following targeted radiotherapy and, in case of surgery, by histopathological examination.

Original article 3 evaluated the use of [^{89}Zr]Zr-PSMA-617 PET/CT in patients with BCR and previously indeterminate findings on conventional PSMA PET/CT imaging. Among 15 patients with a total of 20 lesions classified as indeterminate on prior [^{68}Ga]Ga-PSMA-11 PET/CT, [^{89}Zr]Zr-PSMA-617 PET/CT enabled a precise characterization (6 lesions suspicious for tumor, 14 not suspicious for tumor). Differences in tracer kinetics were observed between the two groups, with tumor lesions showing an increase in tracer uptake during the first 24 hours and a further progressively improving contrast to physiological tissue over time.

In summary, [^{89}Zr]Zr-PSMA-617 PET/CT provides a promising and safe complementary imaging method with acceptable radiation exposure for patients with BCR of prostate cancer. It enables both the detection of tumor lesions not visible on conventional PSMA PET/CT and the further evaluation and precise characterization of previously indeterminate findings. The results of the original articles 1 – 3 thus provide a scientific basis and a clear rationale for future studies, ideally in prospective settings with larger patient cohorts.

III. Einleitung und Zielsetzung

In der Nuklearmedizin kommen Radiopharmaka sowohl zur molekularen Bildgebung als auch zur zielgerichteten Therapie verschiedenster Erkrankungen zum Einsatz [84]. Die Radiopharmaka, auch Tracer (engl. *trace* – Spur) genannt, bestehen typischerweise aus zwei Komponenten, einem biologisch aktiven Molekül (Vektor), welches aktiv in Stoffwechselprozessen interagiert oder an spezifische Zielstrukturen bindet sowie einem Radionuklid (Abbildung 1). Das Radionuklid ist entweder kovalent oder, im Falle von Radiometallen, über einen Chelator an die biologisch aktive Komponente gekoppelt. Durch diese Kombination lassen sich verschiedenste Krankheitsprozesse nach intravenöser Injektion eines solchen Tracers sichtbar machen oder gezielt behandeln. Abhängig vom jeweiligen Ziel (Diagnostik oder Therapie) kommen unterschiedliche Arten ionisierender Strahlung zum Einsatz [80]. Für therapeutische Zwecke werden α-Strahlung oder β^--Strahlung genutzt. Zur molekularen Bildgebung hingegen dienen β^+-Strahler in der Positronenemissionstomographie (PET) sowie γ-Strahler in der Szintigraphie. Um die molekularen Befunde anatomisch präzise zuzuordnen, wird die PET i.d.R. mit einer Computertomographie (CT), als sogenannte Hybridbildgebung in Form einer PET/CT kombiniert [9]. Die PET/CT-Diagnostik wird bei unterschiedlichen Erkrankungen unter Verwendung verschiedener Tracer und Zielstrukturen eingesetzt und hat sich unter anderem in der Diagnostik des Prostatakarzinoms etabliert [25,44,67].

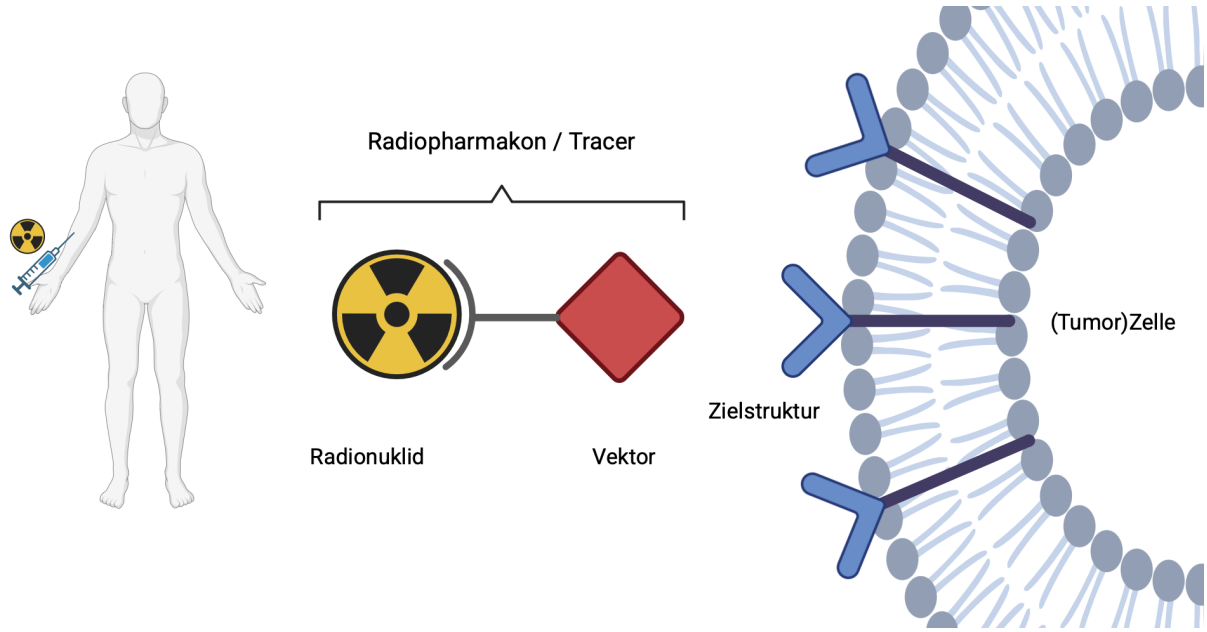

Abbildung 1: Prinzip der nuklearmedizinischen zielgerichteten Diagnostik und Therapie.

In den vergangenen Jahren hat die PSMA-PET/CT, die als Zielstruktur das prostataspezifische Membranantigen (PSMA) verwendet, die Bildgebung des Prostatakarzinoms revolutioniert [34]. Das PSMA ist ein Transmembran-Glykoprotein, das auf der Oberfläche von Prostatakarzinomzellen stark überexprimiert wird und somit eine ideale Zielstruktur für die molekulare Bildgebung und Therapie des Prostatakarzinoms darstellt [30,39,56]. Mit etwa 1,4 Millionen Neuerkrankungen jährlich und einer relativen Inzidenz von 14,1 % aller Tumorerkrankungen ist das Prostatakarzinom weltweit die zweithäufigste Tumorerkrankung und die vierthäufigste tumorbedingte Todesursache bei Männern [7,28]. Die PSMA-PET/CT ist heute ein fester Bestandteil der Diagnostik in verschiedenen Stadien des Prostatakarzinoms [18,73]. Zum Einsatz kommt sie unter anderem im Primärstaging von (Hochrisiko-)Prostatakarzinomen sowie bei der Therapieplanung und -kontrolle im fortgeschrittenen Stadium, beispielsweise im Kontext der PSMA-gerichteten Radioligandentherapie [12,19,27]. Mit am häufigsten wird die PSMA-PET/CT jedoch gegenwärtig zur Lokalisation eines biochemischen Rezidivs (BCR) eingesetzt [4].

Trotz der grundsätzlich hohen Heilungschancen eines lokal begrenzten Prostatakarzinoms durch radikale Prostatektomie oder Strahlentherapie entwickelt ein relevanter Anteil der Patienten im weiteren Verlauf ein Rezidiv, das sich biochemisch bzw. serologisch durch einen Anstieg des prostataspezifischen Antigens (PSA) bemerkbar macht [69,75]. In solchen Fällen ist es wichtig, das BCR frühzeitig und präzise zu lokalisieren, um eine gezielte weiterführende Behandlung, etwa durch zielgerichtete Bestrahlung oder Operation, ermöglichen zu können.

Für die PSMA-PET/CT-Bildgebung wurden in den letzten Jahren diverse PSMA-Tracer entwickelt. Besonders verbreitet in der klinischen Anwendung sind derzeit mit Gallium-68-markierte PSMA-Liganden wie [^{68}Ga]Ga-PSMA-11 oder [^{68}Ga]Ga-PSMA I&T sowie mit Fluor-18-markierte PSMA-Liganden wie [^{18}F]DCFPyl oder [^{18}F]PSMA-1007 [1,17,31,78]. Studien haben gezeigt, dass [^{68}Ga]Ga-PSMA-11 sowie andere etablierte konventionelle PSMA-Tracer eine hohe Sensitivität zur Tumorlokalisation bei BCR aufweisen [4,8,32,52]. Dennoch bleibt insbesondere bei Patienten mit niedrigen PSA-Werten eine relevante Anzahl von Fällen, in denen trotz BCR in der PSMA-PET/CT keine tumorsuspekten Läsionen dargestellt werden können oder nur unklare Befunde vorliegen [50]. In solchen Situationen ist eine gezielte, weiterführende Therapie auf Basis der Bildgebung nicht möglich. Ein limitierender Faktor von ^{68}Ga (sowie auch von ^{18}F) ist die kurze physikalische Halbwertszeit von ca. 67,7 Minuten (bzw. ca. 109,8 Minuten). Diese begrenzt die Bildgebung auf wenige Stunden nach der Injektion des Tracers und verwehrt Bildakquisitionen zu späteren Zeitpunkten.

Der Einsatz von PSMA-Liganden, die mit langlebigen Radionukliden markiert sind, könnte die Sensitivität der PSMA-PET/CT weiter steigern. Durch die Möglichkeit späterer Bildakquisition nach Applikation bleibt theoretisch mehr Zeit für die spezifische intrazelluläre Anreicherung des Tracers in PSMA-exprimierenden Tumorzellen, was potenziell zu einer erhöhten Signalintensität in der PET führen könnte. Gleichzeitigt könnte die unspezifische Hintergrundaktivität durch renale und hepatische Elimination des freien Tracers abnehmen, wodurch sich das Signal-zu-Hintergrund-Verhältnis verbessern könnte und die Detektion sowie Abgrenzung von Läsionen hierdurch erleichtert wird. Basierend aus diesen pharmakokinetischen Überlegungen könnten Spätaufnahmen zudem helfen, unklare Befunde aus der konventionellen PSMA-PET/CT weiter abzuklären und präziser zu charakterisieren.

Aufgrund seiner physikalischen Eigenschaften gilt Zirkonium-89 als ein interessantes und vielversprechendes Radionuklid für die Langzeit-PET-Bildgebung [20,26,82]. ^{89}Zr ist ein Positronenstrahler mit einer Halbwertszeit von ca. 78,4 Stunden und findet bisher vor allem Anwendung in der Antikörper-basierten PET-Bildgebung [40,41,76]. Eine Markierung des PSMA-Liganden PSMA-11 mit ^{89}Zr ist aufgrund seiner chemischen Struktur nicht möglich, da er keinen geeigneten Chelator zur stabilen Komplexierung von Zirkonium enthält. Im Gegensatz dazu können die PSMA-Liganden PSMA-617 und PSMA I&T mit ^{89}Zr markiert werden, da sie die Chelatoren DOTA bzw. DOTAGA enthalten, welche eine stabile Bindung des Radionuklids ermöglichen (Abbildung 2) [49,58]. *Privé et al.* gelang es erstmals PSMA-617 und PSMA I&T mit ^{89}Zr zu markieren, die ^{89}Zr-markierten PSMA-Liganden präklinisch zu charakterisieren und in Xenograft-Mausmodellen eine Anreicherung im Tumorgewebe bis zu einer Woche nach Injektion nachzuweisen [60]. Dabei zeigte [^{89}Zr]Zr-PSMA-617 eine höhere Traceraufnahme im Tumorgewebe als [^{89}Zr]Zr-PSMA I&T. In Zusammenarbeit mit der Arbeitsgruppe um *Privé et al.* wurde am Universitätsklinikum des Saarlandes 2021 weltweit erstmals eine in vivo PET/CT-Bildgebung mit [^{89}Zr]Zr-PSMA-617 durchgeführt.

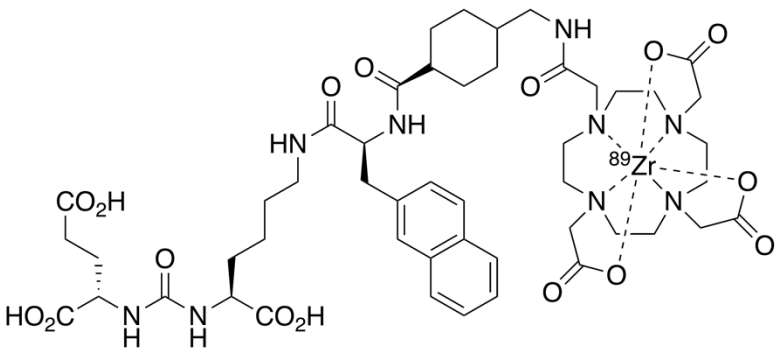

Abbildung 2: Molekülstruktur des PSMA-Tracers [^{89}Zr]Zr-PSMA-617.

Ziel der Dissertation war die klinische Translation der [^{89}Zr]Zr-PSMA-617-PET/CT bei Patienten mit BCR eines Prostatakarzinoms. Neben ersten klinischen Erfahrungen lag der Schwerpunkt auf der Analyse der biologischen Verteilung des Tracers, der Abschätzung der mit der Untersuchung verbundenen Strahlenexposition sowie der Evaluation potenzieller medizinischer Anwendungsfelder.

Nachfolgend werden diese zentralen Inhalte ausführlich erläutert und diskutiert:

1. Biodistribution, Tracerkinetik und Dosimetrie inklusive ersten klinischen Erfahrungen mit der [^{89}Zr]Zr-PSMA-617-PET/CT bei Patienten mit BCR eines Prostatakarzinoms

   (Originalarbeit 1)

2. Einsatz der [^{89}Zr]Zr-PSMA-617-PET/CT bei Patienten mit BCR eines Prostatakarzinoms und zuvor negativer konventioneller PSMA-PET/CT

   (Originalarbeit 2)

3. Einsatz der [^{89}Zr]Zr-PSMA-617-PET/CT bei Patienten mit BCR eines Prostatakarzinoms und unklaren Befunden in der konventionellen PSMA-PET/CT

   (Originalarbeit 3)

IV. Zusammenfassende Darstellung der Originalarbeiten

4.1 Biodistribution, Tracerkinetik und Dosimetrie von [^{89}Zr]Zr-PSMA-617

Originalarbeit 1

***Rosar F**, Schaefer-Schuler A, Bartholomä M, Maus S, Petto S, Burgard C, Privé BM, Franssen GM, Derks YHW, Nagarajah J, Khreish F, Ezziddin S (2022) [^{89}Zr]Zr-PSMA-617 PET/CT in biochemical recurrence of prostate cancer: first clinical experience from a pilot study including biodistribution and dose estimates. Eur J Nucl Med Mol Imaging 49:4736–4747*

Hintergrund und Fragestellung:
Die PSMA-PET/CT hat in der Behandlung des Prostatakarzinoms, insbesondere bei der Lokalisierung eines BCR, zunehmend an Bedeutung gewonnen. Langlebige Radionuklide wie ^{89}Zr (Halbwertszeit: ca. 78,4 Stunden) könnten die PSMA-PET/CT-Diagnostik durch die Möglichkeit späterer Bildaufnahmen weiter verbessern. Diese Studie stellt die ersten klinischen Erfahrungen mit der [^{89}Zr]Zr-PSMA-617-PET/CT bei Patienten mit BCR eines Prostatakarzinoms zusammen und analysiert die Biodistribution und Tracerkinetik von [^{89}Zr]Zr-PSMA-617 sowie die damit verbundene Strahlenexposition.

Methoden:
Bei N = 7 Patienten mit BCR eines Prostatakarzinoms, bei denen in einer [^{68}Ga]Ga-PSMA-11-PET/CT entweder keine tumorsuspekten (n = 4) oder unklare Befunde (n = 3) vorlagen, wurde ergänzend eine [^{89}Zr]Zr-PSMA-617-PET/CT durchgeführt. Die Bildgebung erfolgte zu vier Zeitpunkten: 1, 24, 48 und 72 Stunden nach intravenöser Applikation von 111 ± 11 MBq [^{89}Zr]Zr-PSMA-617. Basierend auf diesen vier Bildgebungen wurde die physiologische Verteilung des Radiotracers und dessen Kinetik in Normalorganen mittels *standardized uptake value* (SUV) und Gewebe-zu-Hintergrund-Verhältnis (*tissue-to-background ratio*, TiBR) analysiert. Für Nieren, Leber, Milz und Speicheldrüsen wurde jeweils organspezifisch die absorbierte Strahlendosis berechnet. Darüber hinaus erfolgte die Ermittlung der effektiven Dosis für den Patienten. Zusätzlich wurde eine quantitative Analyse von tumorsuspekten Läsionen mittels SUV_{max} und Tumor-zu-Hintergrund-Verhältnis (*tumor-to-background ratio*, TBR) durchgeführt.

Ergebnisse:

Bei allen N = 7 Patienten konnte die [^{89}Zr]Zr-PSMA-617-PET/CT-Untersuchung ohne Auftreten von Nebenwirkungen bzw. unerwünschten Reaktionen durchgeführt werden. Ein physiologischer Uptake des Radiotracers [^{89}Zr]Zr-PSMA-617 wurde in den Speichel- und Tränendrüsen, der Leber, der Milz, den Nieren, dem Darm sowie den ableitenden Harnwegen beobachtet (Abbildung 3).

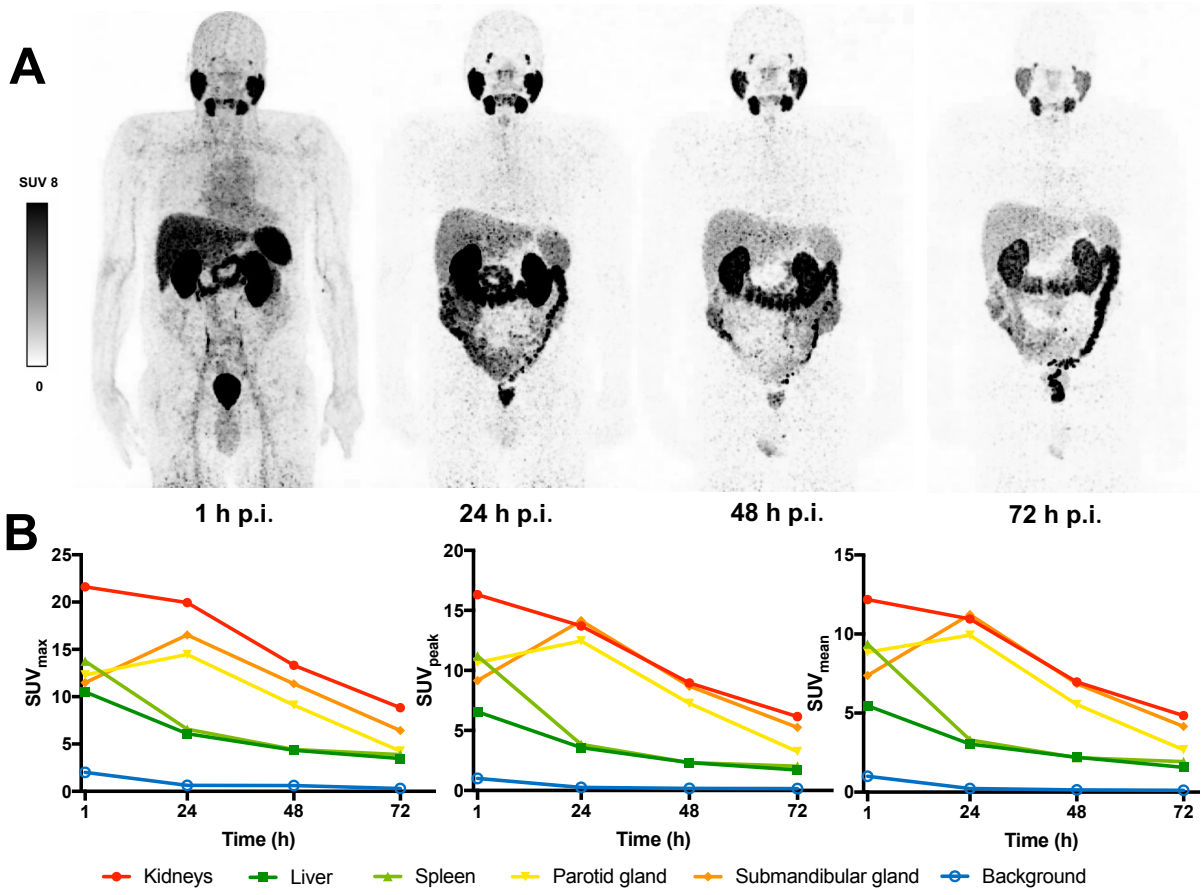

Abbildung 3: Repräsentatives Beispiel der physiologischen Verteilung von [^{89}Zr]Zr-PSMA-617 1 h, 24 h, 48 h und 72 h nach Injektion (*post injectionem*, p.i.) des Radiotracers. **A:** Maximumintensitätsprojektionen (MIP) der [^{89}Zr]Zr-PSMA-617-PET/CT. **B:** Entsprechende Verläufe der Anreicherung des Radiotracers in ausgewählten Normalorganen (Niere, Leber, Milz, Glandula parotidea, Glandula submandibularis) sowie im Hintergrund (Glutealmuskulatur) quantifiziert durch die Parameter SUV_{max}, SUV_{peak} und SUV_{mean}. (Abbildung aus Originalarbeit 1 [62]).

Der höchste durchschnittliche SUV_{max} wurde 1 h nach Injektion (*post injectionem*, p.i.) in den Nieren gemessen (21,15 ± 12,31) und nahm bis 72 h p.i. deutlich ab (7,43 ± 1,56) (Abbildung 4). In den Speichel- und Tränendrüsen zeigte sich der maximale Werte hingegen erst nach 24 h, wobei die Glandula submandibularis mit 17,30 ± 4,69 den höchsten Uptake aufwies. Ab diesem Zeitpunkt sank auch hier der Uptake bis zum Untersuchungsende. Ein kontinuierlicher Anstieg war hingegen nur im Kolon zu beobachten. Hier stieg der SUV_{max} von 3,50 ± 2,21 nach 1 h auf 13,57 ± 5,00 nach 72 h an. Das TiBR nahm im Verlauf der ersten 72 h für die meisten betrachteten Organe zu. Besonders hohe TiBR-Werte (≥ 50) wurden nach 72 h p.i. in den Speicheldrüsen, den Nieren sowie im Kolon festgestellt.

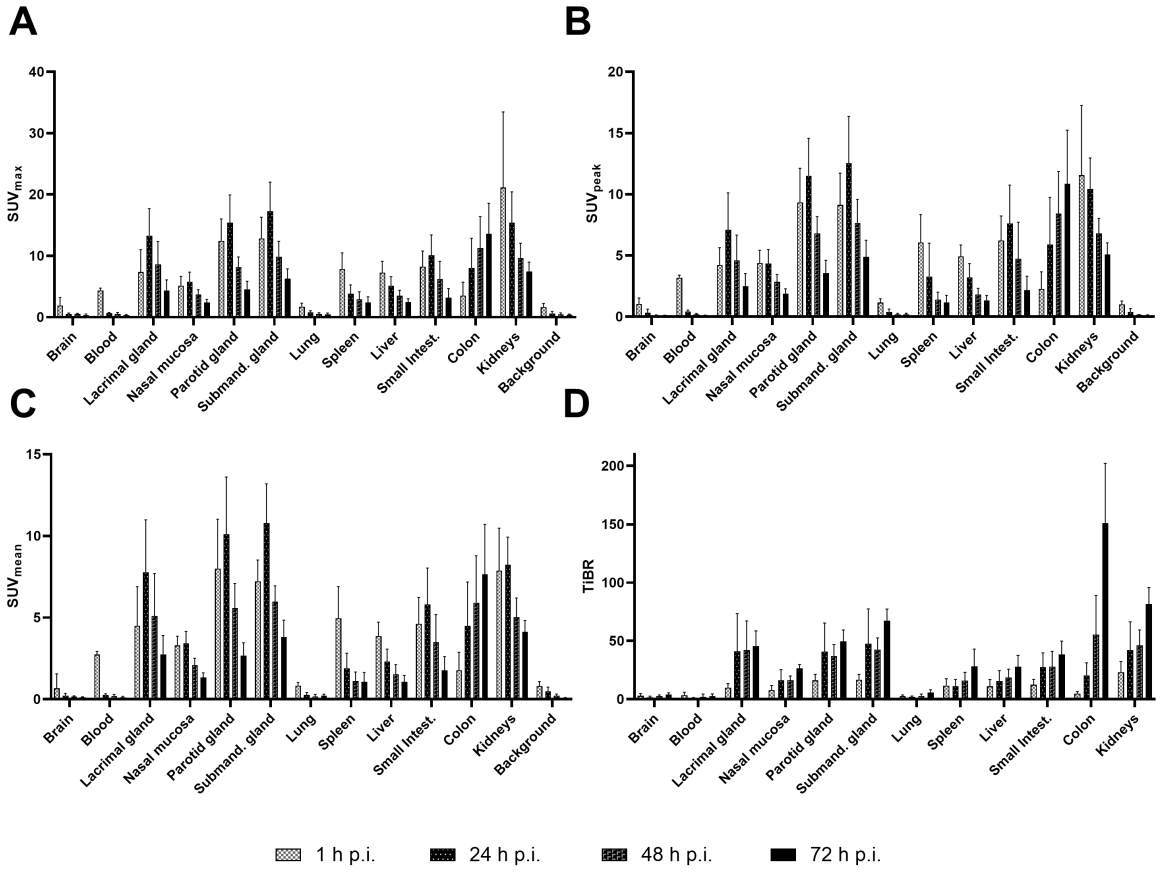

Abbildung 4: Deskriptive Statistik (Mittelwert ± Standardabweichung) der Biodistribution von [^{89}Zr]Zr-PSMA-617 im zeitlichen Verlauf, quantifiziert durch **A**: SUV_{max}, **B**: SUV_{peak}, **C**: SUV_{mean} und **D**: Gewebe-zu-Hintergrund-Verhältnis (TiBR). (Abbildung aus Originalarbeit 1 [62]).

Unter den ausgewählten Organen wies die Glandula parotidea mit 0,601 ± 0,185 mGy/MBq (Minimum – Maximum: 0,368 – 0,859 mGy/MBq) die höchste absorbierte Dosis und damit höchste Strahlenexposition durch [^{89}Zr]Zr-PSMA-617 auf, gefolgt von den Nieren 0,517 ± 0,125 mGy/MBq (Minimum – Maximum: 0,307 – 0,674 mGy/MBq) und der Glandula

submandibularis mit 0,468 ± 0,136 mGy/MBq (Minimum – Maximum: 0,253 – 0,626 mGy/MBq) (Tabelle 1). Basierend auf diesen Werten ergab sich eine mittlere effektive Dosis von 0,0913 ± 0,0118 mSv/MBq (Minimum – Maximum: 0,0702 – 0,1131 mSv/MBq) als Gesamtstrahlenexposition für den Patienten. Bei einer durchschnittlich verabreichten Aktivität von 111 MBq [^{89}Zr]Zr-PSMA-617 entsprach dies einer mittleren effektiven Dosis von 10,1 mSv.

Tabelle 1: Absorbierte Dosis und verschiedene dosimetrische Parameter für [^{89}Zr]Zr-PSMA-617 in ausgewählten Organen. (Tabelle aus Originalarbeit 1 [62]).

Organ	**A** (% injizierter A_0)	**λ** (h^{-1})	**TIAC** (h)	**Absorbierte Dosis** (mGy/MBq)
Niere	3,75 ± 1,24	0,022 ± 0,002	1,74 ± 0,44	0,517 ± 0,125
Leber	6,62 ± 1,39	0,049 ± 0,014	1,54 ± 0,49	0,158 ± 0,051
Milz	1,25 ± 0,70	0,079 ± 0,034	0,21 ± 0,12	0,175 ± 0,068
Glandula parotidea	0,70 ± 0,20	0,031 ± 0,005	0,31 ± 0,10	0,601 ± 0,185
Glandula submandibularis	0,27 ± 0,09	0,029 ± 0,004	0,13 ± 0,04	0,468 ± 0,136
Tränendrüse	0,02 ± 0,01	0,030 ± 0,006	0,10 ± 0,004	0,156 ± 0,070

Abkürzungen: A – Aktivität und λ – Zerfallskonstante als Parameter einer monoexponentiellen Fitfunktion, TIAC – *time-integrated activity coefficient.*

Bei 3 von 4 Patienten (75 %) mit zuvor unauffälliger [^{68}Ga]Ga-PSMA-11-PET/CT konnten mithilfe von [^{89}Zr]Zr-PSMA-617 tumorsuspekte Läsionen identifiziert werden. Bei 2 von 3 Patienten mit unklaren Befunden in der [^{68}Ga]Ga-PSMA-11-PET/CT bestätigte sich der jeweilige Verdacht durch die [^{89}Zr]Zr-PSMA-617-PET/CT. Bei einem Patienten ließ sich jedoch keine entsprechende Traceraufnahme im Bereich des zuvor unklaren Befundes nachweisen, womit der Malignitätsverdacht widerlegt werden konnte. Insgesamt zeigten sich 14 tumorsuspekte Läsionen (1 – 5 pro Patient). In 10/14 Fällen handelte es sich um Lymphknotenmetastasen, in 3/14 um Lokalrezidive und in einem Fall um eine peritoneale Metastase. Der Großteil der Tumorläsionen (11/14 Läsionen) war in den frühen Aufnahmen 1 h p.i. noch nicht sichtbar, konnte jedoch zu späteren Zeitpunkten eindeutig abgegrenzt werden: 9/11 Läsionen erstmals nach 24 h, 2/11 Läsionen nach 48 h. In denjenigen Läsionen, die bereits frühzeitig (nach 1 h) erkennbar waren (3/14 Läsionen), stieg der SUV_{max} bis 24 h p.i. deutlich an. In den späteren Aufnahmen (≥ 24 h p.i.) zeigte sich ein Plateau der SUV_{max}-Werte, während das TBR kontinuierlich mit der Zeit weiter zunahm (Abbildung 5). Eine beispielhafte Tumorläsion und deren zeitlicher Verlauf in der [^{89}Zr]Zr-PSMA-617-PET/CT ist in Abbildung 6 dargestellt.

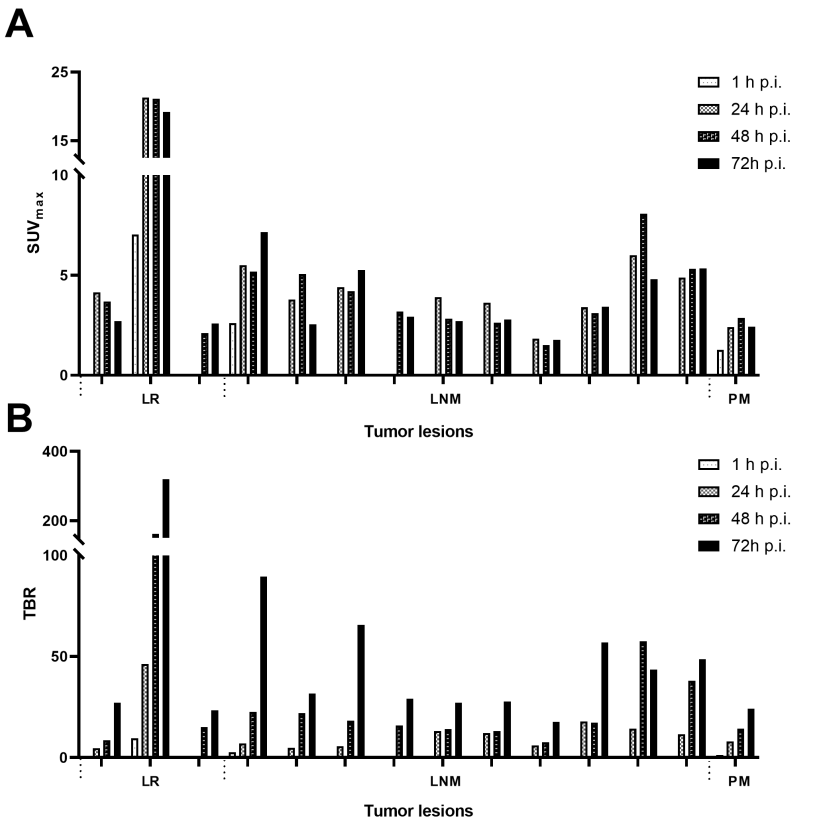

Abbildung 5: A: Uptake quantifiziert durch SUV_{max} und **B:** Tumor-zu-Hintergrund-Verhältnis (TBR) aller Tumorläsionen zu den Zeitpunkten 1 h, 24 h, 48 h und 72 h nach Injektion (p.i.) von [^{89}Zr]Zr-PSMA-617; geordnet nach Lokalisation: Lokalrezidiv (LR), Lymphknotenmetastase (LNM) und peritoneale Metastase (PM). (Abbildung aus Originalarbeit 1 [62]).

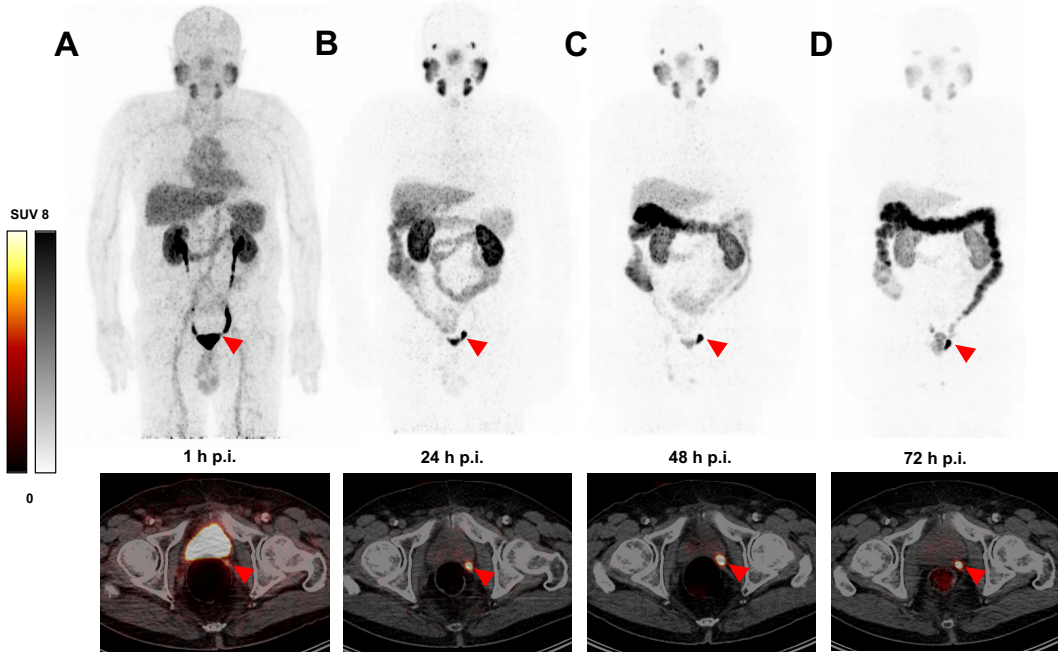

Abbildung 6: Maximumintensitätsprojektionen (MIP) und transversale PET/CT-Schnitte zu den Zeitpunkten **A:** 1 h, **B:** 24 h, **C:** 48 h und **D:** 72 h nach Injektion (p.i.) von [^{89}Zr]Zr-PSMA-617. Rote Pfeile markieren eine tumorsuspekte Traceranreicherung im Bereich der linken Samenblasenloge. (Abbildung aus Originalarbeit 1 [62]).

Hauptaussage:

Die [^{89}Zr]Zr-PSMA-617-PET/CT-Bildgebung stellt ein vielversprechendes neues molekularbildgebendes diagnostisches Verfahren für Patienten mit BCR eines Prostatakarzinoms dar. Der Radiotracer [^{89}Zr]Zr-PSMA-617 zeigt eine mit konventionellen PSMA-Tracern vergleichbare Biodistribution und ist mit einer akzeptablen Strahlenexposition verbunden (effektive Dosis: 10,1 mSv bei Applikation von 111 MBq). Die lange Halbwertszeit von ^{89}Zr ermöglicht im Vergleich zu konventionellen Tracern eine Bildgebung zu späteren Zeitpunkten (in dieser Studie untersucht bis zu 72 h p.i.), was zu einer erhöhten Anreicherung des Tracers in Tumorläsionen und zeitlich zunehmendem Tumor-zu-Hintergrund-Verhältnis führt. Die Ergebnisse dieser Pilotstudie weisen darauf hin, dass dadurch Läsionen erkannt werden können, die in der konventionellen PSMA-PET/CT-Bildgebung nicht oder nicht eindeutig sichtbar sind. Weitere Studien mit größeren Patientenkollektiven sind notwendig, um diese Beobachtung zu bestätigen, die eine entscheidende Bedeutung für das Management des BCR eines Prostatakarzinoms haben könnte.

4.2 Einsatz der [^{89}Zr]Zr-PSMA-617 PET/CT bei zuvor negativer konventioneller PSMA-PET/CT

Originalarbeit 2

***Rosar F**, Khreish F, Marlowe RJ, Schaefer-Schuler A, Burgard C, Maus S, Petto S, Bartholomä M, Ezziddin S (2023) Detection efficacy of [^{89}Zr]Zr-PSMA-617 PET/CT in [^{68}Ga]Ga-PSMA-11 PET/CT-negative biochemical recurrence of prostate cancer. Eur J Nucl Med Mol Imaging 50:2899–2909*

Hintergrund und Fragestellung:
Bei Patienten mit BCR eines Prostatakarzinoms deuten erste Daten eines kleinen Patientenkollektivs (Originalarbeit 1) darauf hin, dass mit [^{89}Zr]Zr-PSMA-617, einem langlebigen ^{89}Zr (Halbwertszeit: ca. 78,4 Stunden)-markierten PSMA-Radiotracer, tumorsuspekte Läsionen nachgewiesen werden können, die bei der Verwendung von konventionellen PSMA-Tracern mit kurzlebigen Radionukliden unentdeckt bleiben. Ziel dieser Studie war es, die Detektionsrate der [^{89}Zr]Zr-PSMA-617-PET/CT bei Patienten mit BCR und zuvor negativer konventioneller PSMA-PET/CT-Bildgebung zu evaluieren.

Methoden:
Zur Evaluation der Detektionsrate der [^{89}Zr]Zr-PSMA-617-PET/CT bei zuvor negativer konventioneller PSMA-PET/CT-Bildgebung wurden N = 23 [^{89}Zr]Zr-PSMA-617-PET/CT-Untersuchungen mit jeweils Bildakquisitionen 1 h, 24 h und 48 h p.i. retrospektiv analysiert. Die Studienkohorte umfasste 23 Männer mit BCR nach radikaler Prostatektomie mit einem medianen PSA-Wert von 0,54 ng/ml (Minimum – Maximum: 0,11 – 2,50 ng/ml). Alle Patienten erhielten eine [^{68}Ga]Ga-PSMA-11-PET/CT im Mittel 40 ± 28 Tage vor der [^{89}Zr]Zr-PSMA-617-PET/CT-Bildgebung, jeweils ohne Nachweis tumorsuspekter Läsionen. Neben der visuellen Bildauswertung der [^{89}Zr]Zr-PSMA-617-PET/CT, bei der die Anzahl und die Lokalisation tumorsuspekter Läsionen erfasst wurde, erfolgte für die identifizierten Läsionen die Bestimmung der quantitativen PET-Parameter SUV_{max}, SUV_{peak} sowie der entsprechenden Tumor-zu-Hintergrund-Verhältnisse TBR_{max} und TBR_{peak}. Zur Validierung der in der [^{89}Zr]Zr-PSMA-617-PET/CT tumorsuspekten Läsionen erfolgte die Erhebung von Daten zu den im Anschluss an die Bildgebung durchgeführten Therapien und interventionellen Maßnahmen sowie deren Ergebnissen.

Ergebnisse:

Bei 18 der 23 Patienten (78 %) mit BCR und zuvor unauffälliger [^{68}Ga]Ga-PSMA-11-PET/CT-Bildgebung konnten mittels [^{89}Zr]Zr-PSMA-617-PET/CT eindeutig tumorsuspekte Läsionen identifiziert werden (exemplarisch Abbildung 7). Insgesamt wurden bei diesen 18 Patienten 36 tumorsuspekte Läsionen detektiert (1 – 4 Läsionen pro Patient). Von diesen nachgewiesenen Läsionen wurden 11 Läsionen als Lokalrezidive in der Prostataloge, 21 als Lymphknotenmetastasen und 4 als Knochenmetastasen gewertet (Abbildung 8 und 9). Von insgesamt 36 Läsionen waren 33 (92 %) in den Aufnahmen 24 h p.i. sichtbar, die ausnahmslos auch nach 48 h nachweisbar blieben. Die restlichen 3 Läsionen (8 %), die jeweils alle als Lokalrezidive in der Prostataloge interpretiert wurden, waren ausschließlich in der Aufnahme 48 h p.i. erkennbar. Lediglich eine Läsion, klassifiziert als Knochenmetastase, kam bereits in der Aufnahme 1 h p.i. zur Darstellung; sie konnte ebenso in den Aufnahmen 24 h und 48 h p.i. abgegrenzt werden.

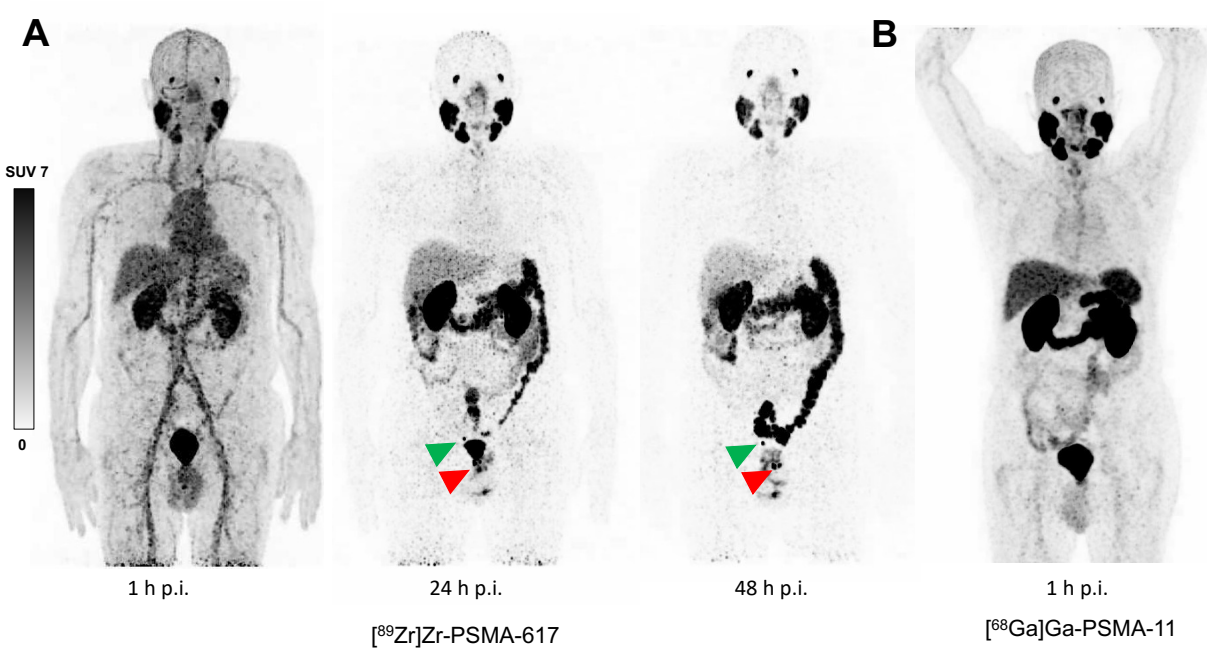

Abbildung 7: Maximumintensitätsprojektionen (MIP) **A:** der [^{89}Zr]Zr-PSMA-617-PET/CT zu den Zeitpunkten 1 h, 24 h, 48 h nach Injektion (p.i.) und **B:** der [^{68}Ga]Ga-PSMA-11-PET/CT zum Zeitpunkt 1 h p.i. eines Patienten mit BCR eines Prostatakarzinoms. Die [^{89}Zr]Zr-PSMA-617-PET/CT zeigte in den Aufnahmen 24 h und 48 h p.i. sowohl eine tumorsuspekte Läsion in der Prostataloge (roter Pfeil) als auch einen tumorsuspekten pelvinen Lymphknoten (grüner Pfeil), die jeweils in der [^{68}Ga]Ga-PSMA-11-PET/CT nicht nachweisbar waren. (Abbildung aus Originalarbeit 2 [63]).

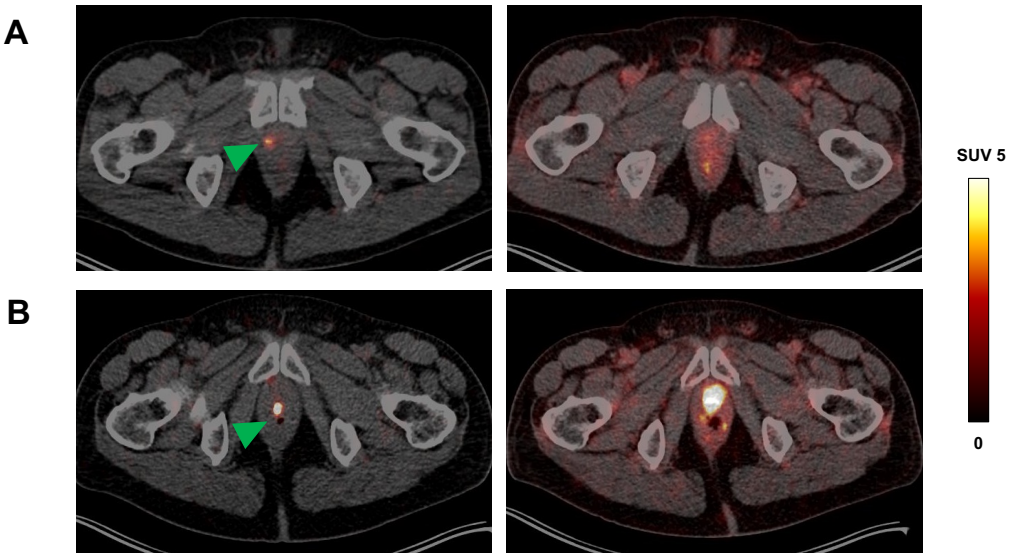

Abbildung 8: PET/CT-Transversalschnitte zweier Patienten (**A** und **B**) mit jeweils Darstellung eines mutmaßlichen Lokalrezidivs in der Prostataloge (grüne Pfeile), das mittels [^{89}Zr]Zr-PSMA-617-PET/CT (linke Spalte) nachgewiesen wurde, jedoch in der [^{68}Ga]Ga-PSMA-11-PET/CT (rechte Spalte) nicht erkennbar war. (Abbildung aus Originalarbeit 2 [63]).

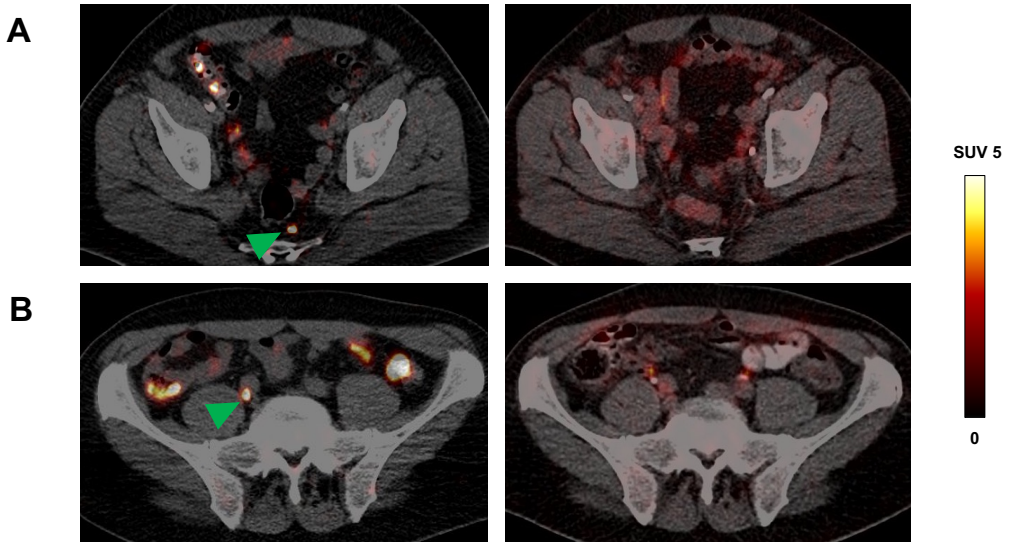

Abbildung 9: PET/CT-Transversalschnitte zweier Patienten (**A** und **B**) mit jeweils Darstellung einer mutmaßlichen pelvinen Lymphknotenmetastase (grüne Pfeile), die mittels [^{89}Zr]Zr-PSMA-617-PET/CT (linke Spalte) nachgewiesen wurde, jedoch in der [^{68}Ga]Ga-PSMA-11-PET/CT (rechte Spalte) nicht erkennbar war. (Abbildung aus Originalarbeit 2 [63]).

Bei der quantitativen Auswertung aller 33 Läsionen, die sowohl in den 24 h als auch in den 48 h p.i. akquirierten Aufnahmen sichtbar waren, zeigte sich kein signifikanter Unterschied im SUV_{max} zwischen den Akquisitionszeitpunkten (p = 0,104). Der SUV_{peak} war hingegen in der Aufnahme 48 h p.i. geringfügig, aber signifikant niedriger (p = 0,010). Im Gegensatz dazu zeigten die Tumor-zu-Hintergrund-Verhältnisse TBR_{max} und TBR_{peak} signifikant höhere Werte in der Aufnahme 48 h p.i. (jeweils p < 0,001) (Abbildung 10). Diese Beobachtung von im zeitlichen Verlauf steigenden Tumor-zu-Hintergrund-Verhältnissen ließ sich konsistent über alle Tumorlokalisationen (Lokalrezidiv, Lymphknoten- und Knochenmetastasen) hinweg beobachten.

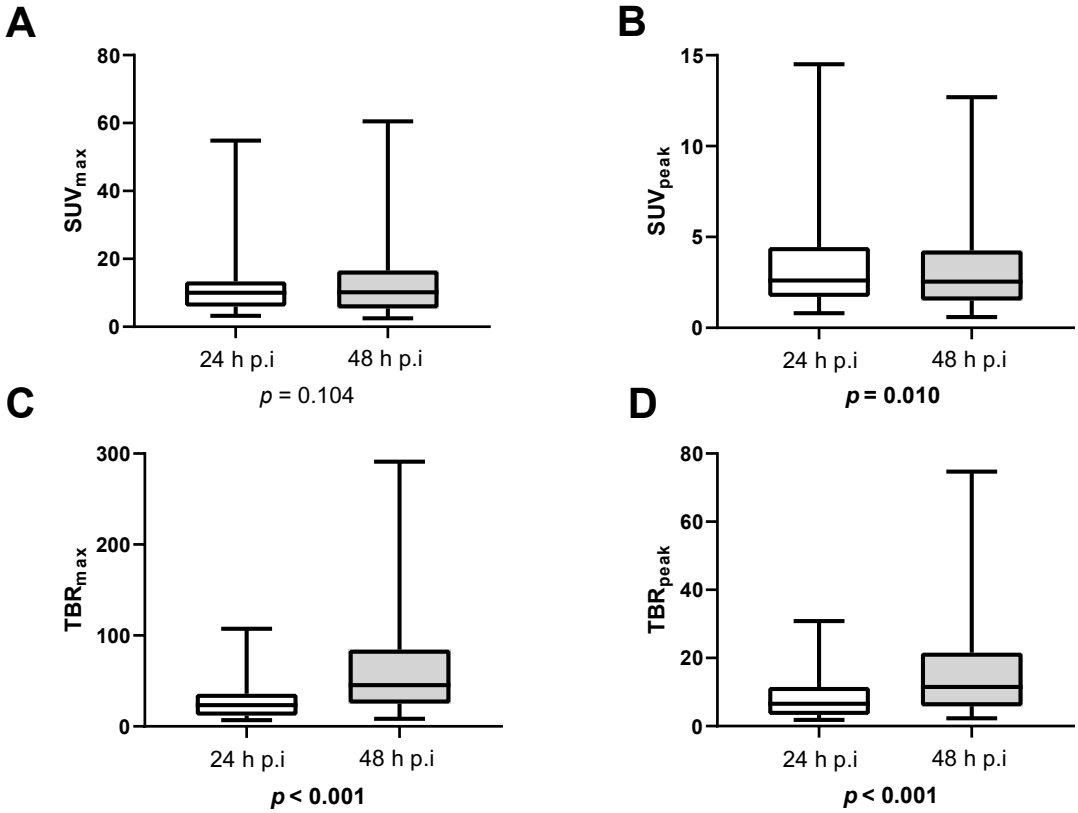

Abbildung 10: Vergleich der quantitativen PET-Parameter **A**: SUV_{max}, **B**: SUV_{peak} sowie der entsprechenden Tumor-zu-Hintergrund-Verhältnisse (TBR) **C**: TBR_{max} und **D**: TBR_{peak} der detektierten tumorsuspekten Läsionen 24 h und 48 h nach Injektion (p.i.) von [^{89}Zr]Zr-PSMA-617. (Abbildung aus Originalarbeit 2 [63]).

Alle 18 Patienten mit Nachweis tumorsuspekter Läsionen in der [^{89}Zr]Zr-PSMA-617-PET/CT erhielten eine Behandlung auf Grundlage der Ergebnisse der [^{89}Zr]Zr-PSMA-617-PET/CT. Ein Patient unterzog sich einer Lymphadenektomie eines solitären tumorsuspekten Lymphknotens. Histopathologisch konnte dieser mittels Immunhistochemie als Lymphknotenmetastase des Prostatakarzinoms bestätigt werden. Die übrigen Patienten erhielten entweder eine gezielte Bestrahlung mit Zielvolumen und Dosisverteilung basierend

auf den Befunden der [^{89}Zr]Zr-PSMA-617-PET/CT (n = 15) oder eine systemische Androgendeprivationstherapie (n = 2). Bei allen Patienten, die eine Strahlentherapie erhielten, kam es im Anschluss an die Behandlung zu einem Abfall des PSA-Werts (im Mittel um 72 ± 25 %). Bei 5 von 15 Patienten lag der PSA-Wert nach Bestrahlung unterhalb der Nachweisgrenze (< 0,05 ng/ml).

Hauptaussage:

Die [^{89}Zr]Zr-PSMA-617-PET/CT zeigt sich bei Männern mit BCR als vielversprechende Methode zur Detektion von Lokalrezidiven und Metastasen, die in der konventionellen PSMA-PET/CT-Bildgebung, wie der [^{68}Ga]Ga-PSMA-11-PET/CT unentdeckt bleiben. In der untersuchten Kohorte lag die Detektionsrate der [^{89}Zr]Zr-PSMA-617-PET/CT bei zuvor unauffälliger konventioneller PSMA-PET/CT-Bildgebung bei 78 %. Die Befunde wurden durch biochemische Ansprechraten nach gezielter Strahlentherapie sowie im Falle einer Operation durch eine histopathologische Untersuchung validiert. Aufgrund des zunehmenden Tumor-zu-Hintergrund-Verhältnisses im zeitlichen Verlauf sowie der Tatsache, dass einzelne Läsionen ausschließlich in den Aufnahmen 48 h p.i. detektiert werden konnten, scheint der spätere Bildgebungszeitpunkt 48 h p.i. dem Zeitpunkt 24 h p.i. überlegen zu sein.

4.3 Einsatz der [^{89}Zr]Zr-PSMA-617-PET/CT bei unklaren Befunden in der konventionellen PSMA-PET/CT

Originalarbeit 3

***Rosar F**, Burgard C, Larsen E, Khreish F, Marlowe RJ, Schaefer-Schuler A, Maus S, Petto S, Bartholomä M, Ezziddin S (2024) [^{89}Zr]Zr-PSMA-617 PET/CT characterization of indeterminate [^{68}Ga]Ga-PSMA-11 PET/CT findings in patients with biochemical recurrence of prostate cancer: lesion-based analysis. Cancer Imaging 24:27*

Hintergrund und Fragestellung:
Der aktuelle Standard zur Bildgebung bei Männern mit BCR eines Prostatakarzinoms ist die PSMA-PET/CT unter Verwendung kurzlebiger Radiotracer wie beispielsweise [^{68}Ga]Ga-PSMA-11 (Halbwertszeit ^{68}Ga: ca. 67,7 Minuten). Allerdings liefern diese Untersuchungen nicht selten unklare Befunde, deren weitere Charakterisierung nach wie vor eine Herausforderung darstellt. Langlebige PSMA-gerichtete Radiotracer, die mit ^{89}Zr (Halbwertszeit: ca. 78,4 Stunden) markiert sind, wie beispielsweise [^{89}Zr]Zr-PSMA-617, ermöglichen spätere Bildgebungszeitpunkte mit zeitlich steigendem Tumor-zu-Hintergrund-Verhältnis (Originalarbeit 1 und 2). Dies könnte eine präzisere Einschätzung von Läsionen erlauben, die in der konventionellen PSMA-PET/CT als unklar beurteilt wurden. Ziel der vorliegenden Studie war es daher zu untersuchen, ob der Malignitätsverdacht unklarer Befunde aus der konventionellen PSMA-PET/CT mithilfe der [^{89}Zr]Zr-PSMA-617-PET/CT präziser bewertet werden kann.

Methoden:
Insgesamt erhielten 15 Patienten mit BCR bei einem medianen PSA-Wert von 0,54 ng/ml (Minimum – Maximum: 0,23 – 1,75 ng/ml) eine [^{89}Zr]Zr-PSMA-617-PET/CT, nach dem bei ihnen in zuvor durchgeführten [^{68}Ga]Ga-PSMA-11-PET/CT-Untersuchungen N = 20 Läsionen als unklar beurteilt wurden (davon 4 mögliche Lokalrezidive, 8 mögliche Lymphknotenmetastasen und 8 mögliche Knochenmetastasen). Die [^{89}Zr]Zr-PSMA-617-PET/CT-Akquisitionen erfolgten jeweils 1 h, 24 h und 48 h nach Applikation von 123 ± 19 MBq [^{89}Zr]Zr-PSMA-617 und fanden im Mittel 35 ± 35 Tage nach der vorangegangenen [^{68}Ga]Ga-PSMA-11-PET/CT-Untersuchung statt. Zusätzlich zur visuellen Beurteilung der 20 Läsionen in der [^{89}Zr]Zr-PSMA-617-PET/CT erfolgte für alle Läsionen eine quantitative Auswertung anhand der Bestimmung des SUV_{max} sowie des Tumor-zu-Leber-Verhältnisses (*tumor-to-liver ratio*, TLR). Zur Validierung der Befundbeurteilung wurden Informationen zu im Anschluss an

die [^{89}Zr]Zr-PSMA-617-PET/CT durchgeführten Therapien und interventionellen Maßnahmen sowie deren Ergebnissen erhoben.

Ergebnisse:

Von insgesamt 20 Läsionen, die in der [^{68}Ga]Ga-PSMA-11-PET/CT als unklar im Hinblick auf Manifestationen des Prostatakarzinoms beurteilt wurden, wurden in der [^{89}Zr]Zr-PSMA-617 6 dieser Läsionen (30%) als tumorsuspekt und 14 Läsionen (70%) als nicht-tumorsuspekt eingestuft. Die in der [^{89}Zr]Zr-PSMA-617 als tumorsuspekt klassifizierten Läsionen umfassten 3 von 4 möglichen Lokalrezidiven, 1 von 8 möglichen Lymphknotenmetastasen sowie 2 von 8 potenziellen Knochenmetastasen (exemplarisch Abbildung 11 und 12).

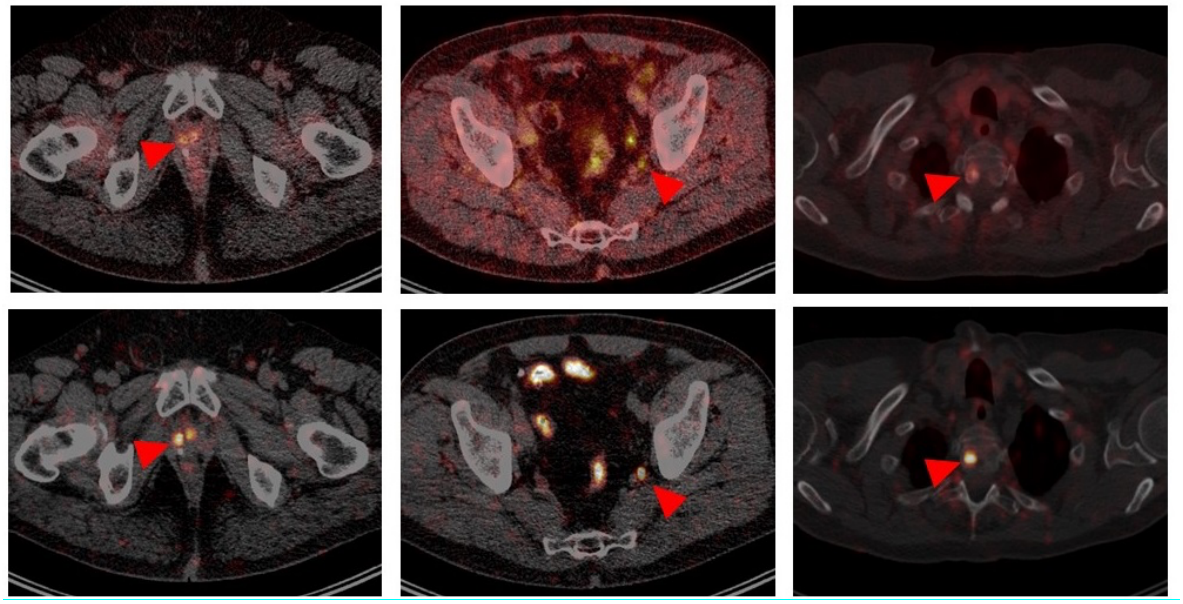

Abbildung 11: PET/CT-Transversalschnitte dreier Patienten (jeweils eine Spalte) mit unklaren Befunden (rote Pfeile) in der [^{68}Ga]Ga-PSMA-11-PET/CT (obere Reihe, Aufnahmen 1 h p.i.), die in der [^{89}Zr]Zr-PSMA-617-PET/CT (untere Reihe, Aufnahmen 48 h p.i.) eindeutig als tumorsuspekt klassifiziert werden konnten, entsprechend (von links nach rechts) als Lokalrezidiv, Lymphknotenmetastase und Knochenmetastase eines Prostatakarzinoms. (Abbildung aus Originalarbeit 3 [64]).

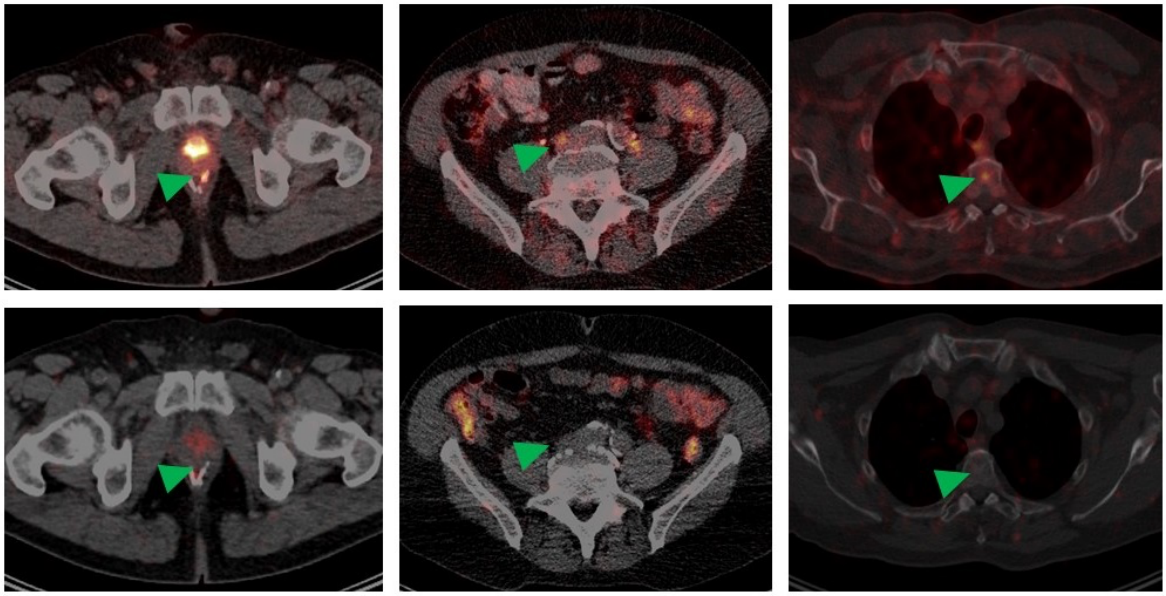

Abbildung 12: PET/CT-Transversalschnitte dreier Patienten (jeweils eine Spalte) mit unklaren Befunden (grüne Pfeile) in der [^{68}Ga]Ga-PSMA-11-PET/CT (obere Reihe, Aufnahmen 1 h p.i.), die jedoch in der [^{89}Zr]Zr-PSMA-617-PET/CT (untere Reihe, Aufnahmen 48 h p.i.) eindeutig als nicht tumorsuspekt klassifiziert werden konnten. (Abbildung aus Originalarbeit 3 [64]).

Bei den als tumorsuspekt bewerteten Läsionen zeigte sich zwischen der 1 h und der 24 h p.i. Aufnahme ein deutlicher Anstieg des Traceruptakes (SUV_{max}). Dieser Uptake blieb im weiteren zeitlichen Verlauf weitgehend stabil. Im Gegensatz dazu nahm der Uptake in den als nicht tumorsuspekt (und als unspezifisch) eingeordneten Läsionen im Verlauf kontinuierlich ab. Entsprechend stieg das TLR bei tumorsuspekten Läsionen im zeitlichen Verlauf deutlich an, während das TLR bei unspezifischen Läsionen unverändert blieb oder abnahm (Abbildung 13).

In der durchgeführten [^{89}Zr]Zr-PSMA-617-PET/CT konnten darüber hinaus bei 7 Patienten insgesamt 11 weitere tumorsuspekte Läsionen identifiziert werden, die in der zuvor erfolgten [^{68}Ga]Ga-PSMA-11-PET/CT nicht abgrenzbar waren. Bei drei dieser neu entdeckten Läsionen handelte es sich um Lokalrezidive, bei acht um Lymphknotenmetastasen. Sämtliche bereits in der [^{68}Ga]Ga-PSMA-11-PET/CT als eindeutig tumorsuspekt bewertete Läsionen, waren auch in der [^{89}Zr]Zr-PSMA-617-PET/CT eindeutig darstellbar.

Im Anschluss an die [^{89}Zr]Zr-PSMA-617-PET/CT-Bildgebung erhielten 12 von 15 Patienten (80 %) eine zielgerichtete Strahlentherapie der in der [^{89}Zr]Zr-PSMA-617-PET/CT als tumorsuspekt bewerteten Läsionen. Nach der gezielten Bestrahlung dieser Befunde sank der PSA-Wert im Mittel um 84 ± 26 % ab. Bei 6 von 12 Patienten lag der PSA-Wert danach unterhalb der Nachweisgrenze.

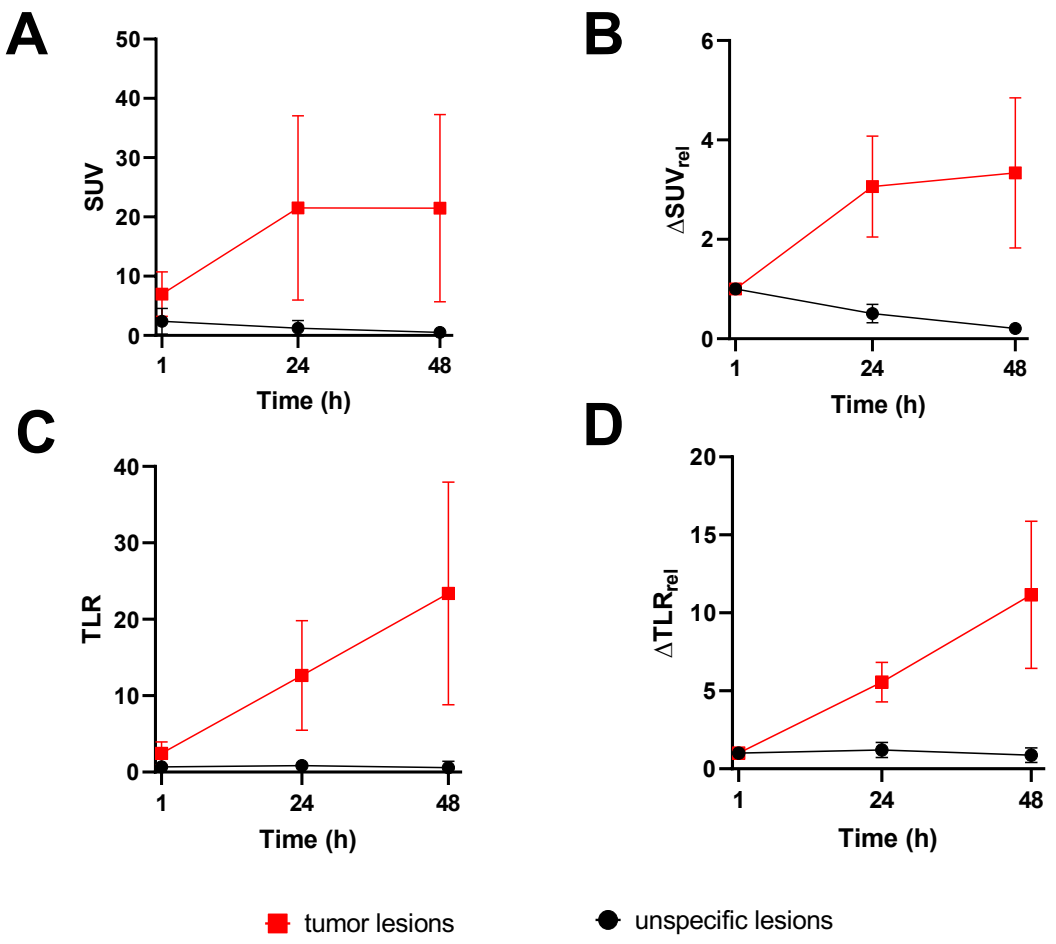

Abbildung 13: Zeitlicher Verlauf des Traceruptakes (SUV_{max}) und des Tumor-zu-Leber-Verhältnisses (TLR) für tumorsuspekte Läsionen (rot) im Vergleich zu als nicht tumorsuspekt bzw. unspezifisch bewerteten Läsionen (schwarz) in der [^{89}Zr]Zr-PSMA-617-PET/CT. **A:** SUV_{max}, **B:** relative Änderung des SUV_{max}, **C:** Tumor-zu-Leber-Verhältnis (TLR) und **D:** relative Änderung der TLR. (Abbildung aus Originalarbeit 3 [64]).

Hauptaussage:

Die [^{89}Zr]Zr-PSMA-617-PET/CT ermöglicht eine weiterführende Abklärung und präzise Einordnung von Läsionen, die in der [^{68}Ga]Ga-PSMA-11-PET/CT zuvor als unklar eingestuft wurden. Tumorsuspekte Läsionen unterscheiden sich dabei durch eine charakteristisch abweichende Tracerkinetik von nicht tumorsuspekten Läsionen. Die [^{89}Zr]Zr-PSMA-617-PET/CT erweist sich somit als vielversprechende Bildgebungsmodalität und sollte als komplementäres Verfahren für die klinische Routine in Betracht gezogen werden.

V. Diskussion

[^{89}Zr]Zr-PSMA-617 ist ein innovativer Tracer zur PET/CT-Diagnostik des Prostatakarzinoms, der sich durch die lange physikalische Halbwertszeit des Radionuklids ^{89}Zr von ca. 78,4 Stunden auszeichnet. Im Rahmen dieser Dissertation werden erste klinische Erfahrungen mit der Anwendung der [^{89}Zr]Zr-PSMA-617-PET/CT bei Patienten mit BCR des Prostatakarzinoms vorgestellt. Der Schwerpunkt lag auf der Analyse der Biodistribution, der Tracerkinetik, der Abschätzung der Strahlenexposition sowie einer ersten Bewertung potenzieller klinischer Einsatzgebiete.

In Originalarbeit 1 lag der Fokus auf der Biodistribution, Tracerkinetik und Dosimetrie von [^{89}Zr]Zr-PSMA-617. Beim Vergleich der Biodistribution von [^{89}Zr]Zr-PSMA-617 mit den etablierten Tracern [^{68}Ga]Ga-PSMA-11 und [^{68}Ga]Ga-PSMA-617 zeigte sich ein ähnliches Verteilungsmuster eine Stunde nach Injektion mit intensiver physiologischer Anreicherung in den Speichel- und Tränendrüsen, Nieren, Leber, Milz und dem Dünndarm [2,3]. Diese Anreicherung ist auf die bekannte physiologische PSMA-Expression in diesen Organen und z.T. auch auf renale Traceraussсheidung zurückzuführen [43,70]. Im Gegensatz zu den konventionellen PSMA-Tracern erlaubt die längere Halbwertszeit von ^{89}Zr auch spätere Bildgebungszeitpunkte mit [^{89}Zr]Zr-PSMA-617. In der vorliegenden Studie wurden Bildakquisitionen bis 72 Stunden nach Injektion durchgeführt. Während der Traceruptake in Nieren, Leber und Milz über die Zeit stetig zurückging, stieg er in Speichel- und Tränendrüsen sowie im Dünndarm bis 24 Stunden nach Injektion weiter an und nahm erst anschließend ab. Zudem zeigte sich ein über die Zeit zunehmender Traceruptake im Kolon, was auf eine, neben einer renalen Exkretion, zunehmende Ausscheidung über den Darm (hepatische Elimination) hinweist. Ähnliche Beobachtungen wurde auch für [^{177}Lu]Lu-PSMA-617 (Halbwertszeit Lutetium-177: ca. 6,6 Tage) im Rahmen von Dosimetrie-Studien beschrieben [21,46]. Im Gegensatz zu der physiologischen Traceranreicherung in den Organen zeigte sich bei den detektierten Tumorläsionen ein zunehmender Traceruptake bis 24 Stunden nach Injektion, der danach bis zum Untersuchungsende nach 72 Stunden stabil blieb. Dies lässt sich durch die Internalisierung des Radioliganden-PSMA-Komplexes und die nachfolgende intrazelluläre Speicherung erklären [48,79]. In Kombination mit der fortschreitenden Clearance des Tracers aus gesundem Gewebe führt dies zu deutlich steigenden Tumor-zu-Hintergrund-Verhältnissen, was die Detektion von Tumoren erheblich verbessert (*vide infra*, Originalarbeiten 2 und 3).

Die geschätzte effektive Dosis von [^{89}Zr]Zr-PSMA-617 bei einer applizierten Aktivität von 111 MBq (3 mCi) betrug 10,1 mSv (0,0913 ± 0,0118 mSv/MBq) und liegt damit etwa zwei- bis

dreimal höher als bei PET-Untersuchungen mit konventionellen PSMA-Tracern in den jeweils üblich verwendeten Aktivitäten. Für [^{68}Ga]Ga-PSMA-11 oder [^{68}Ga]Ga-PSMA-617 ergeben sich bei Standardaktivität von 200 MBq ca. 4,6 mSv (0,023 mSv/MBq) bzw. 4,2 mSv (0,021 mSv/MBq) [2,3]. Analog zu den konventionellen PSMA-Tracern erhielten die Glandula parotidea und die Nieren die höchsten Organdosen, wobei die absoluten Dosen im Vergleich zu den konventionellen Tracern etwa drei- bis viermal höher ausfielen [2,3]. Eine höhere Strahlenexposition durch [^{89}Zr]Zr-PSMA-617 im Vergleich zu konventionellen PSMA-Tracern war aufgrund der deutlich längeren Halbwertszeit von ^{89}Zr zu ^{68}Ga (ca. 78,4 Stunden vs. 67,7 Minuten) grundsätzlich zu erwarten. Die tatsächlich berechnete Dosis fiel jedoch vergleichsweise gering aus – insbesondere im Vergleich zu [^{89}Zr]Zr-PSMA-DFO (0,15 mSv/MBq, entsprechend 16,6 mSv bei 111 MBq), einem zuvor von der Arbeitsgruppe um *Dietlein et al.* entwickelten ^{89}Zr-markierten PSMA-Tracer, sowie deutlich niedriger als für [^{89}Zr]Zr-Df-IAB2M (0,41 mSv/MBq, entsprechend 45 mSv bei 111 MBq), einem ^{89}Zr-markierten PSMA-gerichteten Antikörperfragment (Minibody) [23,57]. Da die Langzeit-PET-Bildgebung mit ^{89}Zr-markierten Antikörpern typischerweise mit einer sehr hohen Strahlenbelastung einhergeht [10,47,57,81], stellt die vergleichsweise niedrige Exposition einen klaren Vorteil für PSMA-Liganden dar. [^{89}Zr]Zr-PSMA-617 ist damit bislang der ^{89}Zr-basierte PSMA-Tracer mit der geringsten Strahlenexposition in vivo. Die Strahlenbelastung durch die [^{89}Zr]Zr-PSMA-617-PET liegt mit etwa 10 mSv somit in einem akzeptablen Bereich und entspricht in ihrer Größenordnung etwa der einer diagnostischen CT von Thorax und Abdomen [11]. Neben dem Aspekt der Strahlenbelastung zeigte sich allgemein die [^{89}Zr]Zr-PSMA-617-PET/CT als sicheres Verfahren ohne Hinweis auf unerwünschte Wirkungen. Nebenwirkungen wie beispielsweise Mundtrockenheit, wie sie typischerweise bei der PSMA-Radioligandentherapie mit therapeutischen Radionukliden (z.B. ^{177}Lu) beobachtet werden [35,42,65], traten nicht auf.

Eine zentrale klinische Beobachtung von Originalarbeit 1 war, dass bei 3 von 4 Patienten (75 %) mit zuvor negativer [^{68}Ga]Ga-PSMA-11-PET/CT in der [^{89}Zr]Zr-PSMA-617-PET/CT tumorsuspekte Läsionen (Lokalrezidiv oder Lymphknotenmetastasen) detektiert werden konnten. Originalarbeit 2 untersuchte daraufhin systematisch den Einsatz und die Detektionsrate der [^{89}Zr]Zr-PSMA-617-PET/CT bei Patienten mit BCR mit zuvor negativer konventioneller PSMA-PET/CT. Bei 18 von 23 Patienten mit BCR und zuvor unauffälliger [^{68}Ga]Ga-PSMA-11-PET/CT-Bildgebung konnten mittels [^{89}Zr]Zr-PSMA-617-PET/CT eindeutig tumorsuspekte Läsionen identifiziert werden (insgesamt 36 Läsionen, jeweils 1 bis 4 Läsionen pro Patient, lokalisiert als Lokalrezidiv, Lymphknoten oder Knochenmetastasen), was einer patientenbasierten Detektionsrate von 78 % entspricht. Ein posttherapeutischer Abfall des PSA-Werts nach gezielter Bestrahlung (in vielen Fällen unter die Nachweisgrenze) sowie eine histopathologische Untersuchung im Falle einer Operation bestätigten, dass es sich bei diesen Läsionen um Tumormanifestationen und damit um richtig-positive Befunde der

PET-Bildgebung handelte. Die diagnostische Überlegenheit der [^{89}Zr]Zr-PSMA-617-PET/CT gegenüber der [^{68}Ga]Ga-PSMA-11-PET/CT liegt in der längeren Halbwertszeit des Tracers begründet. Diese erlaubt, wie zuvor diskutiert, spätere Bildgebungszeitpunkte, wodurch Tumorläsionen zur Darstellung kommen, die mit kurzlebigen PSMA-Tracern nicht abgegrenzt werden können. Die in den ersten 24 Stunden zunehmende und anschließend anhaltende Anreicherung des Tracers in den Tumorläsionen sowie die gleichzeitig im zeitlichen Verlauf deutlich abnehmende Hintergrundaktivität in Blutgefäßen, Weichteilen sowie den ableitenden Harnwegen, insbesondere der Blase, führen zu einem erheblich verbesserten Kontrast zwischen Tumorläsion und Umgebung. Dies führt zu einer verbesserten Detektion kleinster pathologischer Strukturen.

Diese beobachte Überlegenheit einer ^{89}Zr-basierten PSMA-PET/CT stimmt mit den Ergebnissen von *Dietlein et al.* überein, die in 57 % der Patienten mit initial negativer PSMA-PET/CT (mit [^{68}Ga]Ga-PSMA-11 oder [^{18}F]JK-PSMA-7) Tumorläsionen mittels [^{89}Zr]Zr-PSMA-DFO-PET/CT (2 – 3 Tage nach Injektion) nachweisen konnten [23]. Die in Originalarbeit 2 ermittelte Detektionsrate der [^{89}Zr]Zr-PSMA-617-PET/CT von 78 % bei zuvor negativer [^{68}Ga]Ga-PSMA-11-PET/CT wurde durch eine nachfolgende Studie von *Burgard et al.* mit einem erweiterten Patientenkollektiv (N = 33) bestätigt [13]. *Burgard et al.* konnten zudem eine bis zu 100-fache Kontrastzunahme von Tumorläsionen gegenüber dem unmittelbar angrenzenden Gewebe nachweisen [13].

Die ^{89}Zr-basierte PSMA-PET/CT stellt damit eine vielversprechende ergänzende Option für Patienten mit BCR und unklarer Tumorlokalisation in der konventionellen PSMA-PET/CT dar. Trotz der insgesamt hohen diagnostischen Genauigkeit der konventionellen PSMA-PET/CT, die anderen bildgebenden Standardverfahren wie der Magnetresonanztomographie (MRT), der CT oder der Skelettszintigraphie in der Detektion von Metastasen bereits überlegen ist [36,54,85], bleibt ein nicht unerheblicher Anteil an Untersuchungen mit negativem, d.h. ohne pathologischen Befund [4,14]. In der bislang größten Studie zur [^{68}Ga]Ga-PSMA-11-PET/CT bei BCR des Prostatakarzinoms von *Afshar-Oromieh et al.* mit insgesamt 2553 Patienten wurde eine patientenbasierte Gesamtdetektionsrate von 68,9 % berichtet [4]. Diese Rate zeigte jedoch eine klare Abhängigkeit vom PSA-Wert, wobei die Detektionsrate mit steigenden PSA-Werten zunahm [4]. In einer aktuellen multizentrischen Studie von *Burgard et al.,* in der verschiedene konventionelle PSMA-Tracer untersucht wurden, konnte bei einem PSA-Wert ≤ 0,2 ng/ml eine gepoolte Detektionsrate von 29,6 % festgestellt werden [14]. Diese war weitgehend unabhängig davon, ob ein ^{68}Ga- oder ^{18}F-basierter konventioneller Tracer verwendet wurde [14]. Damit gelingt bei einem Großteil der Patienten, insbesondere bei niedrigen PSA-Werten, kein bildgebender Tumornachweis. Eine frühzeitige Strahlentherapie muss daher häufig unspezifisch auf die Prostataloge ausgerichtet werden.

Dies erhöht das Risiko einer unzureichenden oder fehlgerichteten Bestrahlung, falls sich beispielsweise das Rezidiv an anderer Stelle befindet. Insbesondere bei höhergradigen Prostatakarzinomen ist jedoch eine frühzeitige Strahlentherapie bei noch sehr niedrigen PSA-Werten mit einer besseren Prognose verbunden [29,72]. Durch die Lokalisation des BCR mittels molekularer Bildgebung kann das Rezidiv gezielt im Rahmen einer sogenannten PET-gesteuerten *Salvage*-Strahlentherapie mit kurativer Intention behandelt werden [22,24,71]. Eine aktuelle Metaanalyse von 34 Studien zeigt, dass eine PSMA-PET/CT-Untersuchung bei etwa der Hälfte der Patienten mit BCR die therapeutische Behandlung beeinflusst [59]. Sie eröffnet einen individuell zugeschnittenen, personalisierten Therapieansatz. Die präzise Kenntnis der Tumorlage ermöglicht beispielsweise die Strahlendosis im Bereich der Tumorregion gezielt zu erhöhen [77]. Im Falle von größeren Lokalrezidiven oder Lymphknotenmetastasen kann zudem eine *Salvage*-Operation in Erwägung gezogen werden [38,45]. *Calais et al.* konnten nachweisen, dass die molekulare Bildgebung einen maßgeblichen Einfluss auf die Planung der Strahlentherapie hat [15]. In einem großen Teil der Fälle führte sie zu einer Modifikation des Bestrahlungskonzepts bzw. des -plans [15]. In einer prospektiven Phase-3-Studie von *Armstrong et al.* konnte dies kürzlich bestätigt werden [5]. Mehrere Studien mit retrospektiven Vergleichen weisen darauf hin, dass eine PSMA-basierte Strahlentherapie das Outcome der Patienten verbessert [51,66,74,83]. Die Outcome-Daten der Phase-3-Studie von *Armstrong et al.* stehen zum gegenwärtigen Zeitpunkt noch aus [5]. Die zielgerichtete Behandlung von Metastasen, auch bekannt als *metastasis-directed therapy* (MDT), ist nicht nur bei singulären, sondern ebenso bei oligofokalen Metastasen eine vielversprechende Option. Ziel der MDT im oligometastasierten Stadium ist es, das Zeitintervall bis zur Einleitung einer systemischen Therapie zu verlängern und gleichzeitig eine dauerhafte lokale Tumorkontrolle zu erreichen. Mehrere retrospektive Studien konnten für die MDT bereits vielversprechende Ergebnisse liefern [6,37,53,55]. Voraussetzung für den Erfolg dieses Konzepts ist jedoch die zuverlässige Identifikation aller Metastasen. In der konventionellen PSMA-PET/CT-Diagnostik finden sich jedoch nicht selten unklare Befunde, deren weitere Charakterisierung essenziell ist, aber nach wie vor eine Herausforderung darstellt.

In Originalarbeit 1 konnte bei 2 von 3 Patienten mit unklaren Befunden in der [^{68}Ga]Ga-PSMA-11-PET/CT der jeweilige Verdacht durch eine ergänzende [^{89}Zr]Zr-PSMA-617-PET/CT bestätigt werden; bei einem Patienten wurde dieser hingegen widerlegt. Aufbauend aus diesen Erfahrungen wurde in Originalarbeit 3 der Einsatz der [^{89}Zr]Zr-PSMA-617-PET/CT bei Patienten mit zuvor unklaren Befunden in der konventionellen PSMA-PET/CT systematisch in einem größeren Patientenkollektiv untersucht. Dieses umfasste insgesamt 20 unklare Läsionen bei 15 Patienten. Durch die [^{89}Zr]Zr-PSMA-617-PET/CT konnten alle zuvor in der [^{68}Ga]Ga-PSMA-11-PET/CT als unklar beurteilten Läsionen näher eingeordnet werden. Sechs

der insgesamt 20 Läsionen (30 %) wurden als tumorsuspekt eingestuft, während 14 Läsionen (70 %) als nicht-tumorsuspekt bzw. unspezifisch bewertet wurden. Zusätzlich konnten darüber hinaus bei 7 Patienten insgesamt 11 weitere tumorsuspekte Läsionen identifiziert werden, die in der erfolgten [^{68}Ga]Ga-PSMA-11-PET/CT nicht abgrenzbar waren, was im Einklang mit den Beobachtungen aus Originalarbeit 1 und 2 steht. Die weiterführende Abklärung erwies sich als klinisch bedeutsam: zum einen konnten die tumorsuspekten Läsionen nun mit erhöhter diagnostischer Sicherheit einer Strahlentherapie zugeführt werden. Gleichzeitig konnte bei allen anderen Läsionen auf eine Bestrahlung verzichtet werden, was den Patienten eine unnötige Strahlenexposition und potenzielle Nebenwirkungen ersparte. Biochemische PSA-Verläufe nach Therapie verifizierten die Befundbeurteilung der [^{89}Zr]Zr-PSMA-617-PET/CT. Beide Gruppen zeigten ein deutlich unterschiedliches Muster der Tracerkinetik in den Läsionen. In den als tumorsuspekt eingestuften Läsionen ließ sich in Übereinstimmung mit den Ergebnissen aus Originalarbeit 1 und 2 ein Anstieg der Traceraufnahme in den ersten 24 Stunden beobachten, gefolgt von einem stabilen Verlauf. Im Gegensatz dazu zeigte sich in den als nicht tumorsuspekt bewerteten Läsionen ein kontinuierlicher Rückgang der Traceraufnahme über den gesamten Beobachtungszeitraum. Entsprechend zeigten Tumorläsionen eine zeitliche Zunahme des Kontrasts zum physiologischen Gewebe, während dieser bei unspezifischen Läsionen unverändert blieb oder abnahm. Die unterschiedlichen kinetischen Verläufe lassen sich durch die Internalisierung des Tracer-PSMA-Komplexes in Prostatakarzinom-Läsionen im Gegensatz zur fehlenden Internalisierung und damit verbundenen konsekutiven Auswaschung bei unspezifischen Befunden erklären. Zum einen untermauern die Ergebnisse die Annahme einer korrekten Klassifikation der Läsionen in der [^{89}Zr]Zr-PSMA-617-PET/CT, zum anderen legen sie nahe, dass die Quantifizierung spezifischer PET-Parameter die Differenzierung zwischen Tumorläsionen und unspezifischen Veränderungen wesentlich unterstützen kann.

Bezüglich des optimalen Akquisitionszeitpunktes der [^{89}Zr]Zr-PSMA-617-PET/CT lässt sich auf Grundlage der Tracerkinetik sowie Erfahrungen aus den Originalarbeiten 1 – 3 folgendes ableiten: Aufgrund des stabilen Traceruptakes ab ca. 24 Stunden nach Injektion und des zeitlich zunehmenden Tumor-zu-Hintergrund-Verhältnisses scheinen spätere Aufnahmen, beispielsweise nach 48 oder 72 Stunden, einen diagnostischen Vorteil zu bieten. Dies wird auch dadurch gestützt, dass einige Läsionen ausschließlich in den spätzeitigen Aufnahmen (frühstens 48 Stunden nach Injektion) detektiert werden konnten.

Die [^{89}Zr]Zr-PSMA-617-PET/CT erweist sich zusammenfassend als eine vielversprechende, sichere, komplementäre Bildgebungsoption mit akzeptabler Strahlenexposition für Patienten mit BCR eines Prostatakarzinoms. Sie ermöglicht zum einen die Detektion von Tumorläsionen, die in der konventionellen PSMA-PET/CT nicht abgrenzbar sind, und zum anderen die weitere

Abklärung sowie präzise Einordnung zuvor unklarer Befunde. Die Ergebnisse der Originalarbeiten 1 – 3 liefern damit eine wissenschaftliche Grundlage und eine klare Rationale für zukünftige, idealerweise prospektive Studien mit größeren Patientenkohorten.

Bestätigen zukünftige Studien die bisherigen Ergebnisse, sollte die [^{89}Zr]Zr-PSMA-617-PET/CT als wertvolle Ergänzung in die klinische Routine integriert werden. Darüber hinaus könnte sie insbesondere bei Patienten mit BCR eines Prostatakarzinoms und sehr niedrigen PSA-Werten, bei denen die konventionelle PSMA-PET/CT nur eine eingeschränkte Detektionsrate aufweist [14], als primäre Bildgebungsoption erwogen und Studien hierzu initiiert werden. Auch für das Primärstaging bei neu diagnostiziertem Prostatakarzinom sollte die Anwendung einer [^{89}Zr]Zr-PSMA-617-PET/CT in zukünftigen Studien evaluiert werden. In einem nächsten Schritt sollten zudem prädiktive Marker, wie sie bereits für die konventionelle PSMA-PET/CT bekannt sind [16,61], auch für die [^{89}Zr]Zr-PSMA-617-PET/CT identifiziert werden. Die bisherigen Untersuchungen wurden auf Grundlage konventioneller PSMA-PET/CT-Bildgebung mit [^{68}Ga]Ga-PSMA-11 durchgeführt. Es ist anzunehmen, dass sich ähnliche Resultate auch im Vergleich zu anderen etablierten Tracern wie [^{18}F]DCFPyL oder [^{18}F]PSMA-1007, erzielen lassen. Letzterer ist insbesondere für eine erhöhte Rate unspezifischer, falsch-positiver Knochenbefunde bekannt [33,68]. In diesem Kontext könnte die [^{89}Zr]Zr-PSMA-617-PET/CT als komplementäre Untersuchung einen besonders hohen diagnostischen Mehrwert bieten. Trotz der vielversprechenden Ergebnisse gilt es, die Strahlenexposition von ca. 10 mSv zu berücksichtigen. Zukünftige Studien mit größeren Patientenkohorten sollten darauf abzielen, die optimale Aktivität und den idealen Bildgebungszeitpunkt zu definieren, um bei möglichst geringer Strahlenbelastung eine adäquate Bildqualität zu erzielen. Es gilt auch zu untersuchen, welche genauen Auswirkungen eine zusätzliche [^{89}Zr]Zr-PSMA-617-PET/CT auf das klinische Management, insbesondere auf die Bestrahlungsplanung hat und wie sich dadurch das Outcome der Patienten ändert. Die [^{89}Zr]Zr-PSMA-617-PET/CT könnte zukünftig auch im fortgeschrittenen Stadium des Prostatakarzinoms eine entscheidende Rolle spielen, indem sie durch prätherapeutische Dosimetrie eine individuelle Bestimmung der Aktivität für eine personalisierte Radioligandentherapie mit [^{177}Lu]Lu-PSMA-617 ermöglichen könnte. Das Konzept der Langzeit-PET-Bildgebung mit ^{89}Zr sollte auch auf andere Tracer und Anwendungsgebiete übertragen und geprüft werden, um die Diagnostik und Therapieplanung bei verschiedenen Erkrankungen weiter zu optimieren.

VI. Abkürzungsverzeichnis

BCR	Biochemisches Rezidiv
CT	Computertomographie
MDT	*metastasis-directed therapy*
MIP	Maximumintensitätsprojektion
MRT	Magnetresonanztomographie
PET	Positronenemissionstomographie
p.i.	nach Injektion
PSA	Prostataspezifisches Antigen
PSMA	Prostataspezifisches Membranantigen
SUV	*standardized uptake value*
TBR	Tumor-zu-Hintergrund-Verhältnis
TIAC	*time-integrated activity coefficient*
TiBR	Gewebe-zu-Hintergrund-Verhältnis
TLR	Tumor-zu-Leber-Verhältnis

VII. Literaturverzeichnis

1. Afshar-Oromieh A, Malcher A, Eder M, Eisenhut M, Linhart HG, Hadaschik BA, Holland-Letz T, Giesel FL, Kratochwil C, Haufe S, Haberkorn U, Zechmann CM (2013) PET imaging with a [^{68}Ga]gallium-labelled PSMA ligand for the diagnosis of prostate cancer: biodistribution in humans and first evaluation of tumour lesions. Eur J Nucl Med Mol Imaging 40:486–495

2. Afshar-Oromieh A, Hetzheim H, Kratochwil C, Benesova M, Eder M, Neels OC, Eisenhut M, Kübler W, Holland-Letz T, Giesel FL, Mier W, Kopka K, Haberkorn U (2015) The Theranostic PSMA Ligand PSMA-617 in the Diagnosis of Prostate Cancer by PET/CT: Biodistribution in Humans, Radiation Dosimetry, and First Evaluation of Tumor Lesions. J Nucl Med 56:1697–1705

3. Afshar-Oromieh A, Hetzheim H, Kübler W, Kratochwil C, Giesel FL, Hope TA, Eder M, Eisenhut M, Kopka K, Haberkorn U (2016) Radiation dosimetry of ^{68}Ga-PSMA-11 (HBED-CC) and preliminary evaluation of optimal imaging timing. Eur J Nucl Med Mol Imaging 43:1611–1620

4. Afshar-Oromieh A, da Cunha ML, Wagner J, Haberkorn U, Debus N, Weber W, Eiber M, Holland-Letz T, Rauscher I (2021) Performance of [^{68}Ga]Ga-PSMA-11 PET/CT in patients with recurrent prostate cancer after prostatectomy-a multi-centre evaluation of 2533 patients. Eur J Nucl Med Mol Imaging 48:2925–2934

5. Armstrong WR, Kishan AU, Booker KM, Grogan TR, Elashoff D, Lam EC, Clark KJ, Steinberg ML, Fendler WP, Hope TA, Nickols NG, Czernin J, Calais J (2024) Impact of Prostate-specific Membrane Antigen Positron Emission Tomography/Computed Tomography on Prostate Cancer Salvage Radiotherapy Management: Results from a Prospective Multicenter Randomized Phase 3 Trial (PSMA-SRT NCT03582774). Eur Urol 86:52–60

6. Bauersachs L, Beck M, Furth C, Mehrhof F, Amthauer H, Ghadjar P, Rogasch JMM, de Santis M, Tahbaz R, Zips D, Zschaeck S (2025) Metastasis directed radiotherapy versus standard of care for PSMA-PET diagnosed oligometastatic/oligoprogressive castration resistant prostate cancer. Sci Rep 15:27153

7. Bergengren O, Pekala KR, Matsoukas K, Fainberg J, Mungovan SF, Bratt O, Bray F, Brawley O, Luckenbaugh AN, Mucci L, Morgan TM, Carlsson SV (2023) 2022 Update on Prostate Cancer Epidemiology and Risk Factors-A Systematic Review. Eur Urol 84:191–206

8. Berliner C, Tienken M, Frenzel T, Kobayashi Y, Helberg A, Kirchner U, Klutmann S, Beyersdorff D, Budäus L, Wester H-J, Mester J, Bannas P (2017) Detection rate of PET/CT in patients with biochemical relapse of prostate cancer using [^{68}Ga]PSMA I&T and comparison with published data of [^{68}Ga]PSMA HBED-CC. Eur J Nucl Med Mol Imaging 44:670–677

9. Beyer T, Antoch G, Müller S, Egelhof T, Freudenberg LS, Debatin J, Bockisch A (2004) Acquisition protocol considerations for combined PET/CT imaging. J Nucl Med 45 Suppl 1:25S-35S

10. Börjesson PKE, Jauw YWS, de Bree R, Roos JC, Castelijns JA, Leemans CR, van Dongen GAMS, Boellaard R (2009) Radiation dosimetry of ^{89}Zr-labeled chimeric monoclonal antibody U36 as used for immuno-PET in head and neck cancer patients. J Nucl Med 50:1828–1836

11. Bos D, Guberina N, Zensen S, Opitz M, Forsting M, Wetter A (2023) Radiation

Exposure in Computed Tomography. Dtsch Arzteblatt Int 120:135–141

12. Burgard C, Hein C, Blickle A, Bartholomä M, Maus S, Petto S, Schaefer-Schuler A, Ezziddin S, Rosar F (2024) Change in total lesion PSMA (TLP) during [^{177}Lu]Lu-PSMA-617 radioligand therapy predicts overall survival in patients with mCRPC: monocentric evaluation of a prospective registry. Eur J Nucl Med Mol Imaging 51:885–895

13. Burgard C, Rosar F, Larsen E, Khreish F, Linxweiler J, Marlowe RJ, Schaefer-Schuler A, Maus S, Petto S, Bartholomä M, Ezziddin S (2024) Outstanding increase in tumor-to-background ratio over time allows tumor localization by [^{89}Zr]Zr-PSMA-617 PET/CT in early biochemical recurrence of prostate cancer. Cancer Imaging 24:132

14. Burgard C, Frei M, Blickle A, Hartrampf PE, Hoffmann MA, Schreckenberger M, Schmid H-P, Unterrainer L, Rogasch J, Galler M, Ezziddin S, Rosar F (2025) PSMA PET/CT in biochemical recurrence of prostate cancer with PSA levels ≤ 0.2 ng/mL: a German multicenter analysis of conventional PSMA tracers, including [^{68}Ga]Ga-PSMA-11, [^{68}Ga]Ga-PSMA I&T, and [^{18}F]PSMA-1007. Eur J Nucl Med Mol Imaging 52:4368–4376

15. Calais J, Czernin J, Cao M, Kishan AU, Hegde JV, Shaverdian N, Sandler K, Chu F-I, King CR, Steinberg ML, Rauscher I, Schmidt-Hegemann N-S, Poeppel T, Hetkamp P, Ceci F, Herrmann K, Fendler WP, Eiber M, Nickols NG (2018) ^{68}Ga-PSMA-11 PET/CT Mapping of Prostate Cancer Biochemical Recurrence After Radical Prostatectomy in 270 Patients with a PSA Level of Less Than 1.0 ng/mL: Impact on Salvage Radiotherapy Planning. J Nucl Med 59:230–237

16. Ceci F, Bianchi L, Borghesi M, Polverari G, Farolfi A, Briganti A, Schiavina R, Brunocilla E, Castellucci P, Fanti S (2020) Prediction nomogram for ^{68}Ga-PSMA-11 PET/CT in different clinical settings of PSA failure after radical treatment for prostate cancer. Eur J Nucl Med Mol Imaging 47:136–146

17. Chen Y, Pullambhatla M, Foss CA, Byun Y, Nimmagadda S, Senthamizhchelvan S, Sgouros G, Mease RC, Pomper MG (2011) 2-(3-{1-Carboxy-5-[(6-[^{18}F]fluoro-pyridine-3-carbonyl)-amino]-pentyl}-ureido)-pentanedioic acid, [^{18}F]DCFPyL, a PSMA-based PET imaging agent for prostate cancer. Clin Cancer Res 17:7645–7653

18. Cornford P, van den Bergh RCN, Briers E, Van den Broeck T, Brunckhorst O, Darraugh J, Eberli D, De Meerleer G, De Santis M, Farolfi A, Gandaglia G, Gillessen S, Grivas N, Henry AM, Lardas M, van Leenders GJLH, Liew M, Linares Espinos E, Oldenburg J, van Oort IM, Oprea-Lager DE, Ploussard G, Roberts MJ, Rouvière O, Schoots IG, Schouten N, Smith EJ, Stranne J, Wiegel T, Willemse P-PM, Tilki D (2024) EAU-EANM-ESTRO-ESUR-ISUP-SIOG Guidelines on Prostate Cancer-2024 Update. Part I: Screening, Diagnosis, and Local Treatment with Curative Intent. Eur Urol 86:148–163

19. Cytawa W, Seitz AK, Kircher S, Fukushima K, Tran-Gia J, Schirbel A, Bandurski T, Lass P, Krebs M, Połom W, Matuszewski M, Wester H-J, Buck AK, Kübler H, Lapa C (2020) ^{68}Ga-PSMA I&T PET/CT for primary staging of prostate cancer. Eur J Nucl Med Mol Imaging 47:168–177

20. De Feo MS, Pontico M, Frantellizzi V, Corica F, De Cristofaro F, De Vincentis G (2022) ^{89}Zr-PET imaging in humans: a systematic review. Clin Transl Imaging 10:23–36

21. Delker A, Fendler WP, Kratochwil C, Brunegraf A, Gosewisch A, Gildehaus FJ, Tritschler S, Stief CG, Kopka K, Haberkorn U, Bartenstein P, Böning G (2016) Dosimetry for ^{177}Lu-DKFZ-PSMA-617: a new radiopharmaceutical for the treatment of metastatic prostate cancer. Eur J Nucl Med Mol Imaging 43:42–51

22. Di Giorgio A, Siepe G, Serani F, Di Franco M, Malizia C, Castellucci P, Fanti S, Farolfi A (2025) Long-term outcomes of PSMA PET/CT-guided radiotherapy in biochemical failure patients post-radical prostatectomy: a 5-year follow-up analysis. Eur J Nucl Med Mol Imaging 52:3720–3729

23. Dietlein F, Kobe C, Vázquez SM, Fischer T, Endepols H, Hohberg M, Reifegerst M, Neumaier B, Schomäcker K, Drzezga AE, Dietlein M (2022) An ^{89}Zr-Labeled PSMA Tracer for PET/CT Imaging of Prostate Cancer Patients. J Nucl Med 63:573–583

24. Dragonetti V, Colandrea M, Travaini L, Airò Farulla LS, Ceci F, Mattana F (2025) PSMA-PET Guided Radiotherapy in Prostate Cancer: A Critical Review of Current Applications and Future Directions. Semin Radiat Oncol 35:317–324

25. Duclos V, Iep A, Gomez L, Goldfarb L, Besson FL (2021) PET Molecular Imaging: A Holistic Review of Current Practice and Emerging Perspectives for Diagnosis, Therapeutic Evaluation and Prognosis in Clinical Oncology. Int J Mol Sci 22:4159

26. Duvenhage J, Kahts M, Summers B, Zeevaart JR, Ebenhan T (2024) Highlighting New Research Trends on Zirconium-89 Radiopharmaceuticals Beyond Antibodies. Semin Nucl Med 54:801–811

27. Farolfi A, Calderoni L, Mattana F, Mei R, Telo S, Fanti S, Castellucci P (2021) Current and Emerging Clinical Applications of PSMA PET Diagnostic Imaging for Prostate Cancer. J Nucl Med 62:596–604

28. Ferlay J, Colombet M, Soerjomataram I, Parkin DM, Piñeros M, Znaor A, Bray F (2021) Cancer statistics for the year 2020: An overview. Int J Cancer 149:778–789

29. Fossati N, Karnes RJ, Cozzarini C, Fiorino C, Gandaglia G, Joniau S, Boorjian SA, Goldner G, Hinkelbein W, Haustermans K, Tombal B, Shariat S, Karakiewicz PI, Montorsi F, Van Poppel H, Wiegel T, Briganti A (2016) Assessing the Optimal Timing for Early Salvage Radiation Therapy in Patients with Prostate-specific Antigen Rise After Radical Prostatectomy. Eur Urol 69:728–733

30. Ghosh A, Heston WDW (2004) Tumor target prostate specific membrane antigen (PSMA) and its regulation in prostate cancer. J Cell Biochem 91:528–539

31. Giesel FL, Hadaschik B, Cardinale J, Radtke J, Vinsensia M, Lehnert W, Kesch C, Tolstov Y, Singer S, Grabe N, Duensing S, Schäfer M, Neels OC, Mier W, Haberkorn U, Kopka K, Kratochwil C (2017) F-18 labelled PSMA-1007: biodistribution, radiation dosimetry and histopathological validation of tumor lesions in prostate cancer patients. Eur J Nucl Med Mol Imaging 44:678–688

32. Giesel FL, Knorr K, Spohn F, Will L, Maurer T, Flechsig P, Neels O, Schiller K, Amaral H, Weber WA, Haberkorn U, Schwaiger M, Kratochwil C, Choyke P, Kramer V, Kopka K, Eiber M (2019) Detection Efficacy of ^{18}F-PSMA-1007 PET/CT in 251 Patients with Biochemical Recurrence of Prostate Cancer After Radical Prostatectomy. J Nucl Med 60:362–368

33. Grünig H, Maurer A, Thali Y, Kovacs Z, Strobel K, Burger IA, Müller J (2021) Focal unspecific bone uptake on [^{18}F]-PSMA-1007 PET: a multicenter retrospective evaluation of the distribution, frequency, and quantitative parameters of a potential pitfall in prostate cancer imaging. Eur J Nucl Med Mol Imaging 48:4483–4494

34. Hennrich U, Wagner L, Taş H, Kovacs L, Benešová-Schäfer M (2025) Revolutionizing Prostate Cancer Detection: The Role of Approved PSMA-PET Imaging Agents. Pharmaceuticals 18:906

35. Hofman MS, Violet J, Hicks RJ, Ferdinandus J, Thang SP, Akhurst T, Iravani A, Kong G, Ravi Kumar A, Murphy DG, Eu P, Jackson P, Scalzo M, Williams SG, Sandhu S (2018) [^{177}Lu]-PSMA-617 radionuclide treatment in patients with metastatic castration-resistant prostate cancer (LuPSMA trial): a single-centre, single-arm, phase 2 study. Lancet Oncol 19:825–833

36. Hofman MS, Lawrentschuk N, Francis RJ, Tang C, Vela I, Thomas P, Rutherford N, Martin JM, Frydenberg M, Shakher R, Wong L-M, Taubman K, Ting Lee S, Hsiao E, Roach P, Nottage M, Kirkwood I, Hayne D, Link E, Marusic P, Matera A, Herschtal A, Iravani A, Hicks RJ, Williams S, Murphy DG, proPSMA Study Group Collaborators (2020) Prostate-specific membrane antigen PET-CT in patients with high-risk prostate cancer before curative-intent surgery or radiotherapy (proPSMA): a prospective, randomised, multicentre study. Lancet 395:1208–1216

37. Hölscher T, Baumann M, Kotzerke J, Zöphel K, Paulsen F, Müller A-C, Zips D, Thomas C, Wirth M, Troost EGC, Krause M, Löck S, Lohaus F (2022) Local Control after Locally Ablative, Image-Guided Radiotherapy of Oligometastases Identified by Gallium-68-PSMA-Positron Emission Tomography in Castration-Sensitive Prostate Cancer Patients (OLI-P). Cancers 14:2073

38. Horn T, Lischewski F, Gschwend JE (2024) Salvage-Lymphadenektomie beim Prostatakarzinom. Urol 63:234–240

39. Horoszewicz JS, Kawinski E, Murphy GP (1987) Monoclonal antibodies to a new antigenic marker in epithelial prostatic cells and serum of prostatic cancer patients. Anticancer Res 7:927–935

40. Jauw YWS, O'Donoghue JA, Zijlstra JM, Hoekstra OS, Menke-van der Houven van Oordt CW, Morschhauser F, Carrasquillo JA, Zweegman S, Pandit-Taskar N, Lammertsma AA, van Dongen GuusAMS, Boellaard R, Weber WA, Huisman MC (2019) ^{89}Zr-Immuno-PET: Toward a Noninvasive Clinical Tool to Measure Target Engagement of Therapeutic Antibodies In Vivo. J Nucl Med 60:1825–1832

41. Jung K-H, Park JW, Lee JH, Moon SH, Cho YS, Lee K-H (2021) ^{89}Zr-Labeled Anti-PD-L1 Antibody PET Monitors Gemcitabine Therapy-Induced Modulation of Tumor PD-L1 Expression. J Nucl Med 62:656–664

42. Khreish F, Ghazal Z, Marlowe RJ, Rosar F, Sabet A, Maus S, Linxweiler J, Bartholomä M, Ezziddin S (2022) ^{177}Lu-PSMA-617 radioligand therapy of metastatic castration-resistant prostate cancer: Initial 254-patient results from a prospective registry (REALITY Study). Eur J Nucl Med Mol Imaging 49:1075–1085

43. Kinoshita Y, Kuratsukuri K, Landas S, Imaida K, Rovito PM, Wang CY, Haas GP (2006) Expression of prostate-specific membrane antigen in normal and malignant human tissues. World J Surg 30:628–636

44. Kirienko M, Gelardi F, Fiz F, Bauckneht M, Ninatti G, Pini C, Briganti A, Falconi M, Oyen WJG, van der Graaf WTA, Sollini M (2024) Personalised PET imaging in oncology: an umbrella review of meta-analyses to guide the appropriate radiopharmaceutical choice and indication. Eur J Nucl Med Mol Imaging 52:208–224

45. Knipper S, Ascalone L, Ziegler B, Hohenhorst JL, Simon R, Berliner C, van Leeuwen FWB, van der Poel H, Giesel F, Graefen M, Eiber M, Heck MM, Horn T, Maurer T (2021) Salvage Surgery in Patients with Local Recurrence After Radical Prostatectomy. Eur Urol 79:537–544

46. Kratochwil C, Giesel FL, Stefanova M, Benešová M, Bronzel M, Afshar-Oromieh A, Mier W, Eder M, Kopka K, Haberkorn U (2016) PSMA-Targeted Radionuclide Therapy of Metastatic Castration-Resistant Prostate Cancer with ^{177}Lu-Labeled PSMA-617. J Nucl Med 57:1170–1176

47. Laforest R, Lapi SE, Oyama R, Bose R, Tabchy A, Marquez-Nostra BV, Burkemper J, Wright BD, Frye J, Frye S, Siegel BA, Dehdashti F (2016) [^{89}Zr]Trastuzumab: Evaluation of Radiation Dosimetry, Safety, and Optimal Imaging Parameters in Women with HER2-Positive Breast Cancer. Mol Imaging Biol 18:952–959

48. Liu H, Rajasekaran AK, Moy P, Xia Y, Kim S, Navarro V, Rahmati R, Bander NH (1998) Constitutive and antibody-induced internalization of prostate-specific membrane antigen. Cancer Res 58:4055–4060

49. Lyashchenko SK, Tran T, Happel S, Park H, Bauer D, Jones K, Esposito TV, Pillarsetty N, Lewis JS (2024) [^{89}Zr]ZrCl4 for direct radiolabeling of DOTA-based precursors. Nucl Med Biol 136–137:108943

50. Mazzone E, Thomson A, Chen DC, Cannoletta D, Quarta L, Pellegrino A, Gandaglia G, Moon D, Eapen R, Lawrentschuk N, Montorsi F, Siva S, Hofman MS, Chiti A, Briganti A, Perera ML, Murphy DG (2025) The Role of Prostate-specific Membrane Antigen Positron Emission Tomography for Assessment of Local Recurrence and Distant Metastases in Patients with Biochemical Recurrence of Prostate Cancer After Definitive Treatment: A Systematic Review and Meta-analysis. Eur Urol 88:129–141

51. Meijer D, Eppinga WSC, Mohede RM, Vanneste BGL, Meijnen P, Meijer OWM, Daniels LA, van den Bergh RCN, Lont AP, Ettema RH, Oudshoorn FHK, van Leeuwen PJ, van der Poel HG, Donswijk ML, Oprea-Lager DE, Schaake EE, Vis AN (2022) Prostate-specific Membrane Antigen Positron Emission Tomography/Computed Tomography Is Associated with Improved Oncological Outcome in Men Treated with Salvage Radiation Therapy for Biochemically Recurrent Prostate Cancer. Eur Urol Oncol 5:146–152

52. Mena E, Lindenberg ML, Turkbey IB, Shih JH, Harmon SA, Lim I, Lin F, Adler S, Eclarinal P, McKinney YL, Citrin D, Dahut W, Wood BJ, Krishnasamy V, Chang R, Levy E, Merino M, Pinto P, Eary JF, Choyke PL (2020) ^{18}F-DCFPyL PET/CT Imaging in Patients with Biochemically Recurrent Prostate Cancer After Primary Local Therapy. J Nucl Med 61:881–889

53. Mohan R, Kneebone A, Eade T, Hsiao E, Emmett L, Brown C, Hunter J, Hruby G (2023) Long-term outcomes of SBRT for PSMA PET detected oligometastatic prostate cancer. Radiat Oncol 18:127

54. Morawitz J, Kirchner J, Lakes J, Bruckmann NM, Mamlins E, Hiester A, Aissa J, Loberg C, Schimmöller L, Arsov C, Antke C, Albers P, Antoch G, Sawicki LM (2021) PSMA PET/CT vs. CT alone in newly diagnosed biochemical recurrence of prostate cancer after radical prostatectomy: Comparison of detection rates and therapeutic implications. Eur J Radiol 136:109556

55. Nikitas J, Rieger AC, Farolfi A, Seyedroudbari A, Kishan AU, Nickols NG, Steinberg ML, Valle LF, Rettig M, Czernin J, Calais J (2024) Prostate-Specific Membrane Antigen PET/CT–Guided, Metastasis-Directed Radiotherapy for Oligometastatic Castration-Resistant Prostate Cancer. J Nucl Med 65:1387–1394

56. O'Keefe DS, Bacich DJ, Huang SS, Heston WDW (2018) A Perspective on the Evolving Story of PSMA Biology, PSMA-Based Imaging, and Endoradiotherapeutic Strategies. J Nucl

Med 59:1007–1013

57. Pandit-Taskar N, O'Donoghue JA, Ruan S, Lyashchenko SK, Carrasquillo JA, Heller G, Martinez DF, Cheal SM, Lewis JS, Fleisher M, Keppler JS, Reiter RE, Wu AM, Weber WA, Scher HI, Larson SM, Morris MJ (2016) First-in-Human Imaging with ^{89}Zr-Df-IAB2M Anti-PSMA Minibody in Patients with Metastatic Prostate Cancer: Pharmacokinetics, Biodistribution, Dosimetry, and Lesion Uptake. J Nucl Med 57:1858–1864

58. Pandya DN, Bhatt N, Yuan H, Day CS, Ehrmann BM, Wright M, Bierbach U, Wadas TJ (2017) Zirconium tetraazamacrocycle complexes display extraordinary stability and provide a new strategy for zirconium-89-based radiopharmaceutical development. Chem Sci 8:2309–2314

59. Pozdnyakov A, Kulanthaivelu R, Bauman G, Ortega C, Veit-Haibach P, Metser U (2023) The impact of PSMA PET on the treatment and outcomes of men with biochemical recurrence of prostate cancer: a systematic review and meta-analysis. Prostate Cancer Prostatic Dis 26:240–248

60. Privé BM, Derks YHW, Rosar F, Franssen GM, Peters SMB, Khreish F, Bartholomä M, Maus S, Gotthardt M, Laverman P, Konijnenberg MW, Ezziddin S, Nagarajah J, Heskamp S (2022) ^{89}Zr-labeled PSMA ligands for pharmacokinetic PET imaging and dosimetry of PSMA-617 and PSMA-I&T: a preclinical evaluation and first in man. Eur J Nucl Med Mol Imaging 49:2064–2076

61. Rauscher I, Düwel C, Haller B, Rischpler C, Heck MM, Gschwend JE, Schwaiger M, Maurer T, Eiber M (2018) Efficacy, Predictive Factors, and Prediction Nomograms for ^{68}Ga-labeled Prostate-specific Membrane Antigen-ligand Positron-emission Tomography/Computed Tomography in Early Biochemical Recurrent Prostate Cancer After Radical Prostatectomy. Eur Urol 73:656–661

62. Rosar F, Schaefer-Schuler A, Bartholomä M, Maus S, Petto S, Burgard C, Privé BM, Franssen GM, Derks YHW, Nagarajah J, Khreish F, Ezziddin S (2022) [^{89}Zr]Zr-PSMA-617 PET/CT in biochemical recurrence of prostate cancer: first clinical experience from a pilot study including biodistribution and dose estimates. Eur J Nucl Med Mol Imaging 49:4736–4747

63. Rosar F, Khreish F, Marlowe RJ, Schaefer-Schuler A, Burgard C, Maus S, Petto S, Bartholomä M, Ezziddin S (2023) Detection efficacy of [^{89}Zr]Zr-PSMA-617 PET/CT in [^{68}Ga]Ga-PSMA-11 PET/CT-negative biochemical recurrence of prostate cancer. Eur J Nucl Med Mol Imaging 50:2899–2909

64. Rosar F, Burgard C, Larsen E, Khreish F, Marlowe RJ, Schaefer-Schuler A, Maus S, Petto S, Bartholomä M, Ezziddin S (2024) [^{89}Zr]Zr-PSMA-617 PET/CT characterization of indeterminate [^{68}Ga]Ga-PSMA-11 PET/CT findings in patients with biochemical recurrence of prostate cancer: lesion-based analysis. Cancer Imaging 24:27

65. Sartor O, de Bono J, Chi KN, Fizazi K, Herrmann K, Rahbar K, Tagawa ST, Nordquist LT, Vaishampayan N, El-Haddad G, Park CH, Beer TM, Armour A, Pérez-Contreras WJ, DeSilvio M, Kpamegan E, Gericke G, Messmann RA, Morris MJ, Krause BJ, VISION Investigators (2021) Lutetium-177-PSMA-617 for Metastatic Castration-Resistant Prostate Cancer. N Engl J Med 385:1091–1103

66. Schmidt-Hegemann N-S, Stief C, Kim T-H, Eze C, Kirste S, Strouthos I, Li M, Schultze-Seemann W, Ilhan H, Fendler WP, Bartenstein P, Grosu A-L, Ganswindt U, Belka C, Meyer PT, Zamboglou C (2019) Outcome After PSMA PET/CT–Based Salvage Radiotherapy in Patients with Biochemical Recurrence After Radical Prostatectomy: A 2-Institution Retrospective Analysis. J Nucl Med 60:227–233

67. Schwenck J, Sonanini D, Cotton JM, Rammensee H-G, la Fougère C, Zender L, Pichler BJ (2023) Advances in PET imaging of cancer. Nat Rev Cancer 23:474–490

68. Seifert R, Telli T, Opitz M, Barbato F, Berliner C, Nader M, Umutlu L, Stuschke M, Hadaschik B, Herrmann K, Fendler WP (2023) Unspecific ^{18}F-PSMA-1007 Bone Uptake Evaluated Through PSMA-11 PET, Bone Scanning, and MRI Triple Validation in Patients with Biochemical Recurrence of Prostate Cancer. J Nucl Med 64:738–743

69. Shore ND, Moul JW, Pienta KJ, Czernin J, King MT, Freedland SJ (2024) Biochemical recurrence in patients with prostate cancer after primary definitive therapy: treatment based on risk stratification. Prostate Cancer Prostatic Dis 27:192–201

70. Silver DA, Pellicer I, Fair WR, Heston WD, Cordon-Cardo C (1997) Prostate-specific membrane antigen expression in normal and malignant human tissues. Clin Cancer Res 3:81–85

71. Solomonidou N, Germanou D, Strouthos I, Karagiannis E, Farolfi A, Koerber SA, Debus J, Peeken JC, Vogel ME, Vrachimis A, Spohn SKB, Shelan M, Aebersold D, Grosu A-L, Ceci F, Kroeze SGC, Guckenberger M, Fanti S, Belka C, Hruby G, Scharl S, Wiegel T, Bartenstein P, Henkenberens C, Emmett L, Schmidt-Hegemann NS, Ferentinos K, Zamboglou C (2023) PSMA-PET/CT-guided salvage radiotherapy in recurrent or persistent prostate cancer and PSA < 0.2 ng/ml. Eur J Nucl Med Mol Imaging 50:2529–2536

72. Tendulkar RD, Agrawal S, Gao T, Efstathiou JA, Pisansky TM, Michalski JM, Koontz BF, Hamstra DA, Feng FY, Liauw SL, Abramowitz MC, Pollack A, Anscher MS, Moghanaki D, Den RB, Stephans KL, Zietman AL, Lee WR, Kattan MW, Stephenson AJ (2016) Contemporary Update of a Multi-Institutional Predictive Nomogram for Salvage Radiotherapy After Radical Prostatectomy. J Clin Oncol 34:3648–3654

73. Tilki D, van den Bergh RCN, Briers E, Van den Broeck T, Brunckhorst O, Darraugh J, Eberli D, De Meerleer G, De Santis M, Farolfi A, Gandaglia G, Gillessen S, Grivas N, Henry AM, Lardas M, J.L.H. van Leenders G, Liew M, Linares Espinos E, Oldenburg J, van Oort IM, Oprea-Lager DE, Ploussard G, Roberts MJ, Rouvière O, Schoots IG, Schouten N, Smith EJ, Stranne J, Wiegel T, Willemse P-PM, Cornford P (2024) EAU-EANM-ESTRO-ESUR-ISUP-SIOG Guidelines on Prostate Cancer. Part II—2024 Update: Treatment of Relapsing and Metastatic Prostate Cancer. Eur Urol 86:164–182

74. Valle L, Shabsovich D, de Meerleer G, Maurer T, Murphy DG, Nickols NG, Vapiwala N, Calais J, Kishan AU (2021) Use and Impact of Positron Emission Tomography/Computed Tomography Prior to Salvage Radiation Therapy in Men with Biochemical Recurrence After Radical Prostatectomy: A Scoping Review. Eur Urol Oncol 4:339–355

75. Van den Broeck T, van den Bergh RCN, Arfi N, Gross T, Moris L, Briers E, Cumberbatch M, De Santis M, Tilki D, Fanti S, Fossati N, Gillessen S, Grummet JP, Henry AM, Lardas M, Liew M, Rouvière O, Pecanka J, Mason MD, Schoots IG, van Der Kwast TH, van Der Poel HG, Wiegel T, Willemse P-PM, Yuan Y, Lam TB, Cornford P, Mottet N (2019) Prognostic Value of Biochemical Recurrence Following Treatment with Curative Intent for Prostate Cancer: A Systematic Review. Eur Urol 75:967–987

76. van Dongen GAMS, Beaino W, Windhorst AD, Zwezerijnen GJC, Oprea-Lager DE, Hendrikse NH, van Kuijk C, Boellaard R, Huisman MC, Vugts DJ (2021) The Role of ^{89}Zr-Immuno-PET in Navigating and Derisking the Development of Biopharmaceuticals. J Nucl Med 62:438–445

77. Vogel MME, Dewes S, Sage EK, Devecka M, Gschwend JE, Eiber M, Combs SE,

Schiller K (2021) A survey among German-speaking radiation oncologists on PET-based radiotherapy of prostate cancer. Radiat Oncol 16:82

78. Weineisen M, Schottelius M, Simecek J, Baum RP, Yildiz A, Beykan S, Kulkarni HR, Lassmann M, Klette I, Eiber M, Schwaiger M, Wester H-J (2015) ^{68}Ga- and ^{177}Lu-Labeled PSMA I&T: Optimization of a PSMA-Targeted Theranostic Concept and First Proof-of-Concept Human Studies. J Nucl Med 56:1169–1176

79. Winter G, Vogt A, Jiménez-Franco LD, Rinscheid A, Yousefzadeh-Nowshahr E, Solbach C, Beer AJ, Glatting G, Kletting P (2019) Modelling the internalisation process of prostate cancer cells for PSMA-specific ligands. Nucl Med Biol 72–73:20–25

80. Wurzer AN Stephan G; D'Alessandria, Calogero, Nekolla SG, D'Alessandria C (2022) Stand der Technik in der Radiopharmazie. Angew Nukl 45:167–188

81. Yeh R, O'Donoghue JA, Jayaprakasam VS, Mauguen A, Min R, Park S, Brockway JP, Bromberg JF, Zhi WI, Robson ME, Sanford R, Modi S, Agnew BJ, Lyashchenko SK, Lewis JS, Ulaner GA, Zeglis BM (2024) First-in-Human Evaluation of Site-Specifically Labeled ^{89}Zr-Pertuzumab in Patients with HER2-Positive Breast Cancer. J Nucl Med 65:386–393

82. Yoon J-K, Park B-N, Ryu E-K, An Y-S, Lee S-J (2020) Current Perspectives on ^{89}Zr-PET Imaging. Int J Mol Sci 21:4309

83. Zamboglou C, Staus P, Wolkewitz M, Peeken JC, Ferentinos K, Strouthos I, Farolfi A, Koerber SA, Vrachimis A, Spohn SKB, Aebersold DM, Grosu A-L, Kroeze SGC, Fanti S, Hruby G, Wiegel T, Emmett L, Hayoz S, Ceci F, Guckenberger M, Belka C, Schmidt-Hegemann N-S, Ghadjar P, Shelan M (2025) Better Oncological Outcomes After Prostate-specific Membrane Antigen Positron Emission Tomography–guided Salvage Radiotherapy Following Prostatectomy. Eur Urol Focus 11:242–250

84. Zhang S, Wang X, Gao X, Chen X, Li L, Li G, Liu C, Miao Y, Wang R, Hu K (2025) Radiopharmaceuticals and their applications in medicine. Signal Transduct Target Ther 10:1

85. Zhang X, Ma Z (2024) Head-to-head comparison of PSMA PET/CT and mpMRI for detecting biochemical recurrence of prostate cancer: A systematic review and meta-analysis. Curr Urol 18:177–184

VIII. Appendix

8.1 Weitere Publikationen

Ergänzend zu den Originalarbeiten 1 – 3 sind im Rahmen dieser Arbeit folgende weitere Publikationen entstanden:

Originalarbeiten

Privé BM, Derks YHW, **Rosar F**, Franssen GM, Peters SMB, Khreish F, Bartholomä M, Maus S, Gotthardt M, Laverman P, Konijnenberg MW, Ezziddin S, Nagarajah J, Heskamp S (2022) ^{89}Zr-labeled PSMA ligands for pharmacokinetic PET imaging and dosimetry of PSMA-617 and PSMA-I&T: a preclinical evaluation and first in man. Eur J Nucl Med Mol Imaging 49:2064–2076

Burgard C, **Rosar F**, Larsen E, Khreish F, Linxweiler J, Marlowe RJ, Schaefer-Schuler A, Maus S, Petto S, Bartholomä M, Ezziddin S (2024) Outstanding increase in tumor-to-background ratio over time allows tumor localization by [^{89}Zr]Zr-PSMA-617 PET/CT in early biochemical recurrence of prostate cancer. Cancer Imaging 24:132

Fallberichte

Rosar F, Bartholomä M, Maus S, Privé BM, Khreish F, Franssen GM, Derks YHW, Nagarajah J, Ezziddin S (2022) ^{89}Zr-PSMA-617 PET/CT May Reveal Local Recurrence of Prostate Cancer Unidentified by ^{68}Ga-PSMA-11 PET/CT. Clin Nucl Med 47:435–436

Rosar F, Burgard C, Linxweiler J, Wagner M, Ezziddin S (2023) Histologically Confirmed Testicular Metastasis Revealed by [^{89}Zr]Zr-PSMA-617 PET/CT in a Patient with Biochemical Recurrence of Prostate Cancer and Negative Conventional PSMA PET/CT Imaging. Diagnostics 13:1352

Bastian MB, Burgard C, Blickle A, Speicher T, Ezziddin S, **Rosar F** (2024) [^{89}Zr]Zr-PSMA-617 PET/CT in a Patient with Biochemical Recurrence of Prostate Cancer and Prior Indetermined Findings on [^{18}F]PSMA-1007 Imaging. Diagnostics 14:2321

Bastian MB, Burgard C, Blickle A, Ezziddin S, **Rosar F** (2025) Diffuse Peritoneal Carcinomatosis of Prostate Cancer Unveiled by [^{89}Zr]Zr-PSMA-617 PET/CT. Clin Nucl Med 50:191–192

Kongressbeiträge

Dzierma Y, **Rosar F**, Schaefer-Schuler A, Auerbach H, Nüsken F, Schnellhardt S, Hecht M, Ezziddin S, Melchior P (2024). [^{89}Zr]Zr-PSMA-617 PET/CT in der strahlentherapeutischen Behandlung des Prostata-Karzinoms – erste klinische Erfahrungen. 30. Jahreskongress der DEGRO, Kassel, Deutschland, P05-10

Melchior P, **Rosar F**, Schaefer-Schuler A, Fleckenstein J, Palm J, Ezziddin S, Linxweiler J, Auerbach H, Hecht M, Dzierma Y (2024). Änderung der Behandlungs- und Zielvolumenkonzepte unter dem Einsatz einer [^{89}Zr]Zr-PSMA-617 PET-CT basierten Bestrahlungsplanung im Vergleich zum [^{68}Ga]Ga-PSMA-11 PET-CT beim rezidivierten Prostatakarzinom. 30. Jahreskongress der DEGRO, Kassel, Deutschland, VS11-6

8.2 Danksagung

An dieser Stelle möchte ich meinen Dank all jenen aussprechen, die mich auf meinem zurückliegenden Weg unterstützt und damit das Verfassen dieser Dissertation ermöglicht haben.

Mein besonderer Dank gilt Frau *Prof. Dr. Dr. Yvonne Dzierma* für die wissenschaftliche Betreuung dieser Arbeit. Ebenso danke ich Herrn *Prof. Dr. Samer Ezziddin* für seine fachliche Unterstützung und seine prägende Rolle als medizinischer Mentor, insbesondere im Bereich innovativer Radionuklide und Tracer.

Für die stets anregenden und konstruktiven Diskussionen danke ich Frau *Dr. Caroline Burgard* sowie Herrn *PD Dr. Fadi Khreish*. Ein weiterer besonderer Dank gilt Frau *Dr. Andrea Schaefer-Schuler* für ihre fachliche Begleitung und Durchführung der Dosimetrie sowie Herrn *Sven Petto, M.Sc.* für die tatkräftige Unterstützung in diesem Bereich. Herrn *Dipl.-Ing.-Chem. Stephan Maus*, Herrn *PD Dr. Mark Bartholomä* und Herrn *Dr. Tobias Stemler* danke ich für die Organisation und chemische Aufbereitung des Radionuklids sowie die Herstellung des [^{89}Zr]Zr-PSMA-617.

Für die erfolgreiche europäische Zusammenarbeit, die erst die klinische Translation der [^{89}Zr]Zr-PSMA-617 ermöglichte, danke ich den Wissenschaftlerinnen und Wissenschaftlern der Abteilung für Medizinische Bildgebung der Universität Nijmegen, insbesondere Herrn *Prof. Dr. James Nagaraja*h und Herrn *Dr. Bastiaan Privé*. Mein Dank gilt ebenso allen weiteren Koautorinnen und Koautoren sowie den Mitarbeiterinnen und Mitarbeitern der Klinik für Nuklearmedizin des Universitätsklinikums des Saarlandes.

Abschließend möchte ich meiner Familie und meinen Freunden für ihre unermüdliche Unterstützung, ihren stetigen Zuspruch und ihr entgegengebrachtes Verständnis danken. Mein innigster Dank gilt meiner Frau *Mona*, der ich diese Arbeit von Herzen widme. Ohne ihren Rückhalt wäre es mir nicht möglich gewesen diese Arbeit zu verwirklichen.

8.3 Lebenslauf

Aus datenschutzrechtlichen Gründen wird der Lebenslauf in der elektronischen Fassung der Dissertation nicht veröffentlicht.

IX. Originalarbeiten

9.1 Originalarbeit 1

Rosar F, Schaefer-Schuler A, Bartholomä M, Maus S, Petto S, Burgard C, Privé BM, Franssen GM, Derks YHW, Nagarajah J, Khreish F, Ezziddin S (2022) [^{89}Zr]Zr-PSMA-617 PET/CT in biochemical recurrence of prostate cancer: first clinical experience from a pilot study including biodistribution and dose estimates. Eur J Nucl Med Mol Imaging 49:4736–4747

European Journal of Nuclear Medicine and Molecular Imaging (2022) 49:4736–4747
https://doi.org/10.1007/s00259-022-05925-3

ORIGINAL ARTICLE

[^{89}Zr]Zr-PSMA-617 PET/CT in biochemical recurrence of prostate cancer: first clinical experience from a pilot study including biodistribution and dose estimates

Florian Rosar[1] · Andrea Schaefer-Schuler[1] · Mark Bartholomä[1] · Stephan Maus[1] · Sven Petto[1] · Caroline Burgard[1] · Bastiaan M. Privé[2] · Gerben M. Franssen[2] · Yvonne H. W. Derks[2] · James Nagarajah[2] · Fadi Khreish[1] · Samer Ezziddin[1]

Received: 11 April 2022 / Accepted: 22 July 2022 / Published online: 5 August 2022

Abstract

Purpose Prostate-specific membrane antigen (PSMA)-targeted PET/CT has become increasingly important in the management of prostate cancer, especially in localization of biochemical recurrence (BCR). PSMA-targeted PET/CT imaging with long-lived radionuclides as ^{89}Zr ($T_{1/2} = 78.4$ h) may improve diagnostics by allowing data acquisition on later time points. In this study, we present our first clinical experience including preliminary biodistribution and dosimetry data of [^{89}Zr]Zr-PSMA-617 PET/CT in patients with BCR of prostate cancer.

Methods Seven patients with BCR of prostate cancer who revealed no ($n = 4$) or undetermined ($n = 3$) findings on [^{68}Ga]Ga-PSMA-11 PET/CT imaging were referred to [^{89}Zr]Zr-PSMA-617 PET/CT. PET/CT imaging was performed 1 h, 24 h, 48 h, and 72 h post injection (p.i.) of 111 ± 11 MBq [^{89}Zr]Zr-PSMA-617 (mean ± standard deviation). Normal organ distribution and dosimetry were determined. Lesions visually considered as suggestive of prostate cancer were quantitatively analyzed.

Results Intense physiological uptake was observed in the salivary and lacrimal glands, liver, spleen, kidneys, intestine and urinary tract. The parotid gland received the highest absorbed dose (0.601 ± 0.185 mGy/MBq), followed by the kidneys (0.517 ± 0.125 mGy/MBq). The estimated overall effective dose for the administration of 111 MBq was 10.1 mSv (0.0913 ± 0.0118 mSv/MBq). In 6 patients, and in particular in 3 of 4 patients with negative [^{68}Ga]Ga-PSMA-11 PET/CT, at least one prostate cancer lesion was detected in [^{89}Zr]Zr-PSMA-617 PET/CT imaging at later time points. The majority of tumor lesions were first visible at 24 h p.i. with continuously increasing tumor-to-background ratio over time. All tumor lesions were detectable at 48 h and 72 h p.i.

Conclusion [^{89}Zr]Zr-PSMA-617 PET/CT imaging is a promising new diagnostic tool with acceptable radiation exposure for patients with prostate cancer especially when [^{68}Ga]Ga-PSMA-11 PET/CT imaging fails detecting recurrent disease. The long half-life of ^{89}Zr enables late time point imaging (up to 72 h in our study) with increased tracer uptake in tumor lesions and higher tumor-to-background ratios allowing identification of lesions non-visible on [^{68}Ga]Ga-PSMA-11 PET/CT imaging.

Keywords Prostate cancer · PSMA · PET/CT · Zirconium-89 · Biochemical recurrence

Introduction

Over the past decade, prostate-specific membrane antigen (PSMA)-targeted positron emission tomography (PET)/computed tomography (CT) has revolutionized imaging of patients with prostate cancer [1]. PSMA is a transmembrane glycoprotein, which is overexpressed on the cell surface of prostate carcinoma cells [2], providing an ideal and specific target for imaging and therapy [3, 4]. PSMA-targeted PET/CT has become increasingly important in the management of prostate cancer for initial staging, localization of biochemical

This article is part of the Topical Collection on Oncology - Genitourinary

✉ Samer Ezziddin
samer.ezziddin@uks.eu

[1] Department of Nuclear Medicine, Saarland University – Medical Center, Kirrberger Str. 100, Geb. 50, 66421 Homburg, Germany

[2] Department of Medical Imaging, Nuclear Medicine, Radboud University Medical Center, Nijmegen, The Netherlands

recurrence, and screening or monitoring of PSMA-targeted radioligand therapy [5–8]. In recent years, various PSMA-ligands have been developed, of which ^{68}Ga-labeled PSMA-11 and ^{18}F-labeled DCFPyL or PSMA-1007 have become widely used for PET/CT imaging in clinical practice, and ^{177}Lu-labeled PSMA-617 for radioligand therapy [9, 10].

[^{68}Ga]Ga-PSMA-11 has shown a high sensitivity for tumor localization in the setting of biochemical recurrence (BCR) of prostate cancer in various recent prospective studies; however, there remains a non-negligible number of patients with BCR and negative [^{68}Ga]Ga-PSMA-11 PET/CT, particularly in patients with low PSA levels [11–14]. Due to its short half-life of 68 min, ^{68}Ga does not allow late image acquisition (e.g., on the next day after injection); therefore, imaging is usually performed 1 h after injection [15]. Similar applies to ^{18}F-labeled PSMA-ligands with ^{18}F offering a moderately longer half-life of 110 min. However, [^{18}F]F-PSMA-1007 offers a possible advantage for the detection of local recurrences due to a lower urinary excretion [16]. But also for [^{18}F]F-PSMA-1007, a certain number of patients with BCR and negative PSMA PET/CT have been observed [17].

PET/CT imaging with PSMA ligands labeled with long-lived radionuclides may increase sensitivity of PSMA PET/CT by allowing longer clearance from non-target organs and therefore resulting in increased target-to-background ratios. In addition, late acquisitions could also increase specificity by confirming or negating undetermined findings by observing uptake over time. In this context, the use of ^{89}Zr may be of interest [18]. ^{89}Zr is a positron emitter (branching fraction 23%) with a half-life of $T_{1/2} = 78.4$ h and a mean positron energy of 0.395 MeV, which is frequently used for antibody imaging [19–21]. Due to chemical reasons, ^{89}Zr cannot be complexed by PSMA-11, but binds to the commonly used bifunctional chelators DOTA and DOTAGA, thus allowing the radiolabeling of PSMA-617 and PSMA I&T [22, 23]. Recently, we described the preclinical characterization of [^{89}Zr]Zr-PSMA-617 and [^{89}Zr]Zr-PSMA I&T including biodistribution studies in tumor bearing mice [23]. Here, we present our first clinical experience including biodistribution and preliminary dosimetry estimates of [^{89}Zr]Zr-PSMA-617 PET/CT in patients with BCR of prostate cancer.

Methods

Patients and ethics

[^{89}Zr]Zr-PSMA-617 PET/CT imaging was performed in $n = 7$ consecutive patients due to BCR of prostate cancer who revealed no or undetermined findings on [^{68}Ga]Ga-PSMA-11 PET/CT. In 4 patients, [^{68}Ga]Ga-PSMA-11 did not reveal suspicious findings (negative [^{68}Ga]Ga-PSMA-11 PET/CT). Three patients had undetermined findings on [^{68}Ga]Ga-PSMA-11 PET/CT with no definite assignment to pathological or physiological uptake, e.g., faintly accumulating or unusually located tracer uptake. The time interval between both, [^{89}Zr]Zr-PSMA-617 and [^{68}Ga]Ga-PSMA-11 PET/CT, was 31 ± 18 days (range 5–49 days), with no treatment performed in between. Prostate-specific antigen (PSA) serum level at time of imaging ranged from 0.43 to 1.92 ng/ml. All patients were initially treated with radical prostatectomy (RP). Initial Gleason score ranged from 7a to 9. Four patients underwent salvage treatments such as androgen-deprivation therapy (ADT), lymphadenectomy (LA) or radiation therapy (RT). Detailed patient characteristics including age, Gleason score, primary therapy, salvage therapies, time from initial diagnosis (ID) of prostate cancer, PSA and PSA doubling time (DT) are presented in Table 1. [^{89}Zr]Zr-PSMA-617 PET/CT imaging was performed on a compassionate use basis under the German Pharmaceutical Act §13 (2b). The medical indication for the examination and the labeling of the tracer were under the direct responsibility of the applying physician. Patients gave their written consent after being thoroughly informed about the general risks of both radiation exposure and application of a novel PET tracer including possible adverse effects of, e.g., therapeutic PSMA tracers. Furthermore, all patients agreed to the publication of the resulting data in accordance with the Declaration of Helsinki.

Synthesis and quality control

The radiolabeling of PSMA-617 with ^{89}Zr was based on our previously published procedure with further optimizations [23]. Briefly, [^{89}Zr]Zr-oxalate (PerkinElmer, Groningen, The Netherlands) was transformed into [^{89}Zr]$ZrCl_4$ using a QMA cartridge (Waters, Milford, USA), which was activated by each 10 mL of acetonitrile, saline, 1 M hydrochloric acid, and deionized water. [^{89}Zr]Zr-oxalate was then loaded onto the cartridge followed by a washing step with 60 mL of deionized water. The activity was recovered from the QMA cartridge by fractionated elution with two fractions of 700 µL and 800 µL of 0.1 M hydrochloric acid. The latter fraction contained ~ 95% of the initial activity and was used for radiolabeling. To this fraction, 1.5 µg (1.44 nmol) of PSMA-617 per MBq [^{89}Zr]$ZrCl_4$ in 50 µL water were added followed by the addition of 800 µL MES buffer (0.5 M, pH 5.5). The reaction mixture was then heated at 95 °C for 30 min. After cooling to room temperature, the mixture was loaded onto a C_{18} Sep Pak cartridge (Waters, Milford, USA), which was pre-equilibrated with each 10 mL of ethanol and water for injection. The cartridge was washed with 5 mL of water for injection and the activity eluted with 2 mL 50% ethanol (v/v) and 8 mL of saline. The product was finally passed through a 0.22-µm filter for sterilization. This procedure is reliable for up to 800 MBq of initial ^{89}Zr

Table 1 Patient characteristics

Pt. no	Age (years)	Gleason score	Primary therapy	Salvage therapies	Current setting	Time from ID (years)	PSA (ng/ml)	PSA DT (months)	Findings on [^{68}Ga]Ga-PSMA-11 PET/CT	Findings on [^{89}Zr]Zr-PSMA-617 PET/CT
1	66	7a	RP	-	BCR	4	1.92	6	No suspicious findings	Local recurrence
2	64	8	RP	ADT, LA, RT	BCR	3	1.75	> 12	1 × LNM + undetermined finding (suspicion of right iliac LNM)	3 × LNM (no right iliac LNM)
3	69	7b	RP	ADT, RT	BCR	10	0.66	9	No suspicious findings	No suspicious findings
4	74	7b	RP	LA, RT	BCR	8	1.77	4	Undetermined finding (suspicion of peritoneal metastasis)	Peritoneal metastasis + 4 × LNM
5	70	8	RP	ADT, RT	BCR	4	0.63	4	No suspicious findings	1 × LNM
6	72	8	RP	-	BCR	19	0.43	> 12	Undetermined finding (suspicion of local recurrence in seminal vesicle bed)	Local recurrence (in seminal vesicle bed)
7	67	9	RP	-	BCR	1	0.68	> 12	No suspicious findings	Local recurrence + 2 × LNM

ADT, androgen-deprivation therapy; *BCR*, biochemical recurrence; *DT*, doubling time; *ID*, initial diagnosis of prostate cancer; *LA*, lymphadenectomy; *LNM*, lymph node metastasis; *PSA*, prostate-specific antigen; *RP*, radical prostatectomy; *RT*, radiation therapy

activity providing the final product [^{89}Zr]Zr-PSMA-617 in radiochemical yields of 70 ± 5% and radiochemical purities of > 98%. Quality control of the final product was performed according to current Good Manufacturing Practice (cGMP) guidelines checking for pH, clarity and color, radiochemical purity (HPLC and iTLC), chemical purity (HPLC), radionuclidic purity, endotoxin content, and sterility.

PET/CT imaging

Each patient underwent PET/CT imaging scans at 4 time points: 1 h, 24 h, 48 h, and 72 h post intravenous injection (p.i.) of 111 ± 11 MBq (mean ± standard deviation, range 97–129 MBq) [^{89}Zr]Zr-PSMA-617. All PET/CT imaging was performed on a Biograph mCT 40 scanner (Siemens Medical Solutions, Knoxville, TN, USA) comprising whole-body PET/CT scans extending from vertex to mid-femur in 3D mode. PET acquisition time duration was 4 min per bed position on the initial day of injection and extended up to 10 min on the last day. CT data were acquired in low-dose technique using an X-ray tube voltage of 120 keV and a modulation of the tube current (CARE Dose4D, Siemens Erlangen; maximal tube current 30 mA) followed by reconstruction with a soft tissue reconstruction kernel (B31f) to a slice thickness of 5 mm (increment 2–4 mm). PET emission data was corrected for decay, randoms, and scatter. PET image reconstruction was performed applying an iterative 3-dimensional ordered-subset expectation maximization (OSEM) algorithm (3 iterations; 24 subsets) with gaussian filtering to a transaxial resolution of 5 mm at full width half maximum (FWHM). The matrix and the pixel size were 200 × 200 and 3.0 mm, respectively. Attenuation correction was performed using the low-dose CT data.

Adverse events

Any adverse event was recorded during and after examination. Vital parameters as heart rate, blood pressure, body temperature, and oxygen saturation were closely monitored. Within a time interval of 4 weeks after [^{89}Zr]Zr-PSMA-617 PET/CT, patients were additionally interviewed about potential side effects.

Biodistribution and tumor uptake

The biodistribution of [^{89}Zr]Zr-PSMA-617 was quantified by analyzing the standard uptake values (SUV) SUV_{max}, SUV_{peak} and SUV_{mean} at 1 h, 24 h, 48 h, and 72 h p.i.. Considering normal-organs, elliptical volumes of interest (VOI) were manually drawn enclosing regions of relatively homogenous uptake. Activity estimation was performed within the VOI applying a 40% or, in case of faintly accumulating organs, a 20% threshold using the SyngoVia software

(Enterprise VB 60, Siemens, Erlangen, Germany). The following organs were included in this evaluation: the brain, salivary, and lacrimal glands, nasal mucosa, lung, liver, spleen, small and large intestine, and the kidneys. With regard to the large intestine, SUV was determined at the descending colon. Blood pool and background were evaluated in the descending aorta and the gluteal muscle, respectively. Tissue-to-background ratios (TiBR) were calculated by dividing the SUV_{max} of the organs by the SUV_{mean} of the background (gluteal muscle).

Three physicians with long-time experience in PSMA-targeted PET/CT (S.E., F.K., and F.R.) visually identified suspicious lesions taking into account all four imaging time points (1 h, 24 h, 48 h, and 72 h p.i.). Lesions that were visually considered as suggestive for prostate cancer were analyzed by measuring SUV_{max} and by calculating tumor-to-background ratios (TBR), defined as SUV_{max} divided by $SUV_{mean,}$ of the background (gluteal muscle).

Radiation dosimetry

Mean absorbed radiation doses were estimated using the QDOSE program package (ABX-CRO, Dresden, Germany) considering the following organs as source organs: kidneys, liver, spleen, salivary glands (parotid gland and submandibular gland), and lacrimal gland. As a first step, volumetric co-registration of the different time points was performed by taking the first CT scan as reference. PET images, which were coupled to the CT images of the respective imaging session, were transformed according to the CT transformation matrix. Boundary VOIs which solely enclosed the source organs without interfering with the activity concentration of neighboring structures were manually drawn in the PET image that allowed the best organ delineation and then copied onto all other time-point scans. Manual adjustment of the boundary VOI for each time point was done when necessary, using the respective CT. Volume and activity estimation were performed within the boundary applying a fuzzy locally adaptive Bayesian (FLAB) segmentation algorithm for automatic volume delineation [24]. The next step comprised mono-exponential regression of the serial measured activities using weighted least squares method and estimation of both, the time integrated activities (TIA) and the time-integrated activity coefficients (TIAC) in the source regions. As an approximation, a linear increase from $t=0$ to the first acquisition time point was assumed, and the integration method for the first time interval was based on the trapezoidal method. Between the first and the last time point, a trapezoidal integration was used, whereas the TIA from the last time-point to infinity was calculated analytically by applying the mono-exponential fitting curve. The respective TIACs (often termed residence time) of the source organs were calculated by normalizing the TIA to the amount of activity administered. The total body TIA was calculated approximately using the total FOV volume of interest and the injected activity. As a further approximation, constant activity between $t=0$ and the first acquisition time point was assumed, and the integration method for the first-time interval was based on the trapezoidal method. Between the first time point and infinity, the TIA was calculated analytically by using the mono-exponential fitting curve. Estimations of absorbed organ dose and effective dose were performed by the IDAC 2.1 software which is implemented in QDOSE [25–27]. The IDAC reference man was applied for the kidneys, the spleen, the liver, the heart and the intestine, and the sphere model for the salivary and lacrimal glands. Patient-specific organ mass adjustment, which is available in QDOSE, was applied for the kidneys, the liver and the spleen. Respective organ masses were determined using the volume of each organ delineated from the CT images (PACS software, SECTRA, Linköping, Sweden) and the respective biological tissue density. Organ masses for the salivary glands were taken from International Commission on Radiological Protection (ICRP) publication 89 with 25 g estimated weight for the parotid and 12.5 g for the submandibular gland [28].

Results

Adverse events

The examination with [^{89}Zr]Zr-PSMA-617 was not associated with any side effects in all 7 patients. No acute adverse events or other drug-related pharmacologic effects occurred. Monitored vital parameters remained unchanged. No patient complained of any subjective symptoms during examination and follow-up.

Biodistribution

Intense physiological uptake was observed in the salivary and lacrimal glands, liver, spleen, kidneys, intestine, and urinary tract. Figure 1 demonstrates a representative example of [^{89}Zr]Zr-PSMA-617 PET/CT at the predefined time points 1 h, 24 h, 48 h, and 72 h p.i., including the respective biodistribution data of selected organs assessed by SUV kinetics.

Detailed descriptive statistics of tracer distribution of all patients, including SUV_{max}, SUV_{peak}, SUV_{mean} and TiBR (tissue-to-background-ratio) of various organs, are presented in Fig. 2. The highest average SUV_{max} at 1 h p.i. was observed for the kidneys with 21.15 ± 12.31, consequently decreasing to 7.43 ± 1.56 at 72 h p.i.. For salivary glands and lacrimal glands, the maximum SUV_{max} was at 24 h p.i., with the highest value for submandibular gland (17.30 ± 4.69 at 24 h p.i., decreasing to 6.29 ± 1.61 at 72 h p.i.). Only colonic

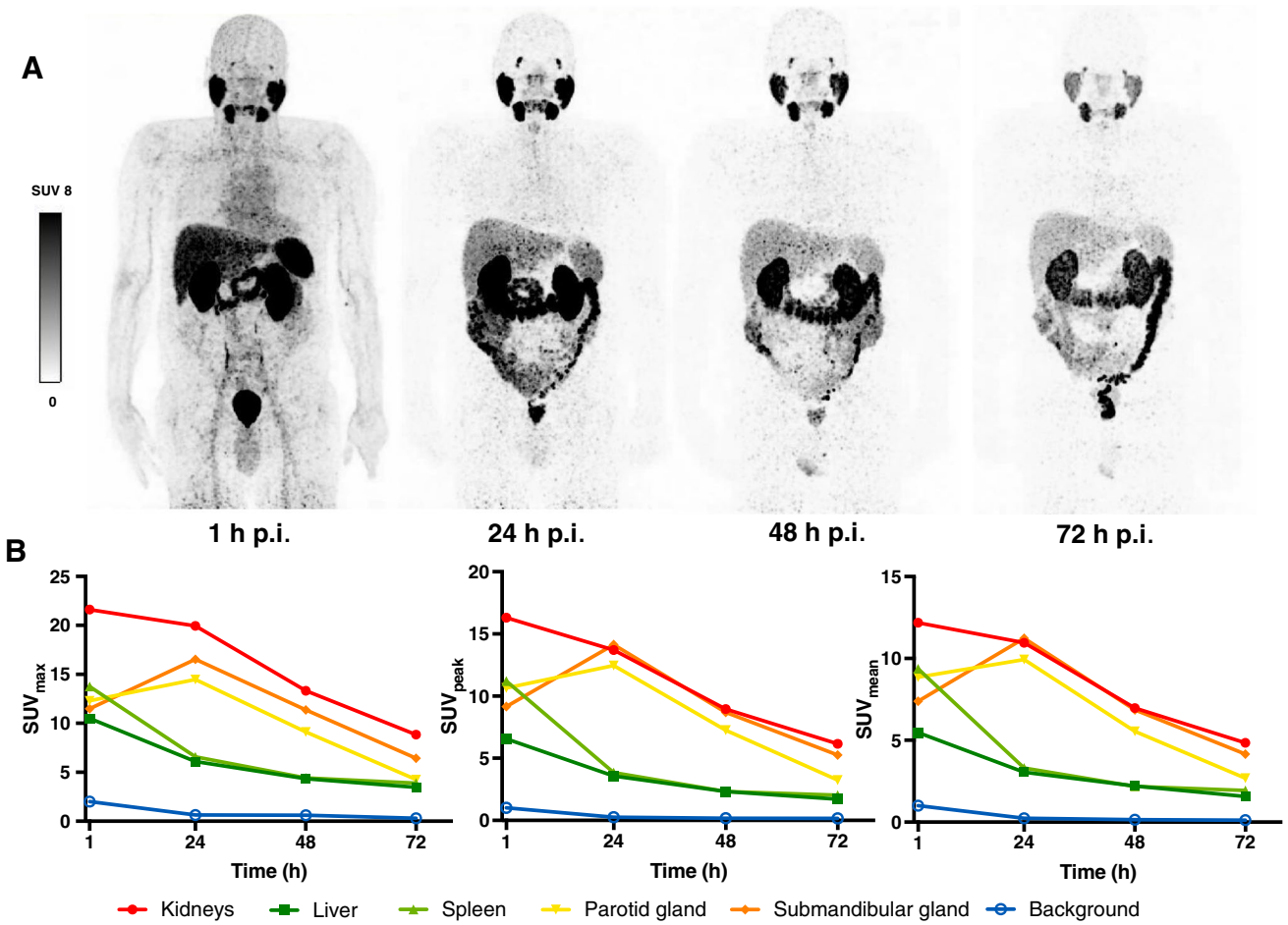

Fig. 1 Representative example (patient no. 2) **A** Maximum intensity projections at 4 time points post injection (p.i.) of [^{89}Zr]Zr-PSMA-617, **B** Respective SUV_{max}, SUV_{peak} and SUV_{mean} kinetics in normal organs (kidneys, liver, spleen, parotid gland, submandibular gland) and background (gluteal muscle)

tracer uptake increased continuously (from 3.50 ± 2.21 at 1 h p.i. to 13.57 ± 5.00 at 72 h p.i.). TiBR increased between 1 and 72 h p.i. for the salivary glands, nasal mucosa, liver, colon, and kidneys. The highest TiBR values (≥ 50) were observed in salivary glands, kidneys, and colon at 72 h p.i.

Radiation dosimetry

The monoexponential curve-fitting parameters, the time-integrated activity coefficients (TIAC) for each source organ, and the respective estimated absorbed doses according to IDAC 2.1 are summarized in Table 2. Among the normal tissues, the parotid gland received the highest absorbed dose of [^{89}Zr]Zr-PSMA-617 with 0.601 ± 0.185 mGy/MBq followed by the kidneys with 0.517 ± 0.125 mGy/MBq and the submandibular gland with 0.468 ± 0.136 mGy/MBq. These values resulted in an average effective dose of 0.0913 ± 0.0118 mSv/MBq. Thus, administration of 111 MBq of [^{89}Zr]Zr-PSMA-617 (mean injected activity) induced a total effective dose of 10.1 mSv.

Clinical findings and tumor uptake

Among 7 patients with either negative (4 patients) or with undetermined findings on [^{68}Ga]Ga-PSMA-11 PET/CT (3 patients), at least one lesion (range 1–5 per patient, in total $n = 14$) that was suggestive for prostate cancer was detected in 6 patients with [^{89}Zr]Zr-PSMA-617 (Table 1). Out of all identified lesions ($n = 14$), 10 were lymph node metastases (in 4 patients), 3 were local recurrence (in 3 patients), and 1 was peritoneal metastasis. The majority of tumor lesions ($n = 11$) were not visible on PET/CT imaging at 1 h p.i., but were delineated at later time points (9 of them first visible at 24 h p.i., and 2 at 48 h p.i.). All tumor lesions were detectable at 48 h p.i. and 72 h p.i.. No additional tumor lesions were found at 72 h p.i.. Three tumor lesions (in 3 patients), which were identified at 1 h

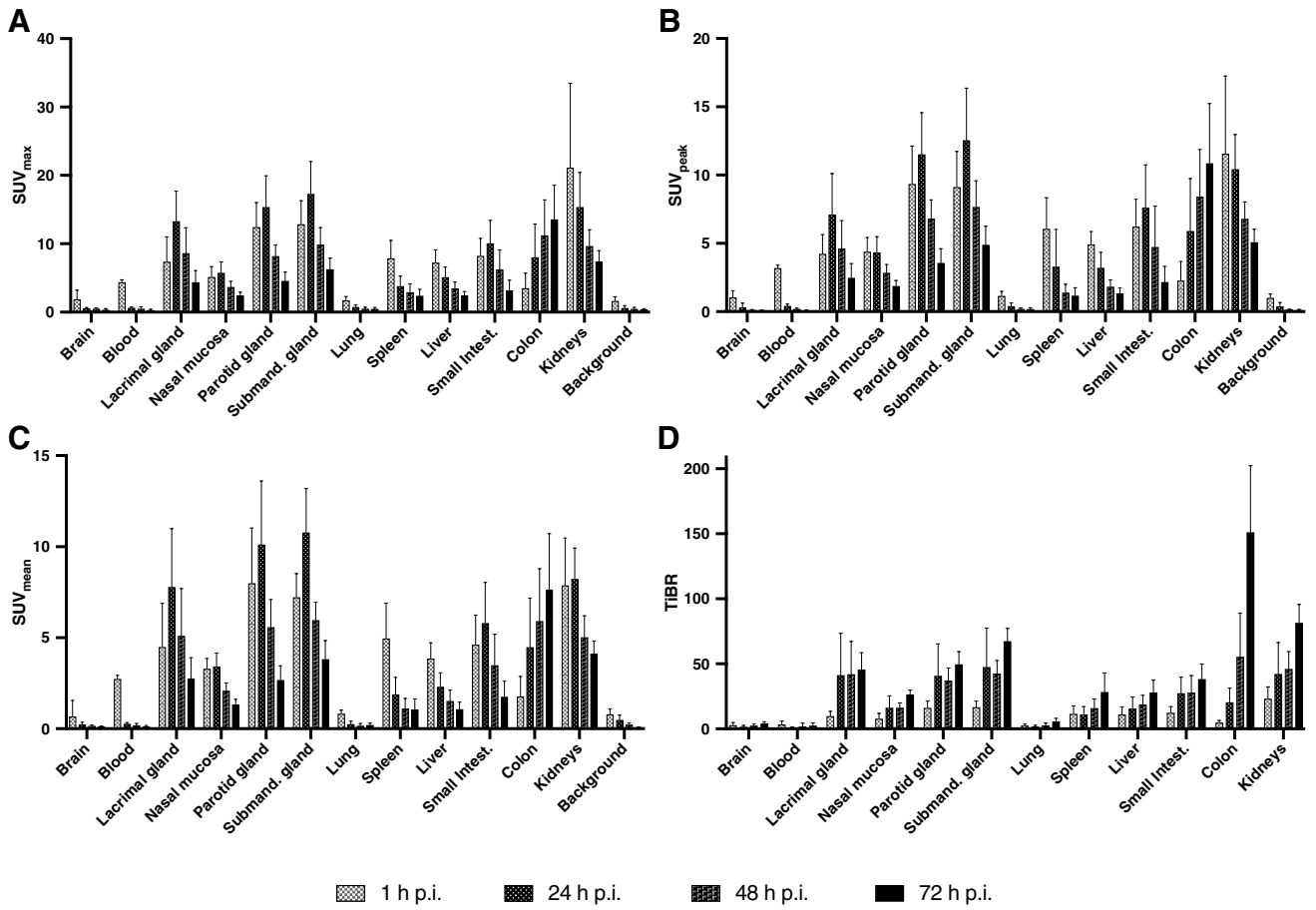

Fig. 2 Biodistribution of [^{89}Zr]Zr-PSMA-617 with descriptive statistics (mean ± standard deviation) of **A** SUV_{max}, **B** SUV_{peak}, and **C** SUV_{mean} and **D** tissue-to-background ratio (TiBR) in normal organs at 1 h, 24 h, 48 h, and 72 h p.i.

Table 2 Monoexponential curve-fitting parameters, time-integrated activity coefficients (TIAC), and mean absorbed dose estimate for [^{89}Zr]Zr-PSMA-617 in selected organs. Results are presented as mean values ± standard deviation

Organ	A (% injected A_0)	l (h^{-1})	TIAC (h^{-1})	Absorbed dose (mGy/MBq)
Kidneys	3.75 ± 1.24	0.022 ± 0.002	1.74 ± 0.44	0.517 ± 0.125
Liver	6.62 ± 1.39	0.049 ± 0.014	1.54 ± 0.49	0.158 ± 0.051
Spleen	1.25 ± 0.70	0.079 ± 0.034	0.21 ± 0.12	0.175 ± 0.068
Parotid gland	0.70 ± 0.20	0.031 ± 0.005	0.31 ± 0.10	0.601 ± 0.185
Submand. gland	0.27 ± 0.09	0.029 ± 0.004	0.13 ± 0.04	0.468 ± 0.185
Lacrimal gland	0.02 ± 0.01	0.030 ± 0.006	0.10 ± 0.004	0.156 ± 0.070

A, activity; *l*, rate constant; *TIAC*, time-integrated activity coefficient

p.i., were also visible in [^{68}Ga]Ga-PSMA-11 PET/CT. An exemplary tumor lesion and its uptake over time is shown in Fig. 3. A graphical representation of the SUV_{max} and TBR values of all lesions in all patients is provided in Fig. 4. In those lesions, which could be identified from early imaging (1 h p.i), SUV_{max} further increased substantially from 1 to 24 h p.i.. In late imaging (≥ 24 h p.i.), SUV_{max} plateaued in all lesions and TBR increased continuously over time.

In 3 of 4 (75%) patients with previously negative [^{68}Ga]Ga-PSMA-11 PET/CT, lesions that were visually considered as suggestive for prostate cancer were identified using [^{89}Zr]Zr-PSMA-617. Two patients were found to have focal uptake in the prostate bed and one of these two and another patient revealed uptake in lymph nodes suggesting local recurrence and lymph node metastases, respectively (Table 1). Figure 5 exemplifies a local recurrence and a lymph node metastasis visible on [^{89}Zr]Zr-PSMA-617 PET/CT at

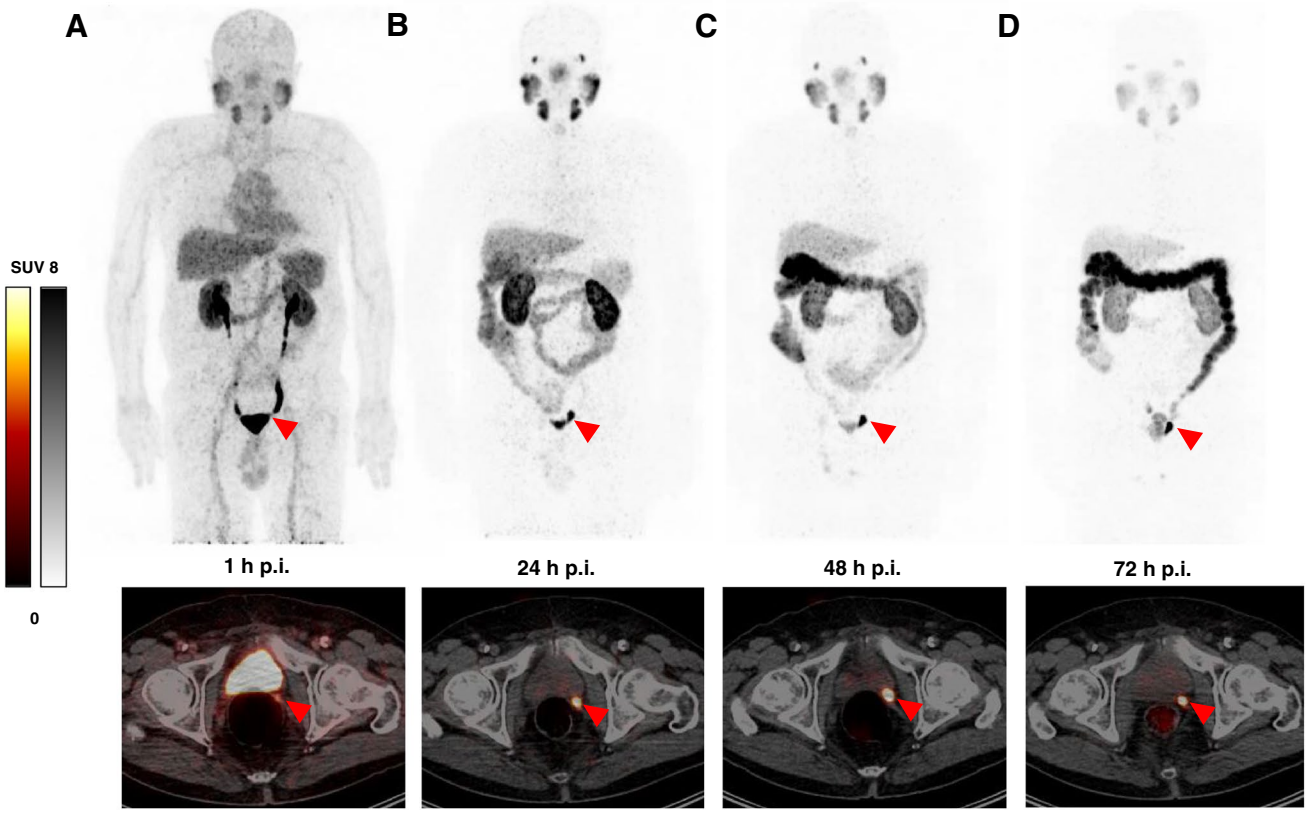

Fig. 3 Maximum intensity projections (MIP) and transversal PET/CT slices of patient no. 6 (PSA 0.43 ng/ml) at 1 h (**A**), 24 h (**B**), 48 h (**C**), and 72 h (**D**) post injection (p.i.) of [^{89}Zr]Zr-PSMA-617. Red arrows point to a suspicious focal uptake in the left seminal vesicle bed showing increased tracer uptake at 24 h p.i., 48 h p.i., and 72 h p.i. compared to 1 h p.i., therefore considered as local recurrence. SUV_{max} at 1 h / 24 h / 48 h and 72 h p.i.: 7.04 / 21.27 / 21.09 / 19.19

48 h p.i., which could not be identified by [^{68}Ga]Ga-PSMA-11 PET/CT. In 2 of 3 patients with undetermined findings in [^{68}Ga]Ga-PSMA-11 PET/CT, the respective findings were confirmed by [^{89}Zr]Zr-PSMA-617 PET/CT, whereas in 1 of 3 patients, no corresponding uptake was identified (Fig. 6). Furthermore, in 2 of these 3 patients, additional lesions were detected in [^{89}Zr]Zr-PSMA-617 PET/CT, which were unidentified by [^{68}Ga]Ga-PSMA-11 PET/CT (Table 1).

Subsequently, five patients received radiotherapy adjusted according to the results of [^{89}Zr]Zr-PSMA-617-PET/CT and in the other two patients, ADT was initiated. There were minor (e.g., additional boost) and also major adjustments on radiation treatment planning (e.g., extension of the radiation field) by the findings on [^{89}Zr]Zr-PSMA-617-PET/CT. In all 5 patients who received radiation therapy, a PSA decrease was achieved, in 4 patients by more than 70% and in 1 patient of 30%.

Discussion

This is a pilot study presenting first clinical experience of [^{89}Zr]Zr-PSMA-617 PET/CT including biodistribution, radiation dosimetry estimates, and analysis of tumor lesion imaging in patients with BCR of prostate cancer.

Comparing the biodistribution of [^{89}Zr]Zr-PSMA-617 with that of [^{68}Ga]Ga-PSMA-617 and [^{68}Ga]Ga-PSMA-11, a similar distribution pattern was observed at 1 h p.i. with intense uptake of radiolabeled PSMA ligands in the salivary glands, lacrimal glands, kidneys, liver, spleen, and small intestine [29, 30]. In contrast to established ^{68}Ga-labeled PSMA tracers, the relatively long half-life of ^{89}Zr with $T_{1/2} = 78.4$ h allowed additional imaging at later time points (up to 72 h in our study). While radiotracer uptake in kidneys, liver, and spleen was continuously decreasing over time, it was highest in the salivary

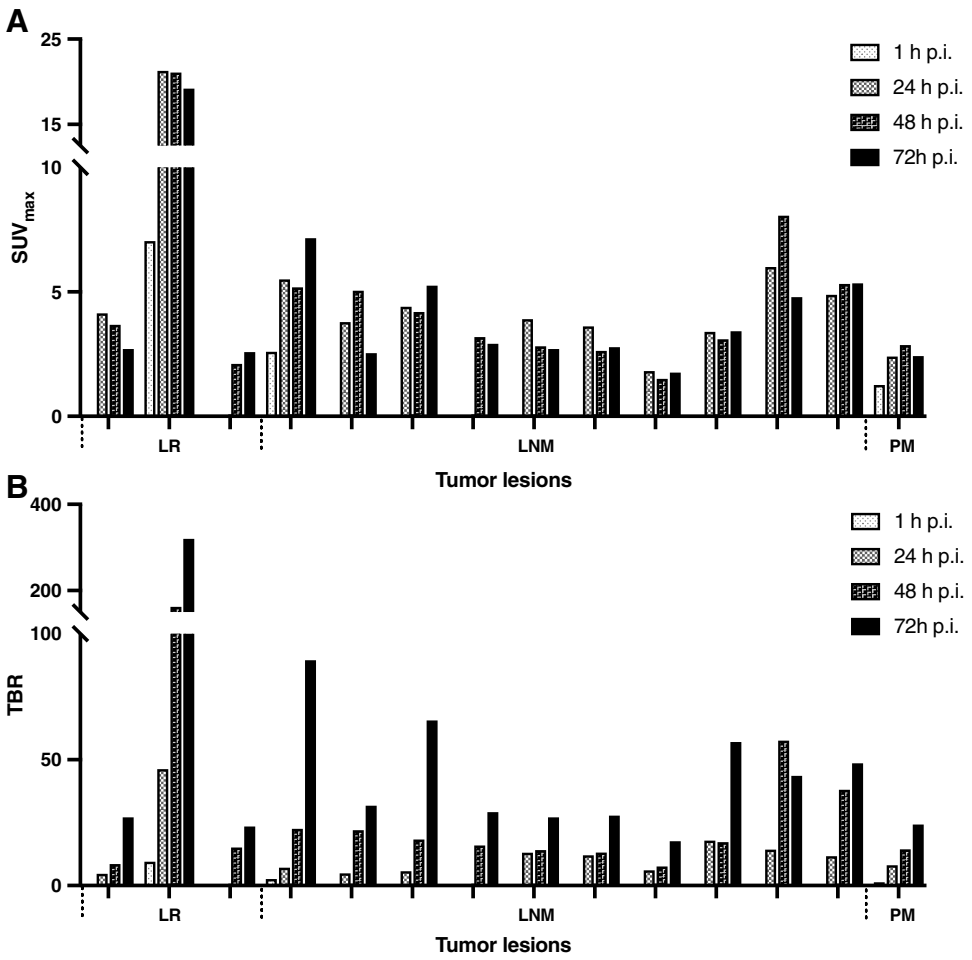

Fig. 4 SUV_{max} (**A**) and tumor-to-background ratio (TBR) (**B**) of all tumor lesions at 1 h, 24 h, 48 h, and 72 h post injection (p.i.) of [^{89}Zr]Zr-PSMA-617. LR, local recurrence; LNM, lymph node metastasis; PM, peritoneal metastasis

glands, lacrimal glands, and small intestine at 24 h p.i. and decreased thereafter. In addition, all of our patients showed increasing [^{89}Zr]Zr-PSMA-617 radiotracer uptake in the colon over time. We suggest that tracer excretion is not only through the urinary system, but more significantly at later time points, also by the intestinal system with intense tracer accumulation in the colon. Comparable observations have also been reported in [^{177}Lu]Lu-PSMA-617 scintigraphy for dosimetry measurements [31, 32]. In contrast to the normal organ uptake, radiotracer accumulation in tumor lesions increased until 24 h p.i. and then remained essentially stable up to 72 h p.i., which may be explained by the internalization process of the radioligand/PSMA complex and subsequent radiotracer trapping. Together with the continuing clearance from non-target tissues, this obviously leads to significantly higher TBR values, which may result in an improved detection of tumor lesions (vide infra).

The estimated overall effective dose of [^{89}Zr]Zr-PSMA-617 PET for the administration of 111 MBq was 10.1 mSv (0.0913 ± 0.0118 mSv/MBq) and therefore about 2–3 times higher than PET with [^{68}Ga]Ga-PSMA-617 or [^{68}Ga]Ga-PSMA-11 with a respective diagnostic activity of 200 MBq [29, 30]. The parotid glands and kidneys were the organs receiving the highest absorbed doses analogue to [^{68}Ga]Ga-PSMA-617 and [^{68}Ga]Ga-PSMA-11, but about 3–4 times higher in absolute numbers. These results could be expected and were attributed to the longer half-life of ^{89}Zr compared to ^{68}Ga. However, our radiation dose estimates are lower than the reported absorbed doses of [^{89}Zr]Zr-PSMA-DFO, another most recently introduced ^{89}Zr-labeled PSMA ligand (effective dose 0.15 ± 0.04 mSv/MBq) [33]. Not surprisingly, the radiation exposure of [^{89}Zr]Zr-PSMA-617 PET/CT did not induce any of the side effects which have been reported for targeted radiotherapy of metastatic prostate cancer with PSMA-ligands, e.g., dry mouth and mucositis. Also, no other side effects were observed. From our pilot experience, [^{89}Zr]Zr-PSMA-617 PET/CT can be considered safe.

The most important clinical finding was that in 3 of 4 patients (75%) with negative [^{68}Ga]Ga-PSMA-11 PET/CT, prostate cancer lesions (local recurrence or lymph node metastases) were identified by [^{89}Zr]Zr-PSMA-617 PET/CT. Furthermore, in 3 patients with undetermined findings on [^{68}Ga]Ga-PSMA-11

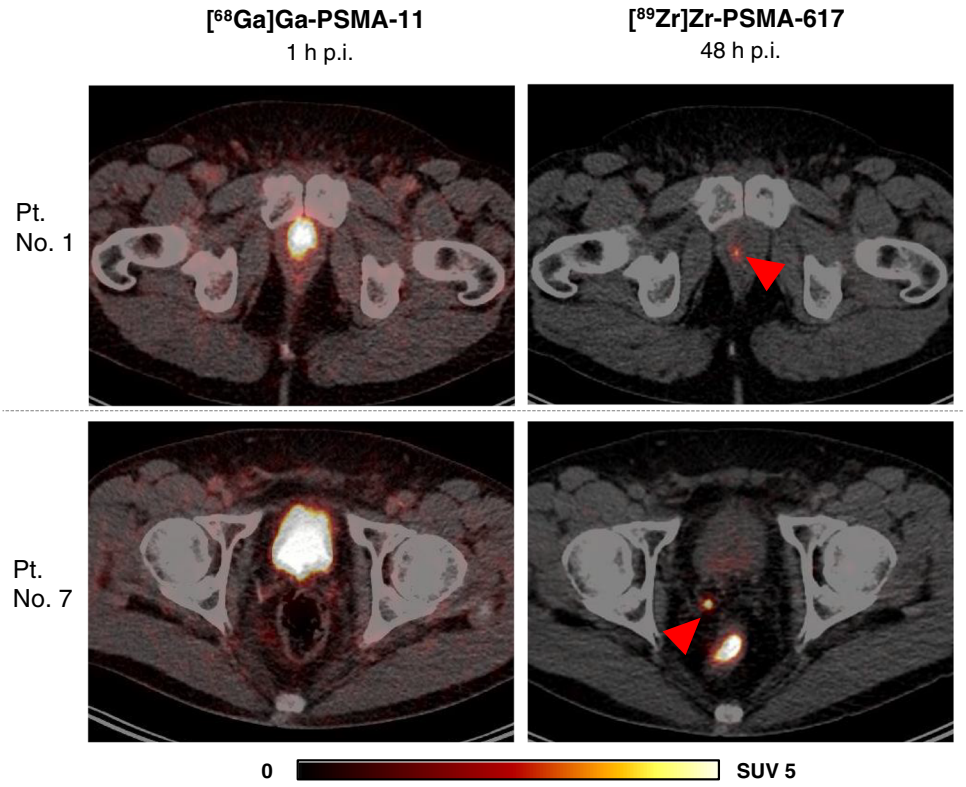

Fig. 5 Transversal slices of [^{89}Zr]Zr-PSMA-617 (right) and [^{68}Ga]Ga-PSMA-11 (left) PET/CT of 2 patients (patient no. 1 and 7) with PSMA-positive lesions detected by [^{89}Zr]Zr-PSMA-617 but unidentified by [^{68}Ga]Ga-PSMA-11. Red arrows point to suspected focal uptake. Patient no. 1 (PSA 1.92 ng/ml) with focal uptake (SUV_{max} 3.68) in the prostate bed considered as local recurrence. Patient no. 7 (PSA 0.68 ng/ml) with focal uptake (SUV_{max} 8.06) in a pelvic lymph node considered as lymph node metastasis

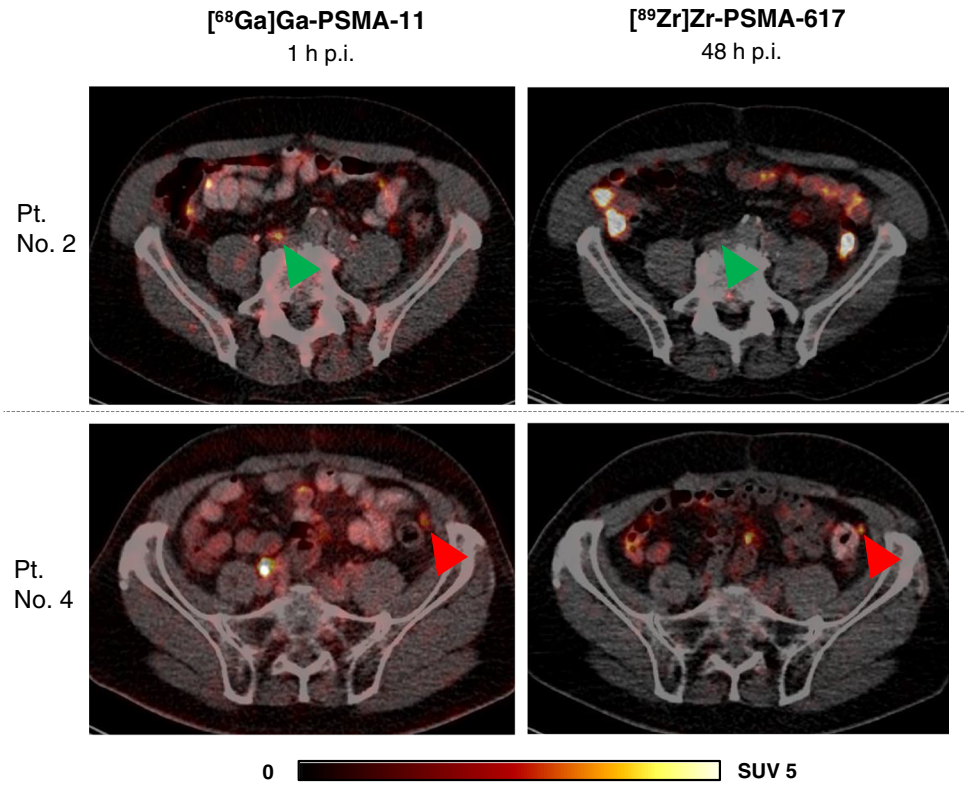

Fig. 6 Transversal slices of [^{89}Zr]Zr-PSMA-617 (right) and [^{68}Ga]Ga-PSMA-11 (left) PET/CT of 2 patients (patient no. 2 and 4) with undetermined PSMA-positive findings on [^{68}Ga]Ga-PSMA-11 PET/CT clarified by [^{89}Zr]Zr-PSMA-617 PET/CT. Green arrows point to pelvic tracer uptake (SUV_{max} 4.47) on [^{68}Ga]Ga-PSMA-11 PET/CT 1 h p.i. with no corresponding uptake on [^{89}Zr]Zr-PSMA-617 PET/CT, considered as unspecific uptake. Red arrows point to faint tracer uptake (SUV_{max} 2.06) in a peritoneal lesion on [^{68}Ga]Ga-PSMA-11 PET/CT 1 h p.i. with corresponding uptake (SUV_{max} 2.87) on [^{89}Zr]Zr-PSMA-617 PET/CT 48 h p.i. considered as peritoneal metastasis

PET/CT, [^{89}Zr]Zr-PSMA-617 PET/CT was able to clarify the results and in 2 of these patients to identify additional tumor lesions. Despite the high diagnostic performance of PET/CT with ^{68}Ga-labeled PSMA radiotracers in patients with BCR of prostate cancer, a considerable proportion of negative findings has also been reported, particularly in patients with low PSA

levels [11–14]. Here, [^{89}Zr]Zr-PSMA-617 PET/CT seems to be a useful complementary examination. The increased radiotracer uptake in tumor lesions at late imaging time points together with decreasing activity in the blood pool, in normal tissues, e.g., the urinary tract and particularly in the bladder, allowed the detection of lesions that were not visible at early imaging time points. Our observations are in accordance with the study of Dietlein et al. who reported detection of prostate cancer lesions by [^{89}Zr]Zr-PSMA-DFO PET/CT (at 2–3 days p.i.) in 8/14 (57%) patients with initially negative PSMA-targeted PET/CT ([^{68}Ga]Ga-PSMA-11 or [^{18}F]-JK-PSMA-7) [33]. The more precise localization of tumor lesions in patients with BCR by ^{89}Zr-labeled PSMA PET/CT is likely to have consequences for therapy management, e.g., in our cohort of patients, radiotherapy treatment was adjusted for all 5 patients who received subsequent salvage radiotherapy (either minor adjustments as, e.g., additional boost or major adjustments as e.g. extension of radiation field). In this respect, PET/CT with ^{89}Zr-labeled PSMA tracers may contribute to an improved and individualized therapy concept for patients with BCR.

Whether [^{18}F]F-PSMA-1007 PET/CT would have detected or clarified the lesions of our cohort due to hepatobiliary excretion with almost complete absence of activity in the bladder and the moderately longer half-life compared to ^{68}Ga remains speculative and requires future studies. Late PET/CT imaging with ^{18}F-labeled PSMA tracers was reported and shown to result in increased tumor-to-background ratios at 3 h after tracer injection when compared to image acquisition 1 h p.i. [16]. However, due to the half-life of ^{18}F of 110 min, respective PET/CT imaging is restricted to the day of tracer injection.

From our preliminary experience, imaging at 48 h p.i. seems to be the optimal time point for [^{89}Zr]Zr-PSMA-617 PET/CT acquisition in patients with BCR. At 1 h and 24 h p.i., not all lesions could be detected, whereas at 48 h p.i. and 72 h p.i., all lesions were well delineated with comparable radiotracer uptake. In addition, compared to 72 h p.i. imaging, there was substantially less uptake of the radiotracer in the sigmoid colon and rectum at 48 h p.i., therefore allowing better identification of small regional lymph nodes. Furthermore, imaging at 48 h p.i. compared to 72 h p.i. is less exhausting for the patient due to shorter acquisition time. However, the most appropriate imaging time point needs further evaluation in larger patient cohorts.

Despite these promising results of [^{89}Zr]Zr-PSMA-617 PET/CT in the detection of lesions and the potential advantage over established [^{68}Ga]Ga-PSMA-11 PET/CT imaging, the increased radiation exposure of about 10 mSv overall effective dose should be considered and further studies are recommended in larger patient cohorts to identify the optimal administered activity to further minimize the radiation dose while still obtaining high-quality PET images at later time points. [^{89}Zr]Zr-PSMA-617 PET/CT should thus be considered primarily when [^{68}Ga]Ga-PSMA-11 PET/CT do not provide a correlate for a BCR or undetermined findings arise.

[^{89}Zr]Zr-PSMA-617 PET/CT may have a paramount impact in the radioligand therapeutic field by enabling pre-therapeutic biokinetic studies. Due to the long half-life, a pre-therapeutic estimation of the resulting absorbed doses of PSMA-targeted radioligand therapy with [^{177}Lu]Lu-PSMA-617 might be possible by [^{89}Zr]Zr-PSMA-617 PET/CT since delayed imaging allows individual determination of the biological half-life of each tumor lesion and of the organs-at-risk. This may allow more personalized treatment regimens with administration of individually calculated activities and also prediction of toxicity. Furthermore, its half-life allows the possibility of centralized production and shipment to more distant imaging sites, which do not have the possibility for in-house production of [^{68}Ga]Ga-PSMA-11. This study may serve as a rational starting point for further studies, ideally in a prospective setting, to confirm and extend our findings.

The results reported herein should be considered in the light of some limitations. The data are based on a retrospective monocenter study with a limited number of patients. Imaging was performed only at 1 h, 24 h, 48 h, and 72 h p.i.. The lack of additional imaging, particularly between 1 and 24 h p.i. and after 72 h, may affect dose estimates. In addition, excretion was not measured quantitatively. Furthermore, imaging findings were only confirmed by clinical course and biochemical follow-up and not by histology. In addition, no standardized companion imaging with MRI was performed. Also, no follow-up [^{89}Zr]Zr-PSMA-617 PET/CT post-treatment is yet available.

Conclusion

[^{89}Zr]Zr-PSMA-617 PET/CT imaging is a promising new diagnostic tool with acceptable radiation exposure for patients with prostate cancer especially when [^{68}Ga]Ga-PSMA-11 PET/CT imaging fails detecting recurrent disease. The long half-life of ^{89}Zr ($T_{1/2}$ = 78.4 h) enables late time point imaging (up to 72 h in our study) with increased tracer uptake in tumor lesions and higher tumor-to-background ratios allowing identification of lesions non-visible on [^{68}Ga]Ga-PSMA-11 PET/CT imaging. Further studies, ideally in a prospective setting with larger patient cohorts, are recommended to confirm this observation of paramount impact for management of biochemical recurrence in prostate cancer.

Abbreviations ADT: Androgen-deprivation therapy; BCR : Biochemical recurrence; cGMP: Current good manufacturing practice; CT: Computed tomography; DT: Doubling time; FLAB: Fuzzy locally adaptive Bayesian; FWHM: Full width half maximum; ID : Initial diagnosis; LA: Lymphadenectomy; OSEM: Ordered-subset expectation maximization; PET: Positron emission tomography; PSA: Prostate-specific

antigen; PSMA: Prostate-specific membrane antigen; RP: Radical prostatectomy; RT: Radiation therapy; SUV: Standard uptake value; TBR: Tumor-to-background ratio; TIA: Time integrated activity; TIAC: Time-integrated activity coefficient; TiBR: Tissue-to-background ratio; VOI: Volume of interest

Funding Open Access funding enabled and organized by Projekt DEAL.

Data availability The datasets used and analyzed during the current study are available from the corresponding author on reasonable request. A case report of one patient included in this study has been previously published [34].

Declarations

Ethics approval and consent to participate All procedures performed in the patients described herein were in accordance with the ethical standards of the Institutional and/or National Research Ethics Committees and with the 1964 Helsinki Declaration and its later amendments, or with comparable ethical standards. Approval of our ethics committee was waived due to the retrospective nature of the scientific analysis. This report does not include any animal studies. Written informed consent was obtained from all participants.

Consent for publication All patients have given written consent to publication.

Conflict of interest The authors declare no competing interests.

References

1. Hofman MS, Iravani A, Nzenza T, Murphy DG. Advances in urologic imaging: prostate-specific membrane antigen ligand PET imaging. Urol Clin North Am. 2018;45:503–24.
2. Ghosh A, Heston WDW. Tumor target prostate specific membrane antigen (PSMA) and its regulation in prostate cancer. J Cell Biochem. 2004;91:528–39.
3. Schwarzenboeck SM, Rauscher I, Bluemel C, Fendler WP, Rowe SP, Pomper MG, et al. PSMA ligands for PET imaging of prostate cancer. J Nucl Med. 2017;58:1545–52.
4. Fendler WP, Rahbar K, Herrmann K, Kratochwil C, Eiber M. 177Lu-PSMA Radioligand therapy for prostate cancer. J Nucl Med. 2017;58:1196–200.
5. Cytawa W, Seitz AK, Kircher S, Fukushima K, Tran-Gia J, Schirbel A, et al. 68Ga-PSMA I&T PET/CT for primary staging of prostate cancer. Eur J Nucl Med Mol Imaging. 2020;47:168–77.
6. Valle L, Shabsovich D, de Meerleer G, Maurer T, Murphy DG, Nickols NG, et al. Use and impact of positron emission tomography/computed tomography prior to salvage radiation therapy in men with biochemical recurrence after radical prostatectomy: a scoping review. Eur Urol Oncol. 2021;4:339–55.
7. Farolfi A, Calderoni L, Mattana F, Mei R, Telo S, Fanti S, et al. Current and emerging clinical applications of PSMA PET diagnostic imaging for prostate cancer. J Nucl Med Off Publ Soc Nucl Med. 2021;62:596–604.
8. Rosar F, Wenner F, Khreish F, Dewes S, Wagenpfeil G, Hoffmann MA, et al. Early molecular imaging response assessment based on determination of total viable tumor burden in [68Ga]Ga-PSMA-11 PET/CT independently predicts overall survival in [177Lu]Lu-PSMA-617 radioligand therapy. Eur J Nucl Med Mol Imaging. 2022;49:1584–94.
9. Afshar-Oromieh A, Babich JW, Kratochwil C, Giesel FL, Eisenhut M, Kopka K, et al. The rise of PSMA ligands for diagnosis and therapy of prostate cancer. J Nucl Med. 2016;57:79S-89S.
10. Neels OC, Kopka K, Liolios C, Afshar-Oromieh A. Radiolabeled PSMA inhibitors. Cancers. 2021;13:6255.
11. Afshar-Oromieh A, Holland-Letz T, Giesel FL, Kratochwil C, Mier W, Haufe S, et al. Diagnostic performance of 68Ga-PSMA-11 (HBED-CC) PET/CT in patients with recurrent prostate cancer: evaluation in 1007 patients. Eur J Nucl Med Mol Imaging. 2017;44:1258–68.
12. Fendler WP, Calais J, Eiber M, Flavell RR, Mishoe A, Feng FY, et al. Assessment of 68Ga-PSMA-11 PET accuracy in localizing recurrent prostate cancer. JAMA Oncol. 2019;5:856–63.
13. Beheshti M, Manafi-Farid R, Geinitz H, Vali R, Loidl W, Mottaghy FM, et al. Multiphasic 68Ga-PSMA PET/CT in the detection of early recurrence in prostate cancer patients with a PSA level of less than 1 ng/mL: a prospective study of 135 patients. J Nucl Med. 2020;61:1484–90.
14. Afshar-Oromieh A, da Cunha ML, Wagner J, Haberkorn U, Debus N, Weber W, et al. Performance of [68Ga]Ga-PSMA-11 PET/CT in patients with recurrent prostate cancer after prostatectomy-a multi-centre evaluation of 2533 patients. Eur J Nucl Med Mol Imaging. 2021;48:2925–34.
15. Fendler WP, Eiber M, Beheshti M, Bomanji J, Ceci F, Cho S, et al. 68Ga-PSMA PET/CT: Joint EANM and SNMMI procedure guideline for prostate cancer imaging: version 1.0. Eur J Nucl Med Mol Imaging. 2017;44:1014–24.
16. Giesel FL, Hadaschik B, Cardinale J, Radtke J, Vinsensia M, Lehnert W, et al. F-18 labelled PSMA-1007: biodistribution, radiation dosimetry and histopathological validation of tumor lesions in prostate cancer patients. Eur J Nucl Med Mol Imaging. 2017;44:678–88.
17. Giesel FL, Knorr K, Spohn F, Will L, Maurer T, Flechsig P, et al. Detection efficacy of 18F-PSMA-1007 PET/CT in 251 patients with biochemical recurrence of prostate cancer after radical prostatectomy. J Nucl Med Off Publ Soc Nucl Med. 2019;60:362–8.
18. Yoon J-K, Park B-N, Ryu E-K, An Y-S, Lee S-J. Current perspectives on 89Zr-PET imaging. Int J Mol Sci. 2020;21:4309.
19. Heskamp S, Raavé R, Boerman O, Rijpkema M, Goncalves V, Denat F. 89Zr-Immuno-positron emission tomography in oncology: state-of-the-art 89Zr radiochemistry. Bioconjug Chem. 2017;28:2211–23.
20. Jung K-H, Park JW, Lee JH, Moon SH, Cho YS, Lee K-H. 89Zr-labeled anti-PD-L1 antibody PET monitors gemcitabine therapy-induced modulation of tumor PD-L1 expression. J Nucl Med. 2021;62:656–64.

21. van Dongen GAMS, Beaino W, Windhorst AD, Zwezerijnen GJC, Oprea-Lager DE, Hendrikse NH, et al. The role of 89Zr-immuno-PET in navigating and derisking the development of biopharmaceuticals. J Nucl Med. 2021;62:438–45.
22. Pandya DN, Bhatt N, Yuan H, Day CS, Ehrmann BM, Wright M, et al. Zirconium tetraazamacrocycle complexes display extraordinary stability and provide a new strategy for zirconium-89-based radiopharmaceutical development. Chem Sci The Royal Society of Chemistry. 2017;8:2309–14.
23. Privé BM, Derks YHW, Rosar F, Franssen GM, Peters SMB, Khreish F, et al. 89Zr-labeled PSMA ligands for pharmacokinetic PET imaging and dosimetry of PSMA-617 and PSMA-I&T: a preclinical evaluation and first in man. Eur J Nucl Med Mol Imaging. 2022;49:2064–76.
24. Hatt M, Cheze le Rest C, Turzo A, Roux C, Visvikis D. A fuzzy locally adaptive Bayesian segmentation approach for volume determination in PET. IEEE Trans Med Imaging. 2009;28:881–93.
25. Andersson M, Johansson L, Eckerman K, Mattsson S. IDAC-Dose 2.1, an internal dosimetry program for diagnostic nuclear medicine based on the ICRP adult reference voxel phantoms. EJNMMI Res. 2017;7:88.
26. Zankl M, Schlattl H, Petoussi-Henss N, Hoeschen C. Electron specific absorbed fractions for the adult male and female ICRP/ICRU reference computational phantoms. Phys Med Biol. 2012;57:4501–26.
27. Menzel H-G, Clement C, DeLuca P. ICRP Publication 110. Realistic reference phantoms: an ICRP/ICRU joint effort. A report of adult reference computational phantoms. Ann ICRP. 2009;39:1–164.
28. ICRP. Basic anatomical and physiological data for use in radiological protection: reference values. A report of age- and gender-related differences in the anatomical and physiological characteristics of reference individuals. ICRP Publication 89. Ann ICRP. 2002;32:5–265.
29. Afshar-Oromieh A, Hetzheim H, Kratochwil C, Benesova M, Eder M, Neels OC, et al. The theranostic PSMA ligand PSMA-617 in the diagnosis of prostate cancer by PET/CT: biodistribution in humans, radiation dosimetry, and first evaluation of tumor lesions. J Nucl Med. 2015;56:1697–705.
30. Afshar-Oromieh A, Hetzheim H, Kübler W, Kratochwil C, Giesel FL, Hope TA, et al. Radiation dosimetry of (68)Ga-PSMA-11 (HBED-CC) and preliminary evaluation of optimal imaging timing. Eur J Nucl Med Mol Imaging. 2016;43:1611–20.
31. Kratochwil C, Giesel FL, Stefanova M, Benešová M, Bronzel M, Afshar-Oromieh A, et al. PSMA-targeted radionuclide therapy of metastatic castration-resistant prostate cancer with 177Lu-labeled PSMA-617. J Nucl Med. 2016;57:1170–6.
32. Delker A, Fendler WP, Kratochwil C, Brunegraf A, Gosewisch A, Gildehaus FJ, et al. Dosimetry for (177)Lu-DKFZ-PSMA-617: a new radiopharmaceutical for the treatment of metastatic prostate cancer. Eur J Nucl Med Mol Imaging. 2016;43:42–51.
33. Dietlein F, Kobe C, Vázquez SM, Fischer T, Endepols H, Hohberg M, et al. An 89Zr-labeled PSMA tracer for PET/CT imaging of prostate cancer patients. J Nucl Med. 2022;63:573–83.
34. Rosar F, Bartholomä M, Maus S, Privé BM, Khreish F, Franssen GM, et al. 89Zr-PSMA-617 PET/CT may reveal local recurrence of prostate cancer unidentified by 68Ga-PSMA-11 PET/CT. Clin Nucl Med. 2022;47:435–6.

9.2 Originalarbeit 2

Rosar F, Khreish F, Marlowe RJ, Schaefer-Schuler A, Burgard C, Maus S, Petto S, Bartholomä M, Ezziddin S (2023) Detection efficacy of [^{89}Zr]Zr-PSMA-617 PET/CT in [^{68}Ga]Ga-PSMA-11 PET/CT-negative biochemical recurrence of prostate cancer. Eur J Nucl Med Mol Imaging 50:2899–2909

European Journal of Nuclear Medicine and Molecular Imaging (2023) 50:2899–2909
https://doi.org/10.1007/s00259-023-06241-0

ORIGINAL ARTICLE

Detection efficacy of [^{89}Zr]Zr-PSMA-617 PET/CT in [^{68}Ga]Ga-PSMA-11 PET/CT-negative biochemical recurrence of prostate cancer

Florian Rosar[1] · Fadi Khreish[1] · Robert J. Marlowe[2] · Andrea Schaefer-Schuler[1] · Caroline Burgard[1] · Stephan Maus[1] · Sven Petto[1] · Mark Bartholomä[1] · Samer Ezziddin[1]

Received: 30 January 2023 / Accepted: 19 April 2023 / Published online: 6 May 2023

Abstract

Rationale In patients with biochemical recurrence of prostate cancer (BCR), preliminary data suggest that prostate-specific membrane antigen (PSMA) ligand radiotracers labeled with zirconium-89 (^{89}Zr; half-life ~ 78.41 h), which allow imaging ≥ 24 h post-injection, detect suspicious lesions that are missed when using tracers incorporating short-lived radionuclides.

Materials and methods To confirm [^{89}Zr]Zr-PSMA-617 positron emission tomography/computed tomography (PET/CT) detection efficacy regarding such lesions, and compare quality of 1-h, 24-h, and 48-h [^{89}Zr]Zr-PSMA-617 scans, we retrospectively analyzed visual findings and PET variables reflecting lesional [^{89}Zr]Zr-PSMA-617 uptake and lesion-to-background ratio. The cohort comprised 23 men with BCR post-prostatectomy, median (minimum–maximum) prostate-specific antigen (PSA) 0.54 (0.11–2.50) ng/mL, and negative [^{68}Ga]Ga-PSMA-11 scans 40 ± 28 d earlier. Primary endpoints were percentages of patients with, and classifications of, suspicious lesions.

Results Altogether, 18/23 patients (78%) had 36 suspicious lesions (minimum–maximum per patient: 1–4) on both 24-h and 48-h scans (n = 33 lesions) or only 48-h scans (n = 3 lesions). Only one lesion appeared on a 1-h scan. Lesions putatively represented local recurrence in 11 cases, and nodal or bone metastasis in 21 or 4 cases, respectively; 1/1 lesion was histologically confirmed as a nodal metastasis. In all 15 patients given radiotherapy based on [^{89}Zr]Zr-PSMA-617 PET/CT, PSA values decreased after this treatment. Comparison of PET variables in 24-h vs 48-h scans suggested no clear superiority of either regarding radiotracer uptake, but improved lesion-to-background ratio at 48 h.

Conclusions In men with BCR and low PSA, [^{89}Zr]Zr-PSMA-617 PET/CT seems effective in finding prostate malignancy not seen on [^{68}Ga]Ga-PSMA-11 PET/CT. The higher detection rates and lesion-to-background ratios of 48-h scans versus 24-h scans suggest that imaging at the later time may be preferable. Prospective study of [^{89}Zr]Zr-PSMA-617 PET/CT is warranted.

Keywords Prostate cancer · Biochemical recurrence · Positron emission tomography/computed tomography (PET/CT) · Prostate-specific membrane antigen (PSMA) · Zirconium-89 (^{89}Zr)

Introduction

The diagnostic performance of imaging in patients with biochemical recurrence of prostate cancer (BCR) has been substantially improved by positron emission tomography/computed tomography (PET/CT) using radiotracers targeted at prostate-specific membrane antigen (PSMA) [1, 2], a transmembrane glycoprotein overexpressed on the surface of prostate carcinoma cells [3–5]. To date, PSMA-targeted radiotracers that are used in everyday practice comprise PSMA ligands labeled with either of two short-lived radionucludes, gallium-68 (^{68}Ga; half-life ~ 1.1 h) or fluorine-18 (^{18}F; half-life ~ 1.8 h) [6–12]. Such tracers combine generally good sensitivity and specificity

This article is part of the Topical Collection on Oncology - Genitourinary.

✉ Samer Ezziddin
samer.ezziddin@uks.eu

[1] Department of Nuclear Medicine, Saarland University – Medical Center, Kirrberger Str. 100, Geb. 50, 66421 Homburg, Germany

[2] Spencer-Fontayne Corporation, Jersey City, NJ, USA

with relatively low radiation exposure and the convenience and workflow efficiency of early image acquisition.

However, PET/CT with ^{68}Ga or ^{18}F tracers cannot detect suspicious lesions in an appreciable proportion of cases of BCR, especially when prostate-specific antigen (PSA) values are low [13, 14]. For example, our group reported a 74.8% rate of negative [^{68}Ga]Ga-PSMA-11 PET/CT in men with PSA levels ≤ 0.2 ng/mL (N = 115) [15], while Afshar-Oromieh et al. reported a 42.5% rate of negative scans in those with PSA > 0.2–0.5 ng/mL (n = 630) and a 27.8% rate in those with PSA > 0.5–≤ 1.0 ng/mL (n = 526) [2].

To some extent, this diagnostic dilemma may be mitigated when image acquisition using ^{68}Ga or ^{18}F tracers is performed at additional, delayed time points, e.g., 3 h post-[^{68}Ga]Ga-PSMA-11 administration [16]. Nonetheless, certain cases of missed lesions may relate to a key limitation of the short-lived tracers: inability to provide interpretable images beyond several hours post-injection. PET/CT with such tracers thus might not visualize lesions requiring longer times to internalize PSMA-targeted radiopharmaceuticals, e.g., lesions with low PSMA expression or low perfusion [17]. Alternatively, residual urinary tract activity associated with hours-long renal clearance of a short-lived radiopharmaceutical may obscure lesions in sites such as the ureter or urinary bladder [17, 18].

Interest therefore has increased in imaging patients with BCR with tracers that combine PSMA ligands with the radionuclide zirconium-89 (^{89}Zr), with its much longer half-life, ~ 78.41 h [13, 17–19]. Building on earlier work by others [20, 21], our group and our collaborators from Radboud University Medical Center/the University of Nijmegen stably conjugated ^{89}Zr to PSMA-617 [17]; we then reported on this radiotracer's biodistribution, organ and whole-body dosimetry, and use in a small number of men with BCR (N = 8). We observed that [^{89}Zr]Zr-PSMA-617 PET/CT at ≥ 24 h post-injection frequently revealed lesions suspicious for prostate cancer that had been missed on ~ 1-h [^{68}Ga]Ga-PSMA-11 PET/CT images [17, 19, 22].

This favorable preliminary clinical experience, and experience reported with additional ^{89}Zr-conjugated PSMA-targeted tracers [13, 17, 18], led us to perform the present retrospective analysis of our use of [^{89}Zr]Zr-PSMA-617 PET/CT in a larger group of patients with BCR and recent prior negative [^{68}Ga]Ga-PSMA-11 PET/CT. Our goal was to confirm the detection efficacy of [^{89}Zr]Zr-PSMA-617 PET/CT, and to gather additional data regarding appropriate timing of image acquisition when using this novel modality.

Materials and methods

Endpoints

The primary endpoints of this analysis were the percentage of the study sample with clear visual evidence of lesions suspicious for prostate cancer, and the classification of those lesions (local recurrence, lymph node metastasis, bone metastasis) on scans performed 1 h, 24 h, or 48 h after [^{89}Zr]Zr-PSMA-617 administration. The 1-h [^{89}Zr]Zr-PSMA-617 scans were performed to evaluate early imaging using an ^{89}Zr-containing radiotracer, and to allow direct comparison with the conventional [^{68}Ga]Ga-PSMA-11 scan; the 24-h and 48-h [^{89}Zr]Zr-PSMA-617 scans were performed to assess image acquisition at times that presumably could be used effectively with the long-lived ^{89}Zr, but not the short-lived ^{68}Ga.

Secondary endpoints were the values on each scan for each suspicious lesion of four key [^{89}Zr]Zr-PSMA-617 PET variables reflecting lesional radiotracer uptake or lesion-to-background ratio, and comparison of these variables between scans at different time points. The variables reflecting lesional radiotracer uptake were the maximum and peak standardized uptake values (SUV_{max} and SUV_{peak}, respectively) of the lesions; the variables reflecting lesion-to-background ratio were the tumor-to-background ratios of SUV_{max} or SUV_{peak} (TBR_{max} or TBR_{peak}, respectively), i.e., the SUV_{max} or SUV_{peak} of the lesion/mean standardized uptake value (SUV_{mean}) of the tissue used as background, healthy gluteal muscle.

An additional secondary endpoint of the analysis was short-term safety, i.e., side effects or vital signs abnormalities that we believed to be associated with [^{89}Zr]Zr-PSMA-617 PET/CT. Also, we compiled data regarding prostate cancer-related interventions post-[^{89}Zr]Zr-PSMA-617 PET/CT and these interventions' results.

Patients and ethics

The cohort comprised 23 consecutive men with BCR, defined as increasing PSA following radical prostatectomy. These patients underwent imaging for that indication at our center between 27 April 2021 and 22 August 2022. They had negative [^{68}Ga]Ga-PSMA-11 PET/CT scans, defined by absence of visual evidence of non-physiological radiotracer uptake. The [^{68}Ga]Ga-PSMA-11 PET/CT was performed per standard procedures [23], with images acquired ~ 1 h after administration of a mean ± standard deviation (SD) 148 ± 21 MBq activity of [^{68}Ga]Ga-PSMA-11. [^{89}Zr]Zr-PSMA-617 PET/CT took place 40 ± 28 (median [minimum–maximum] 35 [6–104]) d thereafter. To avoid a factor that potentially could confound scan interpretation, patients were eligible for this analysis only if they received no treatment for prostate cancer during the interval between [^{68}Ga]Ga-PSMA-11 PET/CT and [^{89}Zr]Zr-PSMA-617 PET/CT.

Table 1 summarizes study sample characteristics. The patients were generally middle-aged to elderly, with Gleason stage ≤7 disease in about two-thirds. The PSA value (median [minimum–maximum]) was 0.53 [0.12–2.49] ng/mL at [^{68}Ga]Ga-PSMA-11 PET/CT and 0.54 [0.11–2.50] ng/mL at [^{89}Zr]Zr-PSMA-617 PET/CT. No patient had a history of any malignancy other than prostate cancer.

Patients underwent [^{89}Zr]Zr-PSMA-617 PET/CT on a compassionate use basis under the German Pharmaceutical Act §13 (2b). Their treating nuclear medicine physicians had direct responsibility for the procedure, including requisitioning the radiopharmaceutical. The analysis was conducted according to the Declaration of Helsinki and was approved by the Institutional Review Board of the Ärztekammer des Saarlandes/Saarbrücken (approval number: 170/22, approval date: 13 September 2022). All patients provided written consent for [^{89}Zr]Zr-PSMA-617 PET/CT after receiving comprehensive information regarding the risks of radiation exposure from the procedure, and regarding the potential for side effects of the novel PET agent. The latter information included a summary of adverse events associated to date with current PSMA-targeted radiotracers, and those associated with PSMA radioligand therapy (RLT). The consent also covered use of the resulting data, in de-identified form, for scientific publications. Data regarding 5/23 cases (22%) were reported previously [17, 19, 22].

Table 1 Patient characteristics

Characteristic	Value
Age	
Median (min.–max.)	67 (53–77)
PSA [ng/mL], median (min.–max.)	
At [^{68}Ga]Ga-PSMA-11 PET/CT	0.53 (0.12–2.49)
At [^{89}Zr]Zr-PSMA-617 PET/CT	0.54 (0.11–2.50)
PSA doubling time, % (n)	
< 3 mo	17% (4)
3–6 mo	39% (9)
7–12 mo	22% (5)
> 12 mo	22% (5)
Gleason Score, % (n)	
6	4% (1)
7a	17% (4)
7b	39% (9)
8	22% (5)
9	17% (4)
Primary treatment, % (n)	
Prostatectomy	100% (23)
Additional treatments before PSMA PET/CT, % (n)	
Radiation therapy	35% (8)
ADT	22% (5)
Lymphadenectomy	4% (1)

ADT, androgen deprivation therapy; max., maximum; min., minimum; PSA, prostate-specific antigen, PSMA, prostate-specific membrane antigen

[^{89}Zr]Zr-PSMA-617 PET/CT

Whole-body images, extending from vertex to mid-femur, were acquired 1 h, 24 h, and 48 h after intravenous injection of a mean ± SD 116 ± 20 (median [minimum–maximum]: 119 [84–163]) MBq of radiotracer, immediately followed by a 500-mL NaCl 0.9% infusion. Patients were instructed to void before each image acquisition. [^{89}Zr]Zr-PSMA-617 was made in-house as described previously [19].

All imaging was performed in 3D mode on a Biograph mCT 40 scanner (Siemens Medical Solutions, Knoxville, TN, USA). PET acquisition time was 3 min/bed position for the 1-h scan, 4 min/bed position for the 24-h scan, and 5 min/bed position for the 48-h scan, with an extended field-of-view of 21.4 cm.

For attenuation correction and anatomical localization, low-dose CT was performed employing a 120-keV x-ray tube voltage and tube current modulation using CARE Dose4D software (Siemens Healthineers, Erlangen, Germany), with 30 mAs as the reference. Data were reconstructed with a soft tissue kernel (B31f/Be32) to a slice thickness of 5 mm (increment: 2–4 mm).

Along with attenuation correction, PET emission data underwent decay correction, random correction, and scatter correction. PET images were reconstructed applying an iterative 3-dimensional ordered-subset expectation maximization algorithm (3 iterations; 24 subsets) with Gaussian filtering to a transaxial resolution of 5 mm at full width at half maximum. The matrix size was 200 × 200 and the pixel size, 3.0 mm.

Interpretation of [^{89}Zr]Zr-PSMA-617 PET/CT images and calculation of PET variables

[^{89}Zr]Zr-PSMA-617 scans were visually interpreted by consensus by three nuclear medicine physicians (SE, FK, FR) with extensive experience in reading PET/CT images acquired with PSMA-targeted radiotracers. Since image interpretation took place within everyday practice rather than within a clinical trial, readers were not blinded to the patient's prostate cancer-related and other history. In interpreting the [^{89}Zr]Zr-PSMA-617 PET/CT scans, [^{68}Ga]Ga-PSMA-11 PET/CT findings were taken into account, as were findings of earlier [^{89}Zr]Zr-PSMA-617 scans in the cases of the 24-h and 48-h scans.

Each lesion that appeared to be suspicious for prostate cancer was analyzed using SyngoVia software (Enterprise VB 60, Siemens, Erlangen, Germany) to measure SUV_{max} and SUV_{peak}, and calculate TBR_{max} and $TBR_{peak.}$ The latter two variables were respectively defined as SUV_{max} or SUV_{peak} of the lesion divided by SUV_{mean} of healthy gluteal muscle, the tissue used as background. SUV_{mean} was calculated within a volume of interest applying a threshold of 20% of SUV_{max}.

Monitoring for potential adverse events related to [^{89}Zr]Zr-PSMA-617 PET/CT

We recorded adverse events and clinically-relevant abnormalities in vital signs that we believed to be related to [^{89}Zr]Zr-PSMA-617 PET/CT and that were observed by health care professionals, reported by the patient, or both during imaging and up to 4 weeks thereafter. Questions about specific potential side effects as well as open-ended queries about the occurrence of side effects in general were posed to patients in telephone calls made shortly after scanning and/or after the first follow-up visit.

Statistics

Data are presented as descriptive statistics, including mean ± SD, median (minimum–maximum), and number (percentage) or vice versa, as appropriate. The Wilcoxon matched-pairs signed rank test was used for intra-individual comparison of values for PET variables between scans acquired at different time points.

Prism version 8 (GraphPad Software, San Diego, USA) was used for the statistical analyses. $p < 0.05$ was considered to be statistically significant.

Results

Visual findings

Eighteen of the 23 patients (78%) included in this analysis had clear visual evidence of lesions suspicious for prostate cancer on one or more [^{89}Zr]Zr-PSMA-617 PET/CT scans, while 5 (22%) had no such findings (Table 2). PSA ranged from 0.19 ng/mL to 2.5 ng/mL in the patients with positive scans and from 0.11 ng/mL to 1.55 ng/mL in the patients with negative scans. Figure 1 shows representative [^{89}Zr]Zr-PSMA-617 PET images 1 h, 24 h, and 48 h post-injection from a patient with a positive scan.

Altogether 36 lesions (minimum–maximum 1–4 per patient) were detected in the 18 patients with positive [^{89}Zr]Zr-PSMA-617 PET/CT scans. Of these lesions, 11 were suspected to be local (prostate bed) recurrence, 21, lymph node metastases, and 4, bone metastases. Figures 2, 3 and 4 display representative images of lesions that were classified as either a local recurrence, a lymph node metastasis, or a bone metastasis.

Thirty-three lesions (92%) were visible on the 24-h scan, all of which also were visible on the 48-h scan. Three additional lesions (8%), all presumed to be local (prostate bed) recurrences, were seen only on the 48-h scan. Of these 36 lesions, only one, which was classified as a bone metastasis, was visible on the 1-h scan; this lesion was also noted on both the 24-h and 48-h scans.

PET variables

In intra-lesion comparisons involving all 33 lesions visible on both scans, SUV_{max} did not differ significantly between 24-h scans versus 48-h scans ($p = 0.104$), while SUV_{peak} was slightly but significantly lower in 48-h scans ($p = 0.01$) (Fig. 5). Results of PET variables across scans and lesion types are compiled in Table 2.

In contrast, intra-lesion comparisons, also involving all 33 lesions visible on both scans, of variables reflecting lesion-to-background ratio, i.e., TBR_{max} and TBR_{peak}, showed that values were significantly higher in the 48-h scan versus the 24-h scan (both $p < 0.001$) (Table 2; Fig. 5). The pattern of improved lesion-to-background ratio from the 24-h scan to the 48-h scan also held true across lesion types (Table 2; Fig. 6).

Safety

No adverse events, including clinically-relevant vital signs abnormalities, were noted during the [^{89}Zr]Zr-PSMA-617 PET/CT or the 4 weeks thereafter.

Follow-up

All patients with positive [^{89}Zr]Zr-PSMA-617 PET/CT imaging (n = 18) received treatment due to scan findings. One patient underwent lymphadenectomy of a solitary nodal lesion. The surgical specimen was histopathologically confirmed to contain prostate cancer using immunohistochemistry. The other patients underwent radiotherapy with the dose and fields based on the [^{89}Zr]Zr-PSMA-617 scan observations (n = 15) or received systemic antiandrogen therapy (n = 2). In the patients who received radiotherapy, PSA decreased following that intervention in all cases, by an average of 72% ± 25%. Post-radiotherapy, the PSA value became undetectable in

Table 2 [^{89}Zr]Zr-PSMA-617 PET/CT findings

Variable	Value		
Suspicious lesions on [^{89}Zr]Zr-PSMA-617 PET/CT	24-h scan	48-h scan	
Number of patients with suspicious lesions	16	18	
Number of lesions			
Any	33	36	
Local recurrence	8	11	
Lymph node metastasis	21	21	
Bone metastasis	4	4	
[^{89}Zr]Zr-PSMA-617 PET variables, mean ± SD [min.–max.]			
SUV_{max}			
	24-h scan	48-h scan	*p*-value
All lesions	12.7 ± 11.4 [3.2–54.8]	14.0 ± 12.5 [2.5–60.5][a] 13.6 ± 12.3 [2.5–60.5][b]	0.104[a]
Local recurrence	15.3 ± 14.1 [3.2–44.5]	16.5 ± 15.5 [3.1–49.5][a] 14.7 ± 14.0 [3.1–49.5][b]	0.55[a]
Lymph node metastasis	10.4 ± 6.0 [3.5–29.7]	11.6 ± 6.8 [2.5–25.5]	0.36
Bone metastasis	19.4 ± 23.7 [5.9–54.8]	21.7 ± 26.8 [7.4–60.5]	0.13
SUV_{peak}			
	24-h scan	48-h scan	*p*-value
All lesions	3.7 ± 3.2 [0.8–14.5]	3.4 ± 2.8 [0.6–12.7][a] 3.3 ± 2.7 [0.6–12.7][b]	0.01[a]
Local recurrence	4.9 ± 4.6 [1.4–14.5]	4.3 ± 4.2 [0.6–12.7][a] 3.8 ± 3.7 [0.6–12.7][b]	0.016[a]
Lymph node metastasis	2.9 ± 1.6 [0.8–7.8]	2.8 ± 1.7 [0.7–7.3]	0.30
Bone metastasis	5.7 ± 5.3 [1.7–12.8]	4.9 ± 4.4 [1.5–11.0]	0.38
TBR_{max}			
	24-h scan	48-h scan	*p*-value
All lesions	29.7 ± 24.9 [7.0–107.5]	64.8 ± 59.7 [8.4–291.2][a] 64.2 ± 59.2 [8.4–291.2][b]	< 0.001[a]
Local recurrence	36.4 ± 30.7 [7.0–94.7]	85.2 ± 94.1 [8.4–291.2][a] 77.7 ± 84.8 [8.4–291.2][b]	< 0.001[a]
Lymph node metastasis	25.4 ± 17.1 [7.7–80.3]	54.0 ± 35.7 [13.2–141.7]	< 0.001
Bone metastasis	39.2 ± 45.7 [12.6–107.5]	89.4 ± 81.6 [24.7–201.7]	0.13
TBR_{peak}			
	24-h scan	48-h scan	*p*-value
All lesions	8.8 ± 7.2 [1.8–30.9]	15.8 ± 14.5 [2.3–74.7][a] 15.6 ± 14.2 [2.3–74.7][b]	< 0.001[a]
Local recurrence	11.6 ± 9.9 [3.3–30.9]	21.9 ± 24.4 [2.3–74.7][a] 19.5 ± 21.6 [2.3–74.7][b]	< 0.001[a]
Lymph node metastasis	7.1 ± 4.8 [1.9–21.1]	12.9 ± 8.5 [3.7–36.5]	< 0.001
Bone metastasis	11.9 ± 10.5 [3.3–25.1]	19.0 ± 13.8 [5.0–36.7]	0.13

max., maximum; min., minimum; PET/CT, positron emission tomography/computed tomography; PSMA, prostate-specific membrane antigen; SD, standard deviation; SUV_{max}, maximum standardized uptake value; SUV_{peak}, peak standardized uptake value; TBR_{max}, tumor-to-background ratio of SUV_{max}: SUV_{max} of presumed tumor lesion/SUV_{mean} of healthy gluteal muscle; TBR_{peak}, tumor-to-background ratio of SUV_{peak}: SUV_{peak} of presumed tumor lesion/SUV_{mean} of healthy gluteal muscle

[a] Calculation based on lesions seen in both 24-h and 48-h post-injection scans

[b] Calculation based on all lesions seen in 48-h post-injection scan

5 of the 15 patients, decreased by > 70% in an additional 5/15, and decreased by 30–70% in the remaining 5/15. Post-treatment PSA became also undetectable in the 2 men given antiandrogen therapy.

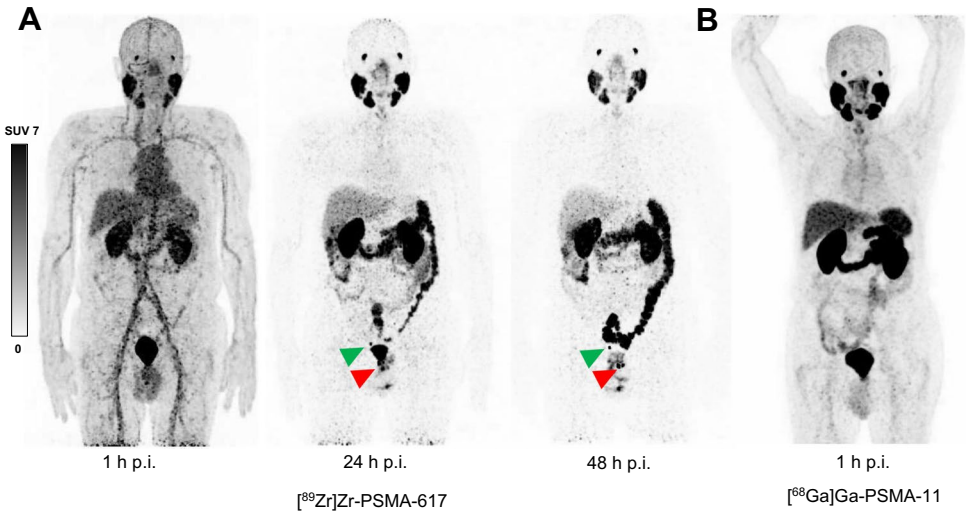

Fig. 1 Maximum intensity projection (MIP) images of a patient with biochemical recurrence of prostate cancer (PSA 2.5 ng/mL, PSA doubling time > 12 months at time of imaging) on a) [^{89}Zr]Zr-PSMA-617 PET/CT 1 h, 24 h, and 48 h post-injection (p.i.) and b) [^{68}Ga]Ga-PSMA-11 PET/CT 1 h post-injection. [^{89}Zr]Zr-PSMA-617 PET/CT revealed a suspected local recurrence (red arrow) and a suspected pelvic lymph node metastasis (green arrow) on 24-h and 48-h post-injection scans, findings that were not discerned on [^{68}Ga]Ga-PSMA-11 PET/CT

Discussion

This analysis of experience with [^{89}Zr]Zr-PSMA-617 PET/CT involves, to our knowledge, the largest yet published cohort of men with BCR and recent negative conventional PSMA-targeted imaging. The study had four principal findings. First, we confirmed in a 23-patient sample the efficacy of [^{89}Zr]Zr-PSMA-617 PET/CT in localizing lesions suspicious for prostate cancer, with a patient-level detection rate of 78% (18/23). The lesions detected were suggestive of the three most common forms of recurrent prostate cancer, local recurrence, lymph node metastasis, and bone metastasis. As would be expected in the BCR setting, each patient had a limited number (1–4 per patient) of suspicious lesions, i.e., structural correlates of the PSA elevation appear to have been detected at the oligometastatic stage or earlier. Notably, high detection efficacy was shown in this study despite low PSA concentrations (median 0.54 ng/mL, minimum–maximum 0.11–2.5 ng/mL).

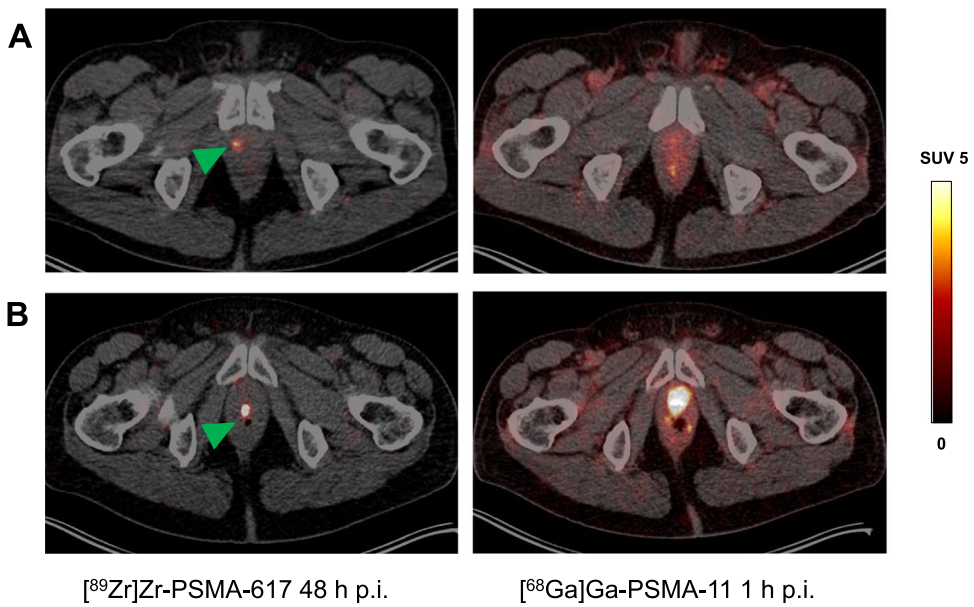

Fig. 2 Transversal slice images showing presumed local recurrence of prostate cancer (green arrows) revealed by [^{89}Zr]Zr-PSMA-617 PET/CT (left-hand column) but not identified on [^{68}Ga]Ga-PSMA-11 PET/CT (right-hand column) in two patients (rows **A** and **B**, respectively). p.i., post-injection; SUV, standardized uptake value

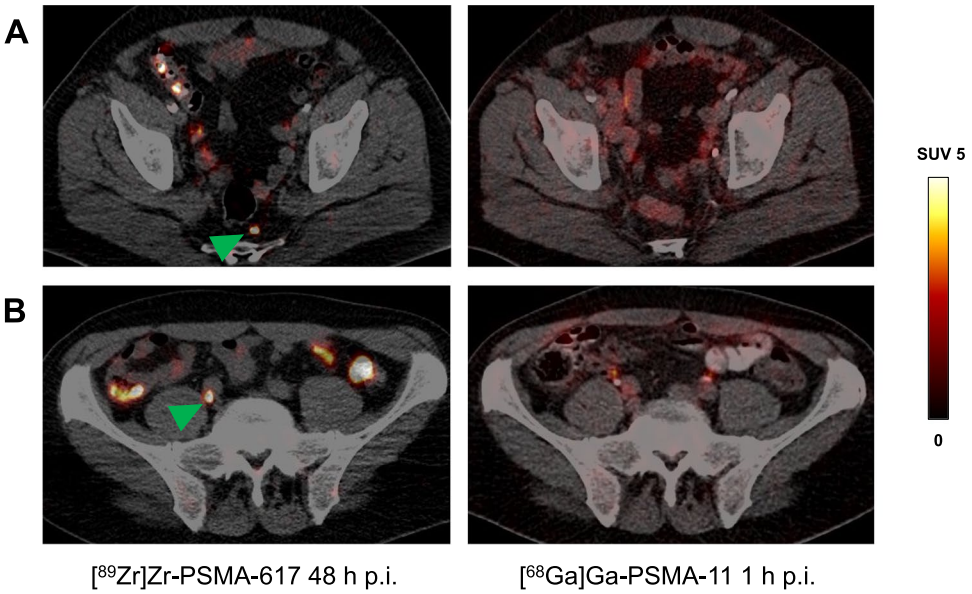

Fig. 3 Transversal slice images showing presumed lymph node metastases of prostate cancer (green arrows) revealed by [^{89}Zr]Zr-PSMA-617 PET/CT (left-hand column) but not identified on [^{68}Ga]Ga-PSMA-11 PET/CT (right-hand column) in two patients (rows **A** and **B**, respectively). p.i., post-injection; SUV, standardized uptake value

Second, our analysis of PET variables of lesional tracer uptake and lesion–to-background ratio confirmed a pair of earlier observations regarding [^{89}Zr]Zr-PSMA-617 pharmacokinetics [19]. Namely, lesional accumulation of this tracer remains broadly stable in the 24-h to 48-h post-administration interval, reflected in the present analysis by the lack of significant differences in SUV_{max} and by only slightly (albeit significantly) lower SUV_{peak} at 48 h. On the other hand, decreased physiological accumulation of [^{89}Zr]Zr-PSMA-617 during that period resulted in an increased lesion-to-background ratio in the later scans, in the form of a statistically-significant, and roughly twofold higher, TBR_{max} and TBR_{peak} at 48 h vs 24 h. These pharmacokinetics likely explain our detection of 33 lesions on both the 24-h and 48-h scans, but 3 additional lesions only on 48-h images. Indeed, these pharmacokinetic findings, along with the persistent visibility on 48-h scans of all lesions seen on 24-h scans, and the greater detection efficacy of the later imaging, suggest that 48-h imaging may be preferable to 24-h imaging. However, it remains for future studies to more definitively determine the most appropriate timing for [^{89}Zr]Zr-PSMA-617 PET/CT scanning.

Third, we found evidence that patients with suspicious lesions on [^{89}Zr]Zr-PSMA-617 PET/CT appeared to have had true-positive scans. One patient underwent surgery based on scan findings, and true positivity was

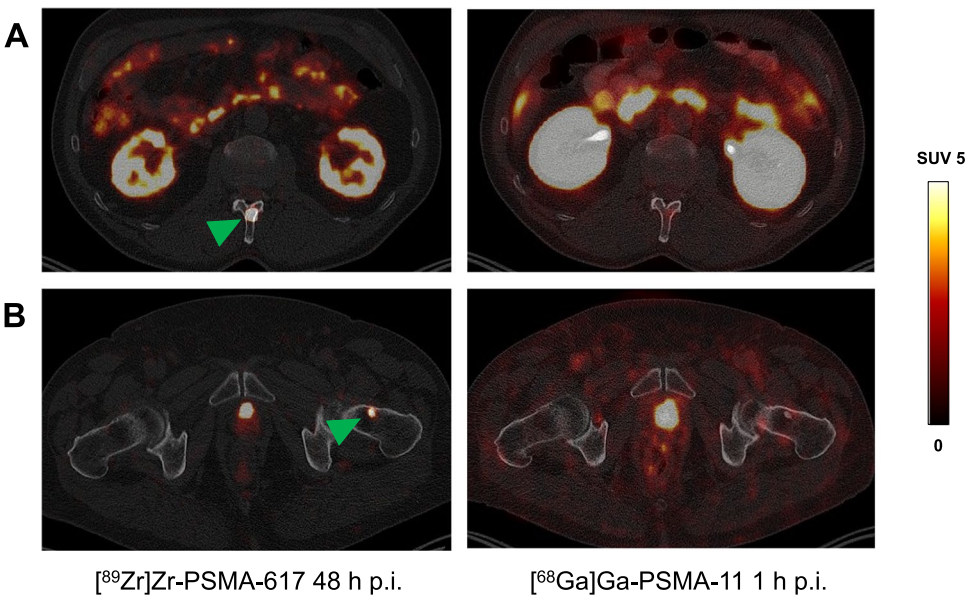

Fig. 4 Transversal slice images showing suspected bone metastases of prostate cancer (green arrows) revealed by [^{89}Zr]Zr-PSMA-617 PET/CT (left-hand column) but not discernible on [^{68}Ga]Ga-PSMA-11 PET/CT (right-hand column) in two patients (rows **A** and **B**, respectively). p.i., post-injection; SUV, standardized uptake value

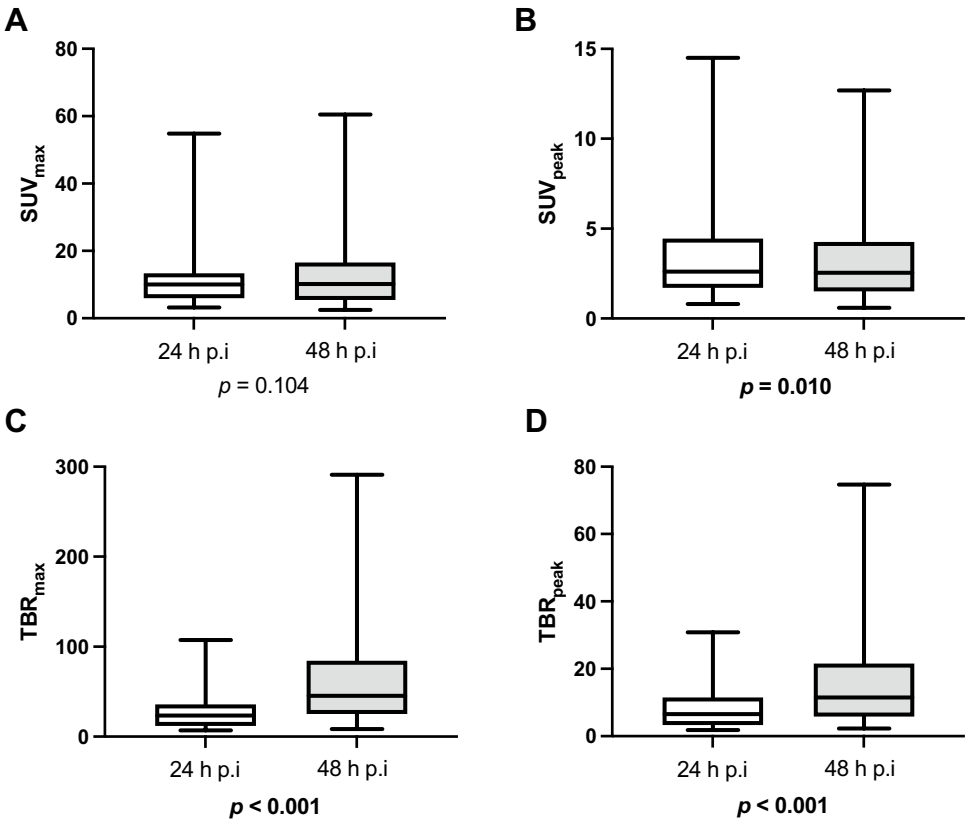

Fig. 5 Aggregate descriptive statistics of PET variables of lesional radiotracer uptake and lesion-to-background ratio of all detected lesions suspicious for prostate cancer in [^{89}Zr]Zr-PSMA-617 PET/CT images acquired at 24 h vs. 48 h post-injection: a) SUV_{max}, b) SUV_{peak}, c) TBR_{max}, and d) TBR_{peak}. *p* values refer to intra-lesion comparisons of the values between the 24-h and 48-h post-injection scans for all lesions visible on both scans (n = 33). SD, standard deviation; SUV_{max}, maximum standardized uptake value; SUV_{peak}, peak standardized uptake; TBR_{max}, tumor-to-background ratio of SUV_{max}: SUV_{max} of presumed tumor lesion/SUV_{mean} of healthy gluteal muscle; TBR_{peak}, tumor-to-background ratio of SUV_{peak}: SUV_{peak} of presumed tumor lesion/SUV_{mean} of healthy gluteal muscle

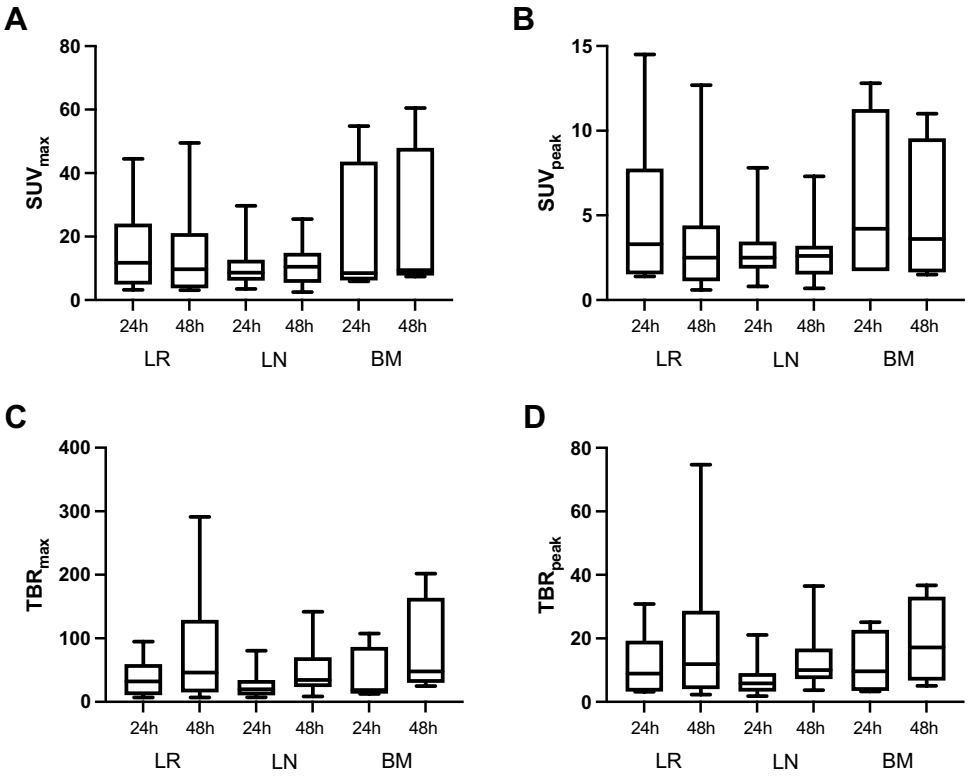

Fig. 6 Aggregate statistics of PET variables of lesional radiotracer uptake and lesion–background ratio by lesion classification in [^{89}Zr]Zr-PSMA-617 PET/CT images acquired 24 h post-injection and 48 h post-injection: a) SUV_{max}, b) SUV_{peak}, c) TBR_{max}, and d) TBR_{peak}. BM, bone metastases; LN, lymph node metastases; LR, local recurrence; SD, standard deviation; SUVmax, maximum standardized uptake value; SUVpeak, peak standardized uptake; TBR_{max}, tumor-to-background ratio of SUV_{max}: SUV_{max} of presumed tumor lesion/SUV_{mean} of healthy gluteal muscle; TBR_{peak}, tumor-to-background ratio of SUV_{peak}: SUV_{peak} of presumed tumor lesion/SUV_{mean} of healthy gluteal muscle

confirmed by surgical specimen histology and by PSA decreases following this procedure, a lymphadenectomy of a solitary nodal lesion. Further, in all 15 additional patients receiving salvage radiotherapy based on [89Zr]Zr-PSMA-617 PET/CT findings, PSA decreased afterwards. The average PSA reduction was 72% ± 25% and the minimum decrease, 30%, with the analyte becoming undetectable in 5 of these men.

Fourth, our analysis supported previous published observations of the safety of [^{89}Zr]Zr-PSMA-617 PET/CT, at least over the short term [19]. No undesirable effects were noted by health care professionals or patients up to 4 weeks post-scanning.

Our observations are quite comparable to those of Dietlein et al. using PET/CT with another ^{89}Zr-based radiotracer, [^{89}Zr]Zr-PSMA-Df [13]. These investigators visually identified altogether 15 suspicious lesions (1–4 per patient) in 8/14 men (57%) with BCR and median (minimum–maximum) PSA of 0.85 (0.31–7.2) ng/mL. The [^{89}Zr]Zr-PSMA-Df scans were acquired 24–144 h post-injection, within 5 weeks after negative [^{68}Ga]Ga-PSMA-11 PET/CT (n = 4) or [^{18}F]-JK-PSMA-7 PET/CT (n = 10). Aligned with our experience, Dietlein and colleagues also detected putative local recurrence, lymph node metastasis, and/or distant metastasis. Additionally, like us, these investigators reported no side effects of the novel imaging procedure.

Limitations of the present work should be kept in mind. This was a single-center, retrospective analysis of a relatively small number of patients, which merits a caveat regarding generalizability. Additionally, in the everyday practice setting reported here, malignancy of 35/36 suspected prostate cancer lesions was not assessed histopathologically. However, 1 patient who underwent excision of a solitary nodal lesion seen on [^{89}Zr]Zr-PSMA-617 PET/CT had this finding histologically confirmed as prostate cancer. Additionally, true scan positivity was suggested by marked to complete biochemical responses following salvage radiotherapy in all 15 additional patients who received that intervention. Nonetheless, presence of detectable PSA post-radiotherapy in some of these men means that the presence of lesions missed by [^{89}Zr]Zr-PSMA-617 PET/CT as well as by [^{68}Ga]Ga-PSMA-11 PET/CT cannot be excluded. Thus, to more definitively characterize the diagnostic performance of this novel radiotracer, it will be useful to more systematically analyze biochemistry, imaging, and clinical follow-up after [^{89}Zr]Zr-PSMA-617 PET/CT.

Additionally, [^{68}Ga]Ga-PSMA-11 PET acquisition at delayed time points, e.g., 3 h post-injection was not performed in our cohort. Further, it cannot be excluded that not only the different radionuclides used in this study, but also the different PSMA ligands played a role in our results. Compared with PSMA-11, PSMA-617 has a longer persistence in the blood pool and is associated with higher background in PET images. However, no clinically relevant differences in tumor uptake of these ligands have been reported, thus an impact on our results seems to be unlikely [24]. Lastly, we did not evaluate longer-term safety of this imaging procedure, or comprehensively assess short-term safety. However, some reassurance is provided by safety having been demonstrated using zirconium-labeled radiopharmaceuticals in other settings [25–28].

[^{89}Zr]Zr-PSMA-617 PET/CT may ultimately be somewhat of a "niche modality", largely reserved for patients with negative or indeterminate conventional (early) PET/CT despite BCR. In such cases, [^{89}Zr]Zr-PSMA-617 may be particularly suitable for patients wishing to avoid systemic treatment in favor of metastasis-directed approaches [13, 29–32]. The potentially treatment-altering and outcome-altering information to be gained from the examination would seem to substantially outweigh its disadvantage of an approximately 2.5 times higher radiation exposure than that associated with conventional PSMA PET/CT [19], and to justify application of this novel procedure, especially in the above-mentioned cases. Given the identical PSMA ligands in this pair of radiopharmaceuticals, another potential application of [^{89}Zr]Zr-PSMA-617 PET/CT may be for pre-lutetium-177-PSMA-617 RLT dosimetry, to attempt to individualize, and thereby optimize, dosing to improve safety and efficacy.

Conclusions

In men with BCR, even when PSA levels are low, [^{89}Zr]Zr-PSMA-617 PET/CT seems to be effective (positivity rate 78% in our cohort) in detecting lesions suspicious for local recurrence and metastasis that eluded detection using conventional imaging such as [^{68}Ga]Ga-PSMA-11 PET/CT. Prospective study of this novel imaging modality in men with BCR is warranted.

Abbreviations ^{18}F: Fluorine-18; ^{68}Ga: Gallium-68; ^{89}Zr: Zirconium-89; ADT: Androgen deprivation therapy ; CT: Computed tomography; DM: Distant metastases; LR: Local recurrence; LN: Lymph node metastases; max.: Maximum; min.: Minimum; MIP: Maximum intensity projection; PET: Positron emission tomography; p.i.: Post-injection; PSA: Prostate-specific antigen; PSMA: Prostate-specific membrane antigen; RLT: Radioligand therapy; SD: Standard deviation; SUV_{max}: Maximum standardized uptake value; SUV_{mean}: Mean standardized uptake value; SUV_{peak}: Peak standardized uptake value; TBR_{max}: Tumor-to-background ratio of SUV_{max}: SUV_{max} of presumed tumor lesion/SUV_{mean} of healthy gluteal muscle; TBR_{peak}: Tumor-to-background ratio of SUV_{peak}: SUV_{peak} of presumed tumor lesion/SUV_{mean} of healthy gluteal muscle

Funding Open Access funding enabled and organized by Projekt DEAL.

Data availability The datasets used and analyzed during the current study are available from the corresponding author on reasonable request.

Declarations

Ethics approval and consent to participate All procedures performed in the patients described herein were in accordance with the ethical standards of the Institutional and/or National Research Ethics Committees and with the 1964 Helsinki Declaration and its later amendments, or with comparable ethical standards. This analysis was approved by the Institutional Review Board of the Ärztekammer des Saarlandes/Saarbrücken (approval number: 170/22, approval date: 13 September 2022). This report does not include any animal studies. Written informed consent was obtained from all participants.

Consent for publication All patients have given written consent to publication.

Conflict of interest The authors declare that they have no conflict of interest.

References

1. Hofman MS, Lawrentschuk N, Francis RJ, Tang C, Vela I, Thomas P, et al. Prostate-specific membrane antigen PET-CT in patients with high-risk prostate cancer before curative-intent surgery or radiotherapy (proPSMA): a prospective, randomised, multicentre study. Lancet. 2020;395:1208–16. https://doi.org/10.1016/S0140-6736(20)30314-7.
2. Afshar-Oromieh A, da Cunha ML, Wagner J, Haberkorn U, Debus N, Weber W, et al. Performance of [(68)Ga]Ga-PSMA-11 PET/CT in patients with recurrent prostate cancer after prostatectomy-a multi-centre evaluation of 2533 patients. Eur J Nucl Med Mol Imaging. 2021;48:2925–34. https://doi.org/10.1007/s00259-021-05189-3.
3. Wright GL Jr, Haley C, Beckett ML, Schellhammer PF. Expression of prostate-specific membrane antigen in normal, benign, and malignant prostate tissues. Urol Oncol. 1995;1:18–28. https://doi.org/10.1016/1078-1439(95)00002-y.
4. Silver DA, Pellicer I, Fair WR, Heston WD, Cordon-Cardo C. Prostate-specific membrane antigen expression in normal and malignant human tissues. Clin Cancer Res. 1997;3:81–5.
5. Sweat SD, Pacelli A, Murphy GP, Bostwick DG. Prostate-specific membrane antigen expression is greatest in prostate adenocarcinoma and lymph node metastases. Urology. 1998;52:637–40. https://doi.org/10.1016/s0090-4295(98)00278-7.
6. Perera M, Papa N, Roberts M, Williams M, Udovicich C, Vela I, et al. Gallium-68 Prostate-specific Membrane Antigen Positron Emission Tomography in Advanced Prostate Cancer-Updated Diagnostic Utility, Sensitivity, Specificity, and Distribution of Prostate-specific Membrane Antigen-avid Lesions: A Systematic Review and Meta-analysis. Eur Urol. 2020;77:403–17. https://doi.org/10.1016/j.eururo.2019.01.049.
7. Pienta KJ, Gorin MA, Rowe SP, Carroll PR, Pouliot F, Probst S, et al. A Phase 2/3 prospective multicenter study of the diagnostic accuracy of prostate specific membrane antigen PET/CT with (18)F-DCFPyL in prostate cancer patients (OSPREY). J Urol. 2021;206:52–61. https://doi.org/10.1097/JU.0000000000001698.
8. Morris MJ, Rowe SP, Gorin MA, Saperstein L, Pouliot F, Josephson D, et al. diagnostic performance of (18)F-DCFPyL-PET/CT in men with biochemically recurrent prostate cancer: Results from the CONDOR Phase III, multicenter study. Clin Cancer Res. 2021. https://doi.org/10.1158/1078-0432.CCR-20-4573.
9. Calais J, Czernin J, Fendler WP, Elashoff D, Nickols NG. Randomized prospective phase III trial of (68)Ga-PSMA-11 PET/CT molecular imaging for prostate cancer salvage radiotherapy planning [PSMA-SRT]. BMC Cancer. 2019;19:18. https://doi.org/10.1186/s12885-018-5200-1.
10. Giesel FL, Hadaschik B, Cardinale J, Radtke J, Vinsensia M, Lehnert W, et al. F-18 labelled PSMA-1007: biodistribution, radiation dosimetry and histopathological validation of tumor lesions in prostate cancer patients. Eur J Nucl Med Mol Imaging. 2017;44:678–88. https://doi.org/10.1007/s00259-016-3573-4.
11. Piron S, Verhoeven J, Vanhove C, De Vos F. Recent advancements in (18)F-labeled PSMA targeting PET radiopharmaceuticals. Nucl Med Biol. 2022;106–107:29–51. https://doi.org/10.1016/j.nucmedbio.2021.12.005.
12. Wurzer A, DiCarlo D, Schmidt A, Beck R, Eiber M, Schwaiger M, et al. Radiohybrid ligands: a novel tracer concept exemplified by (18)F- or (68)Ga-labeled rhPSMA-inhibitors. J Nucl Med. 2019. https://doi.org/10.2967/jnumed.119.234922.
13. Dietlein F, Kobe C, Vazquez SM, Fischer T, Endepols H, Hohberg M, et al. An (89)Zr-labeled PSMA tracer for PET/CT imaging of prostate cancer patients. J Nucl Med. 2022;63:573–83. https://doi.org/10.2967/jnumed.121.262290.
14. Giesel FL, Knorr K, Spohn F, Will L, Maurer T, Flechsig P, et al. Detection efficacy of (18)F-PSMA-1007 PET/CT in 251 patients with biochemical recurrence of prostate cancer after radical prostatectomy. J Nucl Med. 2019;60:362–8. https://doi.org/10.2967/jnumed.118.212233.
15. Burgard C, Hoffmann MA, Frei M, Buchholz HG, Khreish F, Marlowe RJ, et al. Detection efficacy of (68)Ga-PSMA-11 PET/CT in biochemical recurrence of prostate cancer with very low PSA levels: a 7-year, two-center "real-world" experience. Cancers (Basel). 2023;15:1376. https://doi.org/10.3390/cancers15051376.
16. Afshar-Oromieh A, Sattler LP, Mier W, Hadaschik BA, Debus J, Holland-Letz T, et al. The clinical impact of additional late PET/CT imaging with (68)Ga-PSMA-11 (HBED-CC) in the diagnosis of prostate cancer. J Nucl Med. 2017;58:750–5. https://doi.org/10.2967/jnumed.116.183483.
17. Prive BM, Derks YHW, Rosar F, Franssen GM, Peters SMB, Khreish F, et al. (89)Zr-labeled PSMA ligands for pharmacokinetic PET imaging and dosimetry of PSMA-617 and PSMA-I&T: a preclinical evaluation and first in man. Eur J Nucl Med Mol Imaging. 2022;49:2064–76. https://doi.org/10.1007/s00259-021-05661-0.
18. Vazquez SM, Endepols H, Fischer T, Tawadros SG, Hohberg M, Zimmermanns B, et al. Translational development of a Zr-89-labeled inhibitor of prostate-specific membrane antigen for PET imaging in prostate cancer. Mol Imaging Biol. 2022;24:115–25. https://doi.org/10.1007/s11307-021-01632-x.
19. Rosar F, Schaefer-Schuler A, Bartholoma M, Maus S, Petto S, Burgard C, et al. [(89)Zr]Zr-PSMA-617 PET/CT in biochemical recurrence of prostate cancer: first clinical experience from a

pilot study including biodistribution and dose estimates. Eur J Nucl Med Mol Imaging. 2022;49:4736–47. https://doi.org/10.1007/s00259-022-05925-3.
20. Pandya DN, Bhatt N, Yuan H, Day CS, Ehrmann BM, Wright M, et al. Zirconium tetraazamacrocycle complexes display extraordinary stability and provide a new strategy for zirconium-89-based radiopharmaceutical development. Chem Sci. 2017;8:2309–14. https://doi.org/10.1039/c6sc04128k.
21. Pandya DN, Bhatt NB, Almaguel F, Rideout-Danner S, Gage HD, Solingapuram Sai KK, et al. (89)Zr-chloride can be used for immuno-PET radiochemistry without loss of antigen reactivity in vivo. J Nucl Med. 2019;60:696–701. https://doi.org/10.2967/jnumed.118.216457.
22. Rosar F, Bartholoma M, Maus S, Prive BM, Khreish F, Franssen GM, et al. 89Zr-PSMA-617 PET/CT may reveal local recurrence of prostate cancer unidentified by 68Ga-PSMA-11 PET/CT. Clin Nucl Med. 2022;47:435–6. https://doi.org/10.1097/RLU.0000000000004108.
23 Fendler WP, Eiber M, Beheshti M, Bomanji J, Ceci F, Cho S, et al. (68)Ga-PSMA PET/CT: Joint EANM and SNMMI procedure guideline for prostate cancer imaging: version 10. Eur J Nucl Med Mol Imaging. 2017;44:1014–24. https://doi.org/10.1007/s00259-017-3670-z.
24. Guhne F, Radke S, Winkens T, Kuhnel C, Greiser J, Seifert P, et al. Differences in distribution and detection rate of the [(68)Ga]Ga-PSMA ligands PSMA-617, -I&T and -11-inter-individual comparison in patients with biochemical relapse of prostate cancer. Pharmaceuticals (Basel). 2021;15:9. https://doi.org/10.3390/ph15010009.
25. Yoon JK, Park BN, Ryu EK, An YS, Lee SJ. Current perspectives on (89)Zr-PET imaging. Int J Mol Sci. 2020;21:4309 https://doi.org/10.3390/ijms21124309.
26. Pandit-Taskar N, O'Donoghue JA, Beylergil V, Lyashchenko S, Ruan S, Solomon SB, et al. (8)(9)Zr-huJ591 immuno-PET imaging in patients with advanced metastatic prostate cancer. Eur J Nucl Med Mol Imaging. 2014;41:2093–105. https://doi.org/10.1007/s00259-014-2830-7.
27. Pandit-Taskar N, O'Donoghue JA, Durack JC, Lyashchenko SK, Cheal SM, Beylergil V, et al. A phase I/II study for analytic validation of 89Zr-J591 immunoPET as a molecular imaging agent for metastatic prostate cancer. Clin Cancer Res. 2015;21:5277–85. https://doi.org/10.1158/1078-0432.CCR-15-0552.
28. Pandit-Taskar N, Postow MA, Hellmann MD, Harding JJ, Barker CA, O'Donoghue JA, et al. First-in-humans imaging with (89)Zr-Df-IAB22M2C anti-CD8 minibody in patients with solid malignancies: preliminary pharmacokinetics, biodistribution, and lesion targeting. J Nucl Med. 2020;61:512–9. https://doi.org/10.2967/jnumed.119.229781.
29. Deek MP, Van der Eecken K, Sutera P, Deek RA, Fonteyne V, Mendes AA, et al. Long-term outcomes and genetic predictors of response to metastasis-directed therapy versus observation in oligometastatic prostate cancer: analysis of STOMP and ORIOLE trials. J Clin Oncol. 2022;40:3377–82. https://doi.org/10.1200/JCO.22.00644.
30. Jadvar H, Abreu AL, Ballas LK, Quinn DI. Oligometastatic prostate cancer: current status and future challenges. J Nucl Med. 2022;63:1628–35. https://doi.org/10.2967/jnumed.121.263124.
31. von Deimling M, Rajwa P, Tilki D, Heidenreich A, Pallauf M, Bianchi A, et al. The current role of precision surgery in oligometastatic prostate cancer. ESMO Open. 2022;7:100597. https://doi.org/10.1016/j.esmoop.2022.100597.
32. Berghen C, Joniau S, Ost P, Poels K, Everaerts W, Decaestecker K, et al. Progression-directed therapy for oligoprogression in castration-refractory prostate cancer. Eur Urol Oncol. 2021;4:305–9. https://doi.org/10.1016/j.euo.2019.08.012.

9.3 Originalarbeit 3

Rosar F, Burgard C, Larsen E, Khreish F, Marlowe RJ, Schaefer-Schuler A, Maus S, Petto S, Bartholomä M, Ezziddin S (2024) [^{89}Zr]Zr-PSMA-617 PET/CT characterization of indeterminate [^{68}Ga]Ga-PSMA-11 PET/CT findings in patients with biochemical recurrence of prostate cancer: lesion-based analysis. Cancer Imaging 24:27

Cancer Imaging

RESEARCH ARTICLE Open Access

[^{89}Zr]Zr-PSMA-617 PET/CT characterization of indeterminate [^{68}Ga]Ga-PSMA-11 PET/CT findings in patients with biochemical recurrence of prostate cancer: lesion-based analysis

Florian Rosar[1], Caroline Burgard[1], Elena Larsen[1], Fadi Khreish[1], Robert J. Marlowe[2], Andrea Schaefer-Schuler[1], Stephan Maus[1], Sven Petto[1], Mark Bartholomä[1] and Samer Ezziddin[1*]

Abstract

Background The state-of-the-art method for imaging men with biochemical recurrence of prostate cancer (BCR) is prostate-specific membrane antigen (PSMA)-targeted positron emission tomography/computed tomography (PET/CT) with tracers containing short-lived radionuclides, e.g., gallium-68 (^{68}Ga; half-life: ~67.7 min). However, such imaging not infrequently yields indeterminate findings, which remain challenging to characterize. PSMA-targeted tracers labeled with zirconium-89 (^{89}Zr; half-life: ~78.41 h) permit later scanning, which may help in classifying the level of suspiciousness for prostate cancer of lesions previously indeterminate on conventional PSMA-targeted PET/CT.

Methods To assess the ability of [^{89}Zr]Zr-PSMA-617 PET/CT to characterize such lesions, we retrospectively analyzed altogether 20 lesions that were indeterminate on prior [^{68}Ga]Ga-PSMA-11 PET/CT, in 15 men with BCR (median prostate-specific antigen: 0.70 ng/mL). The primary endpoint was the lesions' classifications, and secondary endpoints included [^{89}Zr]Zr-PSMA-617 uptake (maximum standardized uptake value [SUV_{max}]), and lesion-to-background ratio (tumor-to-liver ratio of the SUV_{max} [TLR]). [^{89}Zr]Zr-PSMA-617 scans were performed 1 h, 24 h, and 48 h post-injection of 123 ± 19 MBq of radiotracer, 35 ± 35 d post-[^{68}Ga]Ga-PSMA-11 PET/CT.

Results Altogether, 6/20 previously-indeterminate lesions (30%) were classified as suspicious (positive) for prostate cancer, 14/20 (70%), as non-suspicious (negative). In these two categories, [^{89}Zr]Zr-PSMA-617 uptake and lesional contrast showed distinctly different patterns. In positive lesions, SUV_{max} and TLR markedly rose from 1 to 48 h, with SUV_{max} essentially plateauing at high levels, and TLR further steeply increasing, from 24 to 48 h. In negative lesions, uptake, when present, was very low, and decreasing, while contrast was minimal, from 1 to 48 h. No adverse events

*Correspondence:
Samer Ezziddin
samer.ezziddin@uks.eu

Full list of author information is available at the end of the article

or clinically-relevant vital signs changes related to [^{89}Zr]Zr-PSMA-617 PET/CT were noted during or ~4 weeks after the procedure.

Conclusions In men with BCR, [^{89}Zr]Zr-PSMA-617 PET/CT may help characterize as suspicious or non-suspicious for prostate cancer lesions that were previously indeterminate on [^{68}Ga]Ga-PSMA-11 PET/CT.

Trial registration Not applicable.

Keywords Prostate cancer, Biochemical recurrence, Positron emission tomography/computed tomography (PET/CT), Indeterminate findings, Prostate-specific membrane antigen (PSMA), Zirconium-89 (^{89}Zr)

Background

The state-of-the-art method for imaging men with biochemical recurrence of prostate cancer (BCR) is prostate-specific membrane antigen (PSMA)-targeted positron emission tomography/computed tomography (PET/CT) [1–3]. Most widely used for this purpose at present are PSMA-targeted tracers containing short-lived radionuclides, e.g., gallium-68 (^{68}Ga; half-life: ~67.7 min) or fluorine-18 (^{18}F, half-life ~109.8 min) [4–8].

Besides improving sensitivity and specificity of prostate cancer imaging, PSMA-targeted PET/CT has reduced the rate of equivocal findings compared to that seen with the previous standard procedures, CT and bone scan. For example, in the proPSMA study (N=295) in the primary staging setting, [^{68}Ga]Ga-PSMA-11 PET/CT was associated with a 7% (95% confidence interval: 4–13%) rate of equivocal scans, versus 23% (95% confidence interval: 17–31%) for the older modalities [9]. Nonetheless, indeterminate lesions remain an appreciably frequent challenge in whole-body prostate cancer staging. In many cases, characterization of such lesions may be decisive in optimizing treatment planning, and is therefore of high clinical importance [10].

PSMA-targeted PET/CT with tracers incorporating zirconium-89 (^{89}Zr) are a potential means of characterizing lesions that are indeterminate on conventional PSMA-targeted PET/CT, i.e., that conducted using ^{68}Ga-labeled or ^{18}F-labeled radiotracers. Due to the much longer half-life of ^{89}Zr, ~78.41 h, tracers conjugated with that radionuclide allow much later imaging, i.e., at ≥24 h post-injection. For this reason, ^{89}Zr tracers may clearly visualize lesions that more slowly internalize PSMA ligands, e.g., those with weak PSMA expression or poor perfusion [11–16]. Additionally, late scanning allows greater time for radiopharmaceutical clearance from non-target tissue, thereby increasing tumor-to-background ratio [14].

We, our collaborators from Radboud University Medical Center/the University of Nijmegen, and others have reported that PET/CT at ≥24 h post-injection with [^{89}Zr]Zr-PSMA-617 or other ^{89}Zr-labeled tracers frequently detects lesions suspicious for prostate cancer that were not apparent on conventionally-acquired PET/CT images [11–16]. Our group also reported promising preliminary experience using [^{89}Zr]Zr-PSMA-617 in 3 patients with indeterminate findings on [^{68}Ga]Ga-PSMA-11 PET/CT [13]. However, to our knowledge, the literature contains no additional data regarding the ability of [^{89}Zr]Zr-PSMA-617 PET/CT to characterize as suspicious or non-suspicious for prostate cancer lesions that were indeterminate on conventional PSMA-targeted PET/CT. We therefore sought to assess the use of this novel imaging modality in a larger cohort of patients with indeterminate findings on PET using tracers with short-lived radionuclides.

Methods

Study design and endpoints

This was a retrospective, lesion-based analysis. The primary endpoint was the visual classification on [^{89}Zr]Zr-PSMA-617 PET/CT of lesions that on a prior [^{68}Ga]Ga-PSMA-11 PET/CT scan, had been judged to be indeterminate. Additional secondary endpoints comprised the values of and changes over time in [^{89}Zr]Zr-PSMA-617 PET variables for each previously-indeterminate lesion, and the number and sites of lesions detected on [^{89}Zr]Zr-PSMA-617 PET/CT, but not on [^{68}Ga]Ga-PSMA-11 PET/CT.

The remaining secondary endpoints were near-term safety, i.e., side effects or vital signs abnormalities observed during or shortly after the procedure that we deemed to be related to [^{89}Zr]Zr-PSMA-617 PET/CT, and results of follow-up of patients in the study sample.

Patients and ethics

The cohort included 15 consecutive men with BCR who had ≥1 indeterminate lesion on prior [^{68}Ga]Ga-PSMA-11 PET/CT. BCR was defined as increasing prostate-specific antigen (PSA) after primary (curative-intent) treatment. Imaging took place between 25 October 2021 and 6 February 2023 at Saarland University Medical Center, Homburg, Germany. The [^{68}Ga]Ga-PSMA-11 PET/CT was conducted following standard procedures [17], ~1 h after infusion of, on average, 151±25 MBq of radiotracer. Indeterminate lesions were defined as those that could not be clearly attributed to pathological or physiological uptake, e.g., visually faint foci at typical sites of prostate cancer recurrence, foci at sites unusual for recurrence,

or foci that lacked an apparent anatomical correlate on the concurrent CT. [^{68}Ga]Ga-PSMA-11 PET/CT images were classified visually by consensus among three experienced nuclear medicine specialists (SE, FK, FR). To eliminate a potential confounder in [^{89}Zr]Zr-PSMA-617 scan interpretation, patients were excluded from the analysis if their prostate cancer treatment changed in the time between the [^{68}Ga]Ga-PSMA-11 scan and the [^{89}Zr]Zr-PSMA-617 scan.

Table 1 summarizes patient and imaging characteristics of the study sample. This cohort was typically middle-aged to elderly, with Gleason stage 8 or 9 disease in 60% of cases. PSA values were (median [minimum–maximum] 0.70 [0.10–10.2] ng/mL). Data regarding 3/15 patients were previously published [13].

Table 1 Patient and imaging characteristics of 15 men with indeterminate [^{68}Ga]Ga-PSMA-11 PET/CT

Characteristic	Value
Age [yr]	
Median (min.–max.)	71 (59–77)
PSA [ng/mL]	
Median (min.–max.)	0.70 (0.10–10.2)
PSA doubling time category, % (n)	
<3 mo.	33% (5)
3–6 mo.	33% (5)
7–12 mo.	13% (2)
>12 mo.	20% (3)
Gleason Score category, % (n)	
6	7% (1)
7a	13% (2)
7b	20% (3)
8	27% (4)
9	33% (5)
Primary treatment, % (n)	
Prostatectomy alone	40% (6)
Prostatectomy + lymphadenectomy	47% (7)
Radiation therapy	13% (2)
Additional treatments before study imaging, % (n)	
Radiation therapy	20% (3)
ADT	20% (3)
Number of indeterminate lesions on [^{68}Ga]Ga-PSMA-11 PET/CT	
Total	20
Median (min.–max.) per patient	1 (1–3)
Percentage (number) of patients with multiple indeterminate lesions	27% (4)
Sites(s) of indeterminate lesions on [^{68}Ga]Ga-PSMA-11 PET/CT, % (n)	
Local	20% (4)
Lymph node	40% (8)
Bone	40% (8)

Because of rounding, percentages may not add up to 100% for certain characteristics

ADT: androgen deprivation therapy or antiandrogen therapy; max.: maximum; min.: minimum; PSA: prostate-specific antigen; SD: standard deviation

Altogether 20 indeterminate lesions had been described on [^{68}Ga]Ga-PSMA-11 PET/CT, 4 located in the prostate bed, 8 in or adjacent to lymph nodes, and 8 in the skeleton. Each patient had a limited number of such lesions: 1 each in 11 men, 2 each in 3 patients, and 3 in 1 patient. Besides the indeterminate lesion(s), 7/15 (47%) men had lesions that could be clearly classified as suspicious on [^{68}Ga]Ga-PSMA-11 PET/CT; in 8/15 (53%) patients, the indeterminate lesion(s) were the only findings on the conventional PSMA-targeted scan.

[^{89}Zr]Zr-PSMA-617 PET/CT was performed on a compassionate use basis under the German Pharmaceutical Act § 13 (2b). Attending nuclear medicine physicians had direct responsibility for the procedure, including ordering the radiopharmaceutical. The analysis conformed to the Declaration of Helsinki and received approval from the Institutional Review Board of the Ärztekammer des Saarlandes/Saarbrücken (approval number: 170/22, approval date: 13 September 2022). Written consent for [^{89}Zr]Zr-PSMA-617 PET/CT was obtained from all patients after they received detailed information on the risks of radiation exposure associated with this procedure, and on the potential for side effects of the novel radiotracer. The consent also permitted the patient's data to be reported in de-identified form in scientific publications.

[^{89}Zr]Zr-PSMA-617 PET/CT

[^{89}Zr]Zr-PSMA-617 PET/CT took place 35±35 (median [minimum–maximum] 25 [7–140]) d after the [^{68}Ga]Ga-PSMA-11 PET/CT. One hr, 24 h, and 48 h after intravenous injection of [^{89}Zr]Zr-PSMA-617, whole-body PET/CT images, extending from vertex to mid-femur, were acquired. The mean±standard deviation (SD) [^{89}Zr]Zr-PSMA-617 activity was 123±19 MBq, the median (minimum–maximum) activity was 125 (85–157) MBq, and radiotracer administration was immediately followed by a 500-mL NaCl 0.9% infusion. Patients were asked to void before each image acquisition. [^{89}Zr]Zr-PSMA-617 was manufactured in-house [13]. Imaging was performed on a Biograph mCT 40 system (Siemens Medical Solutions, Knoxville, TN, USA). Acquisition time was 3 min/bed position for the 1-hr scan, 4 min/bed position for the 24-hr scan, and 5 min/bed position for the 48-hr scan. For attenuation correction and anatomical localization, low-dose CT was carried out using a 120-keV x-ray tube voltage and tube current modulation with CARE Dose4D software (Siemens Healthineers, Erlangen, Germany), with 30 mAs as the reference. A soft tissue kernel (B31f/Be32) and a slice thickness of 5 mm (increment: 2–4 mm) were employed

for data reconstruction. PET emission data also underwent decay correction, random correction, and scatter correction. An iterative 3-dimensional ordered-subset expectation maximization algorithm (3 iterations; 24 subsets) with Gaussian filtering to a transaxial resolution of 5 mm at full width at half maximum was applied to reconstruct the PET images. Matrix and pixel sizes were 200×200 and 3.0 mm, respectively.

[^{89}Zr]Zr-PSMA-617 PET/CT image interpretation

[^{89}Zr]Zr-PSMA-617 PET/CT findings were classified visually, by consensus among the same nuclear medicine specialists who had interpreted the [^{68}Ga]Ga-PSMA-11 PET/CT images. Lesions were considered to be positive on [^{89}Zr]Zr-PSMA-617 PET/CT if they were visible on the 24-h scan and/or the 48-h scan as foci of clear uptake. Lesions were deemed to be negative if they could not be visualized on late imaging. Because [^{89}Zr]Zr-PSMA-617 PET/CT images were interpreted within everyday practice and not a clinical study, the readers could access the patient's prostate cancer-related and other medical history and prior images.

Calculation of PET variables

In separate analyses of lesions that respectively had been classified as indeterminate or as positive on the prior conventional scan, two key on [^{89}Zr]Zr-PSMA-617 PET variables were measured. First, the maximum standardized uptake value (SUV_{max}), reflecting lesional uptake of [^{89}Zr]Zr-PSMA-617, was determined. SyngoVia Enterprise VB 60 software (Siemens) was used. Second, the tumor-to-liver ratio (TLR), reflecting lesional contrast, was calculated. TLR was defined as the SUV_{max} of the lesion divided by the mean standardized uptake value (SUV_{mean}) of the tissue representing background, in this analysis, healthy liver. The SUV_{mean} was calculated in a spherical volume of interest within the liver.

Monitoring for potential adverse events related to [^{89}Zr]Zr-PSMA-617 PET/CT

Adverse events and clinically-relevant vital signs abnormalities that were believed to be associated with [^{89}Zr]Zr-PSMA-617 PET/CT and were noted by health care professionals, the patient, or both during imaging and up to 4 weeks thereafter were recorded. In telephone calls made shortly after scanning and/or after the first follow-up visit, patients were questioned about specific side effects and, in open-ended fashion, about the occurrence of side effects in general.

Patient follow-up

Data were compiled regarding subsequent therapy and biochemical follow-up of patients in the study sample. This compilation was performed via retrospective analysis of medical records or via personal interview.

Statistics

Data are presented as descriptive statistics including, as appropriate, mean ± SD, median (minimum–maximum), and number (percentage) or vice versa.

Results

Of altogether 20 lesions considered to be indeterminate for prostate cancer on [^{68}Ga]Ga-PSMA-11 PET/CT, 6 (30%) were classified as suspicious (positive) and the remaining 14 (70%) as non-suspicious (negative) on [^{89}Zr]Zr-PSMA-617 PET/CT. Figure 1 shows [^{89}Zr]Zr-PSMA-617 PET/CT images at 1 h, 24 h, and 48 h post-injection, and the corresponding [^{68}Ga]Ga-PSMA-11 PET/CT scan 1 h post-injection from a patient whose indeterminate lesion was confirmed to be suspicious (positive) on [^{89}Zr]Zr-PSMA-617 PET/CT; also illustrated is a quantitative analysis of this lesion.

As seen in Table 2, the lesions classified as positive on the [^{89}Zr]Zr-PSMA-617 scan comprised 3 of 4 possible local recurrences, 1 of 8 possible lymph node metastases, and 2 of 8 possible bone metastases.

Representative images of positive and negative lesions for each category of anatomical site appear in Figs. 2 and 3.

As reflected by SUV_{max}, collectively, [^{89}Zr]Zr-PSMA-617 uptake (Fig. 4A) and changes in that variable over time (Fig. 4B) distinctly differed between the 6 previously-indeterminate lesions that were classified as positive on [^{89}Zr]Zr-PSMA-617 PET/CT versus their 14 counterparts that were classified as negative. In the positive lesions, radiotracer uptake rose markedly from the 1-hr to the 24-hr scan, and then essentially plateaued at a high level through 48 h post-injection. In the negative lesions, the already very low degree of [^{89}Zr]Zr-PSMA-617 uptake at 1

hr post-injection declined in the subsequent two measurements, or the lesions did not show any clear radiotracer uptake. Additionally, TLR, a marker of lesional contrast, was markedly higher in the [^{89}Zr]Zr-PSMA-617-positive lesions than in the [^{89}Zr]Zr-PSMA-617-negative lesions at 24 and 48 h (Fig. 4C). Furthermore, in distinction with findings in the negative lesions, TLR increased continuously over time in the positive lesions (Fig. 4D).

[^{89}Zr]Zr-PSMA-617 PET/CT also identified altogether 11 lesions suspicious for prostate cancer that had not been visualized at all on [^{68}Ga]Ga-PSMA-11 PET/CT (Table 2; representative images in Fig. 5, left column). Of the newly-discovered suspicious lesions, 3 were presumed to be local recurrences, and 8, lymph node metastases. Altogether 7/15 patients (47%) had lesions newly

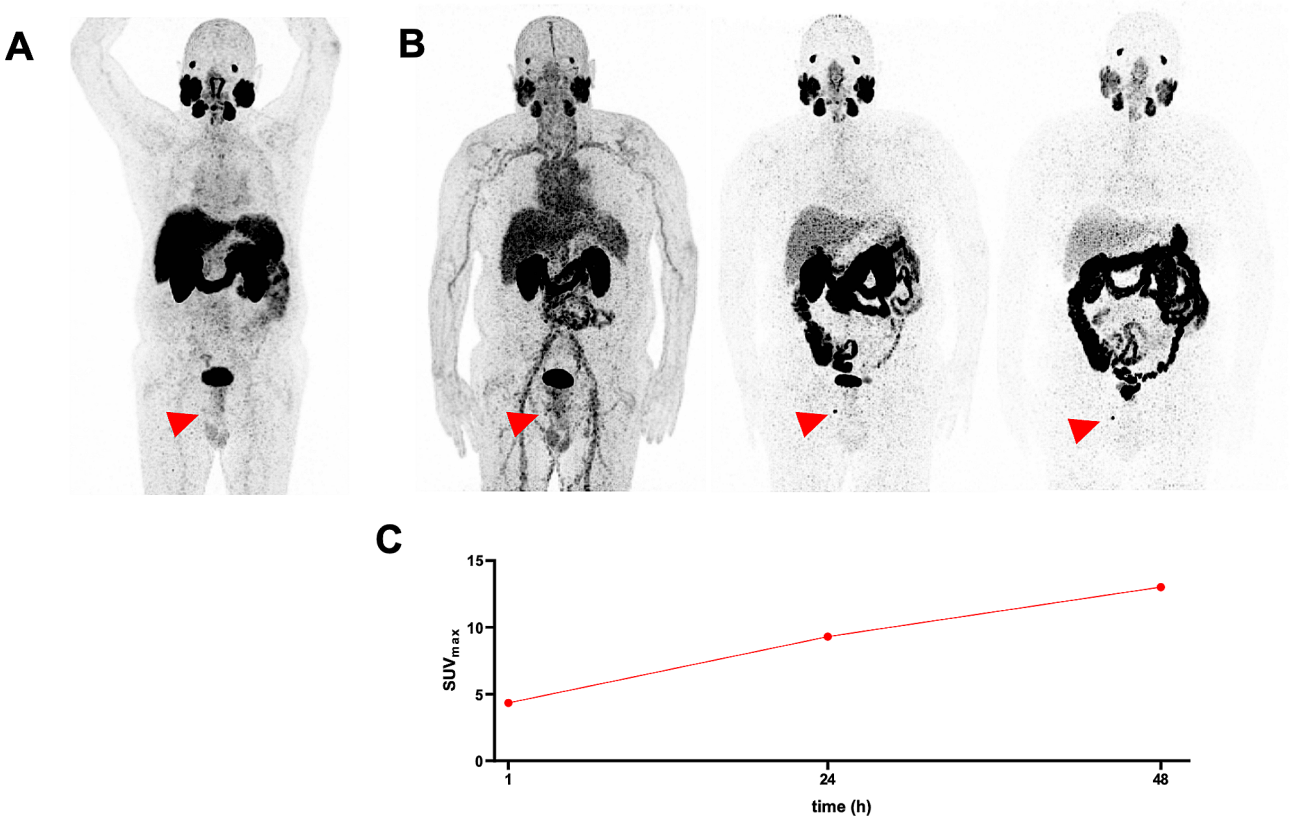

Fig. 1 Maximum intensity projection (MIP) images of a patient with biochemical recurrence of prostate cancer on A) [68Ga]Ga-PSMA-11 PET/CT 1 h post-injection and B) (right to left) [89Zr]Zr-PSMA-617 PET/CT 1 h, 24 h, and 48 h post-injection. As denoted by the red arrows, a lesion faintly visible on the [68Ga]Ga-PSMA-11 scan, although not clearly discernible on the 1-hr [89Zr]Zr-PSMA-617 image, was clearly discernible as a presumed bone metastasis on the 24-hr and 48-hr [89Zr]Zr-PSMA-617 scans. Supporting the visual findings, [89Zr]Zr-PSMA-617 uptake, reflected by C) the SUVmax curve for the lesion, showed a sharp increase from 1 to 24 h, and then a slower increase from 24 to 48 h

Table 2 Classification of [^{68}Ga]Ga-PSMA-11 PET/CT-indeterminate lesions and new positive findings on [^{89}Zr]Zr-PSMA-617 PET/CT

Lesion type	Number of indeterminate lesions on [^{68}Ga]Ga-PSMA-11 PET/CT	Classification of [^{68}Ga]Ga-PSMA-11 PET/CT-indeterminate lesions on [^{89}Zr]Zr-PSMA-617 PET/CT		New positive findings on [^{89}Zr]Zr-PSMA-617 PET/CT
		Positive, n (% of category)	Negative, n (% of category)	
Any	20	6/20 (30%)	14/20 (70%)	11
Local	4	3/4 (75%)	1/4 (25%)	3
Lymph node	8	1/8 (13%)	7/8 (88%)	8
Bone	8	2/8 (25%)	6/8 (75%)	0

Due to rounding, percentages may not add up to 100% for certain categories of lesions

found on [^{89}Zr]Zr-PSMA-617 PET/CT. Every lesion that was positive on [^{68}Ga]Ga-PSMA-11 PET/CT also was clearly seen on the [^{89}Zr]Zr-PSMA-617 scans (representative images in Fig. 5, right column). Figure 6 shows the SUVmax and TLR of the [^{89}Zr]Zr-PSMA-617 PET/CT of these lesions, which were already suspicious on the [^{68}Ga]Ga-PSMA-11 PET/CT. The kinetics of these parameters were similar to those of the [^{68}Ga]Ga-PSMA-11 indeterminate lesions, which were classified as positive by [^{89}Zr]Zr-PSMA-617 PET/CT.

During the [^{89}Zr]Zr-PSMA-617 PET/CT procedure and the 4 wks thereafter, no adverse events, including clinically-relevant vital signs abnormalities, that appeared to be related to the imaging procedure were noted.

Subsequently to [^{89}Zr]Zr-PSMA-617 PET/CT imaging, 12/15 (80%) patients received a [^{89}Zr]Zr-PSMA-617 PET/CT-guided radiotherapy, 1/15 (7%) androgen deprivation therapy (ADT) and 1/15 (7%) PSMA-targeted radioligand therapy. The remaining one decided to wait and postpone treatment. After [^{89}Zr]Zr-PSMA-617 PET/CT-guided radiotherapy PSA serum level decreased by 84±26%; in 6/12 (50%) patients PSA levels were below the detection limit.

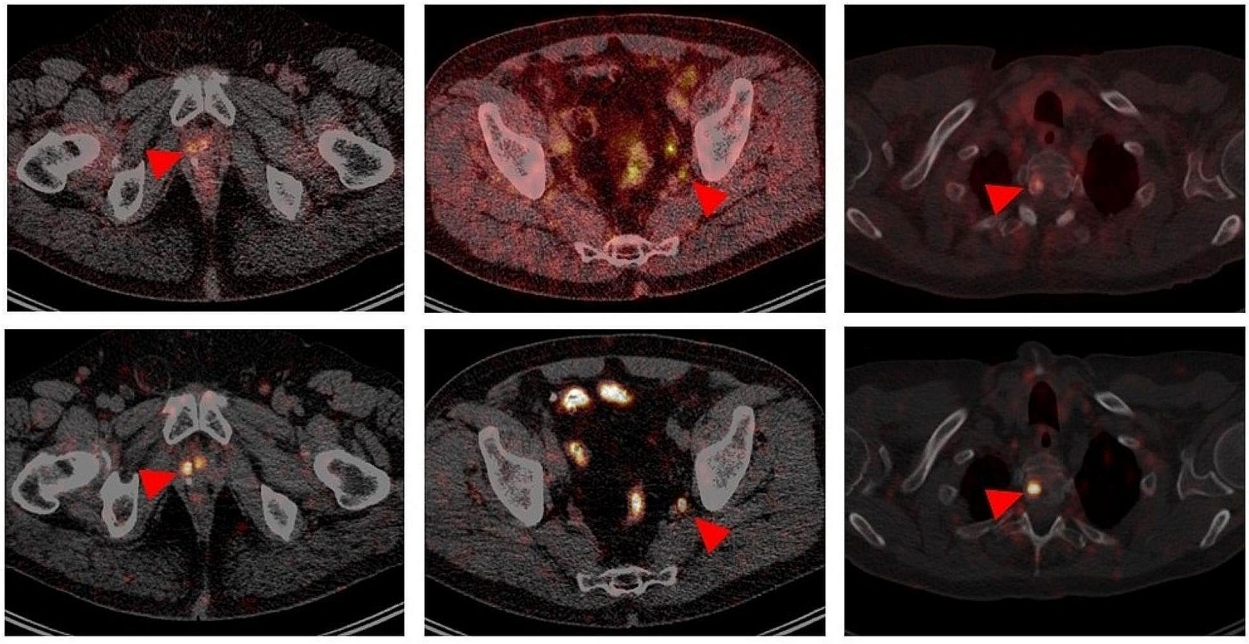

Fig. 2 Representative transversal slice images, from 3 different patients (one per column), showing lesions (indicated by red arrows) that were indeterminate on [^{68}Ga]Ga-PSMA-11 PET/CT (top row) but could be visually classified as suspicious (positive) for, respectively (bottom row, left to right), local recurrence, lymph node metastasis, and bone metastasis of prostate cancer on [^{89}Zr]Zr-PSMA-617 PET/CT (48-hr scans shown here)

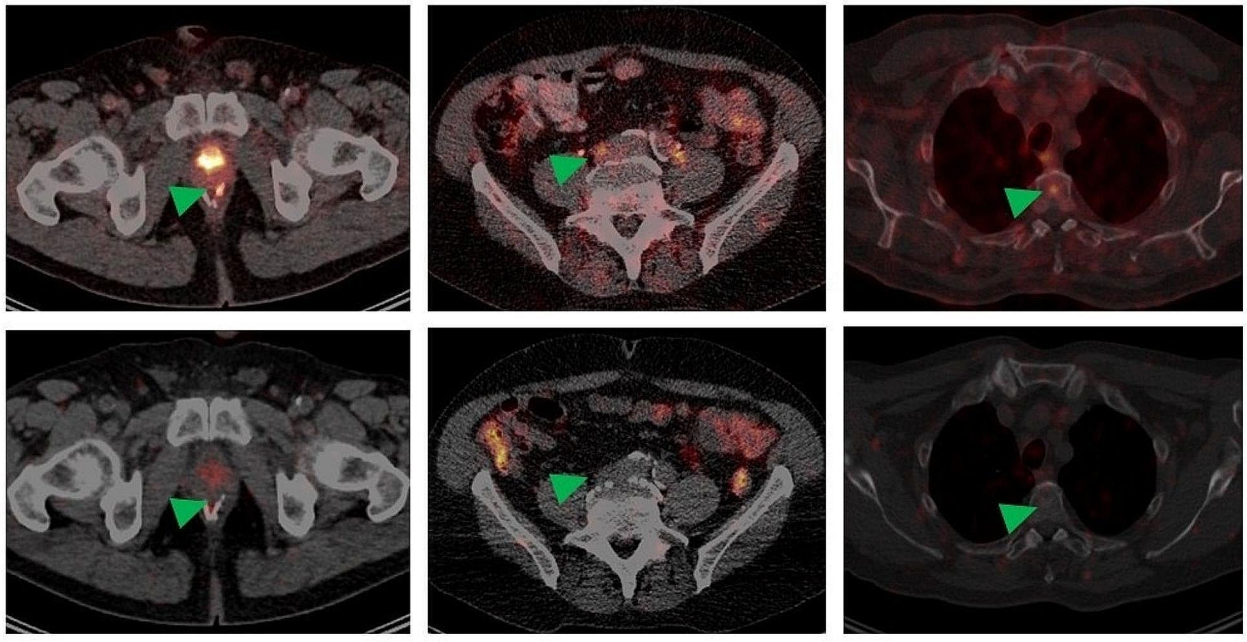

Fig. 3 Representative transversal slice images, from 3 different patients (one per column) showing lesions (indicated by green arrows), that were indeterminate on [^{68}Ga]Ga-PSMA-11 PET/CT (top row) but could be visually classified as non-suspicious (negative) for prostate cancer on [^{89}Zr]Zr-PSMA-617 images (48-hr scan shown here). The lesions indeterminate on [^{68}Ga]Ga-PSMA-11 PET/CT were considered possibly suspicious for local recurrence, lymph node metastasis, and bone marrow metastasis, respectively (left to right), of prostate cancer

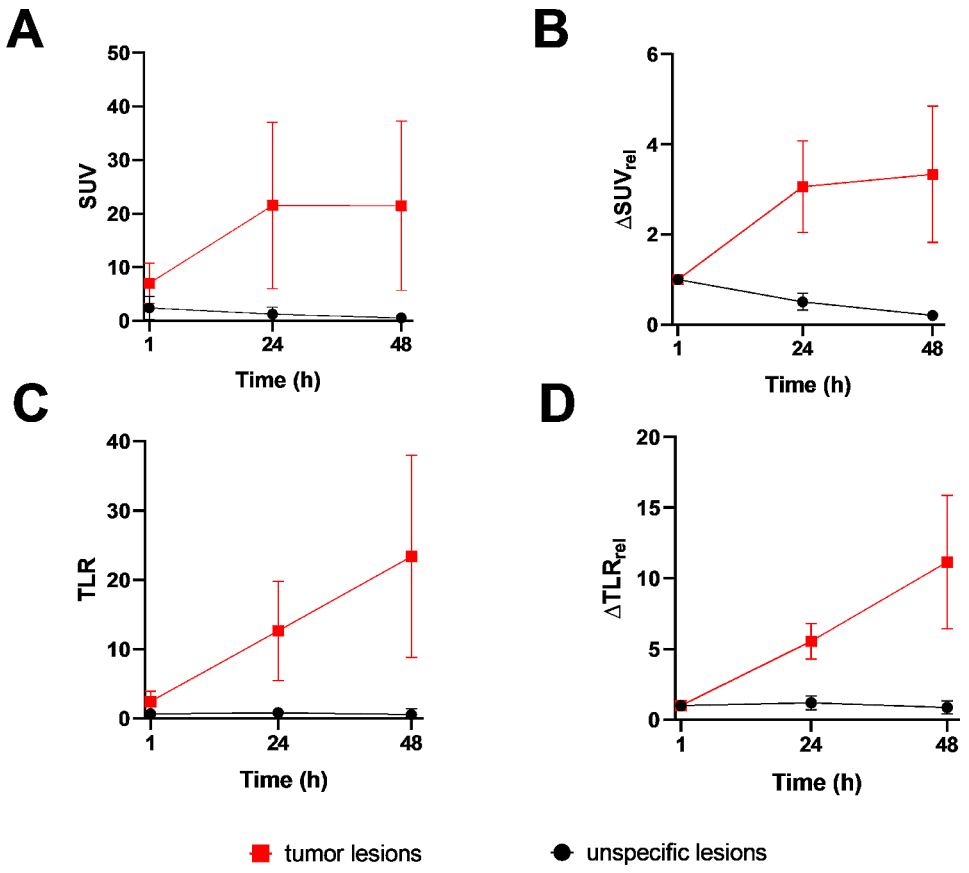

Fig. 4 [^{89}Zr]Zr-PSMA-617 PET variables by scan time and their relative changes over time of [^{68}Ga]Ga-PSMA-11-indeterminate lesions visually classified as positive ($n=6$ lesions) versus negative ($n=14$ lesions) on [^{89}Zr]Zr-PSMA-617 PET/CT. (**A**) SUV_{max}, (**B**) ΔSUV_{rel}, (**C**) TLR, and (**D**) ΔTLR_{rel}. ΔSUV_{rel}, relative change in SUV_{max}; ΔTLR_{rel}, relative change in TLR

Discussion

This is, to our knowledge, the largest analysis ($N=15$) published to date assessing the ability of [^{89}Zr]Zr-PSMA-617 PET/CT to characterize as suspicious or non-suspicious for prostate cancer lesions that were indeterminate on recent prior [^{68}Ga]Ga-PSMA-11 PET/CT. The analysis had three main findings. First, even in the setting of BCR with low PSA levels, and across the three major types of putative prostate cancer recurrence, i.e., prostate bed, lymph node, and bone lesions, previously-indeterminate foci appeared to be readily amenable to such dichotomization on 24-hr and 48-hr [^{89}Zr]Zr-PSMA-617 PET/CT images. This observation suggests that, using this novel method might in many cases solve an important diagnostic dilemma associated with conventional PSMA-targeted imaging. Our observations in additional patients align with our preliminary experience in 3 men with indeterminate conventional PSMA-targeted imaging findings [13].

Second, negative and positive lesions showed distinctly different patterns of [^{89}Zr]Zr-PSMA-617 kinetics. This observation was reflected by lesional radiotracer uptake, represented by SUV_{max}, and by lesional contrast, represented by TLR, as well as by patterns of change in these variables over the 1 to 48 h post-injection. The PET kinetics of the [^{68}Ga]Ga-PSMA-11 indeterminate lesions, which were classified as positive by [^{89}Zr]Zr-PSMA-617 PET/CT were similar to those of the clearly suspicious lesions on [^{68}Ga]Ga-PSMA-11, strengthening the assumption of correct classification by [^{89}Zr]Zr-PSMA-617 PET/CT.

Lastly, [^{89}Zr]Zr-PSMA-617 PET/CT that was performed to characterize previously-indeterminate lesions not infrequently had incidental but clinically-relevant findings of additional lesions that had been entirely missed on [^{68}Ga]Ga-PSMA-11 PET/CT. This observation further supports the efficacy of PSMA-targeted PET/CT with ^{89}Zr tracers in localizing sources of BCR, that has been documented in all preliminary analyses published to date [11–16].

Classification of indeterminate conventional PSMA-targeted imaging findings is highly clinically relevant, as this additional information can significantly influence treatment decisions. These decisions may involve the selection of a therapeutic modality or modalities, as well as the regimen of the treatment(s) chosen. Our results

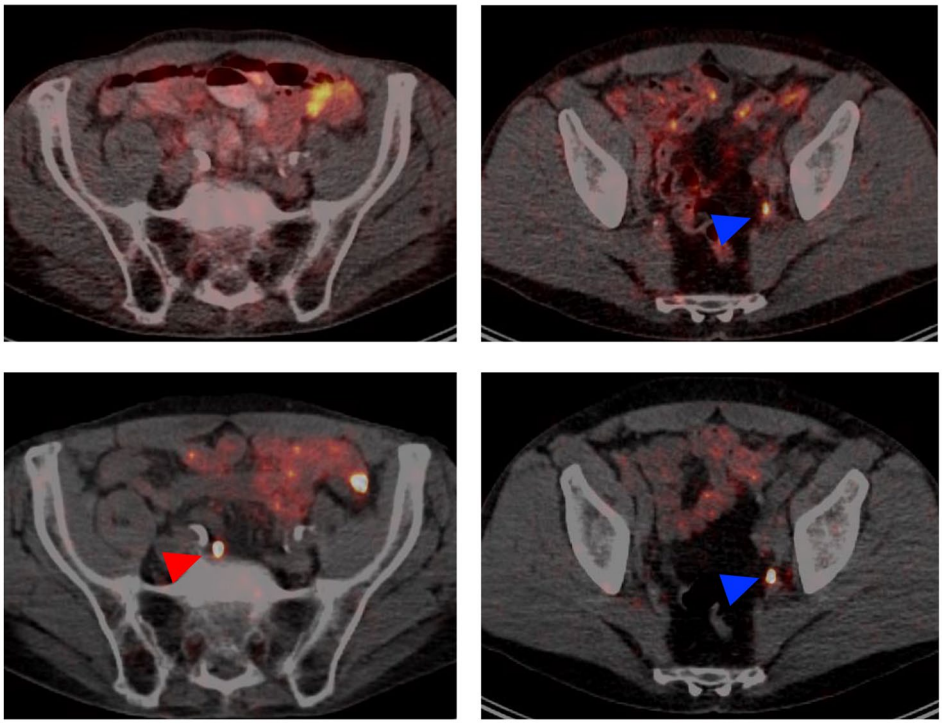

Fig. 5 Representative transversal slice images, from two patients (one per column). The left-hand column shows a lesion (red arrow, bottom image) suspicious for lymph node metastasis of prostate cancer that was detected by [^{89}Zr]Zr-PSMA-617 PET/CT (48-hr scan shown here) but not [^{68}Ga]Ga-PSMA-11 PET/CT (top image). As exemplified in the right-hand column, all lesions detected on [^{68}Ga]Ga-PSMA-11 PET/CT also were detected on [^{89}Zr]Zr-PSMA-617 PET/CT (lesions indicated by blue arrows)

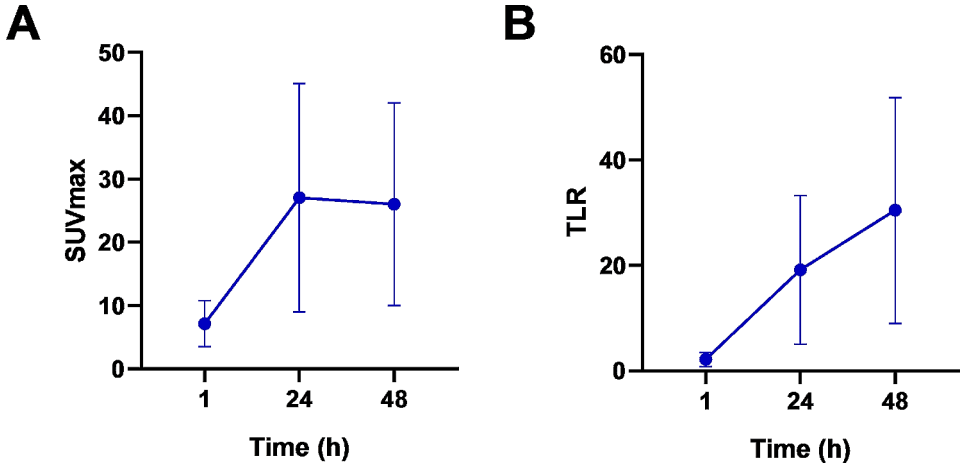

Fig. 6 [^{89}Zr]Zr-PSMA-617 PET variables by scan time of lesions, which were already suspicious on the [^{68}Ga]Ga-PSMA-11 PET/CT: (**A**) SUV_{max} and (**B**) TLR

suggest that depending on the [^{89}Zr]Zr-PSMA-617 PET/CT findings, a precise, individually-adjusted, targeted intervention may be feasible, i.e., metastasis-directed therapy [18–21]. In our cohort, 12/15 patients could receive such a targeted radiotherapy based on [^{89}Zr]Zr-PSMA-617 PET/CT with adequate biochemical response. On the other hand, our confirmation of some indeterminate findings as non-suspicious suggests that [^{89}Zr]Zr-PSMA-617 PET/CT also might help spare certain patients from over-treatment, including, for example, unnecessarily large radiation fields. As seen here and in our earlier reports [11, 12, 14], [^{89}Zr]Zr-PSMA-617 PET/CT appears to be safe. Moreover, the potential benefit of the additional information provided by the procedure would seem to clearly outweigh the main apparent downside of this PET imaging modality, its radiation exposure, which, at ~10 mSv [13], is ~2–3 times higher than that of PET with

[^{68}Ga]Ga-PSMA-11 or other short-lived PSMA-targeted PET tracers [8, 22–24].

Limitations of this work should be noted. First, the analysis was retrospective and observational, and involved a small, single-center series, weakening strength of evidence and decreasing generalizability. Further studies in larger cohorts, ideally with a randomized, prospective design, are recommended.

Second, in the day-to-day practice setting reported here, no lesion had its malignancy evaluated histopathologically and no follow-up imaging was available. Also, because in this context, experimental imaging could not be applied before conventional imaging, [^{68}Ga]Ga-PSMA-11 in all cases preceded [^{89}Zr]Zr-PSMA-617 PET/CT. Additionally, more information (results of follow-up during the interval between scans and [^{68}Ga]Ga-PSMA-11) was available when interpreting the [^{89}Zr]Zr-PSMA-617 images versus the conventional scans. Further, due to the sometimes weeks-long interval between these scans, it cannot be excluded that disease progression may partly accounted for the increased clarity of the previously-indeterminate lesions and/or for the additional lesions seen on the [^{89}Zr]Zr-PSMA-617 images. Moreover, the kinetics of benign lesions on [^{68}Ga]Ga-PSMA-11 should also be analyzed on [^{89}Zr]Zr-PSMA-617 PET/CT in future studies.

Furthermore, it should be noted that we did not evaluate safety of [^{89}Zr]Zr-PSMA-617 PET/CT over the long term. Reassurance is provided, though, by the lack of long-term side effects noted to date [11–14], and by the favorable safety profile of zirconium-labeled radiopharmaceuticals deployed in other settings [25–28].

Despite these limitations of our data, and although this analysis must be considered hypothesis-generating, our results suggest that [^{89}Zr]Zr-PSMA-617 PET/CT may prove to be a beneficial imaging intervention that can be offered to patients with BCR not only as a complementary procedure in cases of negative conventional PSMA-targeted PET/CT, but also to better characterize indeterminate findings of conventional scans.

Conclusions

[^{89}Zr]Zr-PSMA-617 PET/CT appears to allow characterization of lesions that were previously indeterminate on [^{68}Ga]Ga-PSMA-11 PET/CT as suspicious or non-suspicious for prostate cancer. [^{89}Zr]Zr-PSMA-617 radiotracer kinetics differ markedly between previously-indeterminate lesions classified into these categories. Because of this ability to differentiate, the potential to identify lesions that entirely elude detection using conventional PSMA-targeted imaging, and the apparent safety of this novel procedure, [^{89}Zr]Zr-PSMA-617 PET/CT appears to be a promising imaging method.

Abbreviations

ΔSUV_{rel}	Relative change in maximum standardized uptake value
ΔTLR_{rel}	Relative change in tumor-to-liver ratio
^{18}F	Fluorine-18
^{68}Ga	Gallium-68
^{89}Zr	Zirconium-89
ADT	Androgen deprivation therapy or antiandrogen therapy
CT	Computed tomography
max.	Maximum
min.	Minimum
MIP	Maximum intensity projection
p.i.	Post-injection
PET	Positron emission tomography
PSA	Prostate-specific antigen
PSMA	Prostate-specific membrane antigen
SD	Standard deviation
SUV_{max}	Maximum standardized uptake value
SUV_{mean}	Mean standardized uptake value
TLR	Tumor-to-liver ratio of SUV_{max}: SUV_{max} of presumed tumor lesion/SUV_{mean} of healthy liver

Author contributions

FR, CB, EL, and SE designed and conducted the analysis and interpreted the data. FR, CB, EL, FK, AS-S, SM, SP, MB, and SE performed the imaging reported on herein and/or collected and calculated the analyzed data. FR and RJM wrote the first draft of the manuscript, and prepared subsequent drafts. All authors read and edited all drafts of the manuscript and read and approved the final version.

Funding

Nothing to disclose.
Open Access funding enabled and organized by Projekt DEAL.

Data availability

The datasets analyzed during the current study are available from the corresponding author on reasonable request.

Declarations

Ethics approval and consent to participate

All procedures performed in the patients described herein were in accordance with the ethical standards of the Institutional and/or National Research Ethics Committees and with the 1964 Helsinki Declaration and its later amendments, or with comparable ethical standards. This analysis was approved by the Institutional Review Board of the Ärztekammer des Saarlandes/Saarbrücken (approval number: 170/22, approval date: 13 September 2022). This report does not include any animal studies. Written informed consent was obtained from all participants.

Consent for publication

All patients have given written consent to publication.

Competing interests

The authors declare that they have no competing interests.

Author details

[1]Department of Nuclear Medicine, Saarland University– Medical Center, Kirrberger Str. 100, Geb. 50, D-66421 Homburg, Germany
[2]Spencer-Fontayne Corporation, Jersey City, NJ, USA

Received: 4 October 2023 / Accepted: 7 February 2024
Published online: 22 February 2024

References

1. Afshar-Oromieh A, da Cunha ML, Wagner J, Haberkorn U, Debus N, Weber W, et al. Performance of [^{68}Ga]Ga-PSMA-11 PET/CT in patients with recurrent prostate cancer after prostatectomy-a multi-centre evaluation of 2533 patients. Eur J Nucl Med Mol Imaging. 2021;48(9):2925–34.

2. Fendler WP, Eiber M, Beheshti M, Bomanji J, Calais J, Ceci F, et al. PSMA PET/CT: joint EANM procedure guideline/SNMMI procedure standard for prostate cancer imaging 2.0. Eur J Nucl Med Mol Imaging. 2023;50(5):1466–86.
3. Bagguley D, Ong S, Buteau JP, Koschel S, Dhiantravan N, Hofman MS, et al. Role of PSMA PET/CT imaging in the diagnosis, staging and restaging of prostate cancer. Future Oncol. 2021;17(17):2225–41.
4. Perera M, Papa N, Roberts M, Williams M, Udovicich C, Vela I, et al. Gallium-68 prostate-specific membrane antigen positron emission tomography in advanced prostate cancer-updated diagnostic utility, sensitivity, specificity, and distribution of prostate-specific membrane antigen-avid lesions: a systematic review and meta-analysis. Eur Urol. 2020;77(4):403–17.
5. Pienta KJ, Gorin MA, Rowe SP, Carroll PR, Pouliot F, Probst S et al. A phase 2/3 prospective multicenter study of the diagnostic accuracy of prostate specific membrane antigen PET/CT with ^{18}F-DCFPyL in prostate cancer patients (OSPREY). J Urol. 2021:101097JU0000000000001698.
6. Morris MJ, Rowe SP, Gorin MA, Saperstein L, Pouliot F, Josephson D et al. Diagnostic performance of ^{18}F-DCFPyL-PET/CT in men with biochemically recurrent prostate cancer: results from the CONDOR phase III, multicenter study. Clin Cancer Res. 2021.
7. Calais J, Czernin J, Fendler WP, Elashoff D, Nickols NG. Randomized prospective phase III trial of ^{68}Ga-PSMA-11 PET/CT molecular imaging for prostate cancer salvage radiotherapy planning [PSMA-SRT]. BMC Cancer. 2019;19(1):18.
8. Giesel FL, Hadaschik B, Cardinale J, Radtke J, Vinsensia M, Lehnert W, et al. F-18 labelled PSMA-1007: biodistribution, radiation dosimetry and histopathological validation of tumor lesions in prostate cancer patients. Eur J Nucl Med Mol Imaging. 2017;44(4):678–88.
9. Hofman MS, Lawrentschuk N, Francis RJ, Tang C, Vela I, Thomas P, et al. Prostate-specific membrane antigen PET-CT in patients with high-risk prostate cancer before curative-intent surgery or radiotherapy (proPSMA): a prospective, randomised, multicentre study. Lancet. 2020;395(10231):1208–16.
10. Grunig H, Maurer A, Thali Y, Kovacs Z, Strobel K, Burger IA, et al. Focal unspecific bone uptake on [^{18}F]-PSMA-1007 PET: a multicenter retrospective evaluation of the distribution, frequency, and quantitative parameters of a potential pitfall in prostate cancer imaging. Eur J Nucl Med Mol Imaging. 2021;48(13):4483–94.
11. Prive BM, Derks YHW, Rosar F, Franssen GM, Peters SMB, Khreish F, et al. ^{89}Zr-labeled PSMA ligands for pharmacokinetic PET imaging and dosimetry of PSMA-617 and PSMA-I&T: a preclinical evaluation and first in man. Eur J Nucl Med Mol Imaging. 2022;49(6):2064–76.
12. Rosar F, Bartholoma M, Maus S, Prive BM, Khreish F, Franssen GM, et al. ^{89}Zr-PSMA-617 PET/CT may reveal local recurrence of prostate Cancer unidentified by ^{68}Ga-PSMA-11 PET/CT. Clin Nucl Med. 2022;47(5):435–6.
13. Rosar F, Schaefer-Schuler A, Bartholoma M, Maus S, Petto S, Burgard C, et al. [^{89}Zr]Zr-PSMA-617 PET/CT in biochemical recurrence of prostate cancer: first clinical experience from a pilot study including biodistribution and dose estimates. Eur J Nucl Med Mol Imaging. 2022;49(13):4736–47.
14. Rosar F, Khreish F, Marlowe RJ, Schaefer-Schuler A, Burgard C, Maus S et al. Detection efficacy of [^{89}Zr]Zr-PSMA-617 PET/CT in [^{68}Ga]Ga-PSMA-11 PET/CT-negative biochemical recurrence of prostate cancer. Eur J Nucl Med Mol Imaging. 2023.
15. Vazquez SM, Endepols H, Fischer T, Tawadros SG, Hohberg M, Zimmermanns B, et al. Translational development of a Zr-89-labeled inhibitor of prostate-specific membrane antigen for PET imaging in prostate cancer. Mol Imaging Biol. 2022;24(1):115–25.
16. Dietlein F, Kobe C, Vazquez SM, Fischer T, Endepols H, Hohberg M, et al. An ^{89}Zr-labeled PSMA tracer for PET/CT imaging of prostate cancer patients. J Nucl Med. 2022;63(4):573–83.
17. Fendler WP, Eiber M, Beheshti M, Bomanji J, Ceci F, Cho S, et al. ^{68}Ga-PSMA PET/CT: Joint EANM and SNMMI procedure guideline for prostate cancer imaging: version 1.0. Eur J Nucl Med Mol Imaging. 2017;44(6):1014–24.
18. Deek MP, Van der Eecken K, Sutera P, Deek RA, Fonteyne V, Mendes AA, et al. Long-term outcomes and genetic predictors of response to metastasis-directed therapy versus observation in oligometastatic prostate cancer: analysis of STOMP and ORIOLE trials. J Clin Oncol. 2022;40(29):3377–82.
19. von Deimling M, Rajwa P, Tilki D, Heidenreich A, Pallauf M, Bianchi A, et al. The current role of precision surgery in oligometastatic prostate cancer. ESMO Open. 2022;7(6):100597.
20. Berghen C, Joniau S, Ost P, Poels K, Everaerts W, Decaestecker K, et al. Progression-directed therapy for oligoprogression in castration-refractory prostate cancer. Eur Urol Oncol. 2021;4(2):305–9.
21. Jadvar H, Abreu AL, Ballas LK, Quinn DI. Oligometastatic prostate cancer: current status and future challenges. J Nucl Med. 2022;63(11):1628–35.
22. Afshar-Oromieh A, Hetzheim H, Kratochwil C, Benesova M, Eder M, Neels OC, et al. The theranostic PSMA ligand PSMA-617 in the diagnosis of prostate cancer by pet/ct: biodistribution in humans, radiation dosimetry, and first evaluation of tumor lesions. J Nucl Med. 2015;56(11):1697–705.
23. Afshar-Oromieh A, Hetzheim H, Kubler W, Kratochwil C, Giesel FL, Hope TA, et al. Radiation dosimetry of ^{68}Ga-PSMA-11 (HBED-CC) and preliminary evaluation of optimal imaging timing. Eur J Nucl Med Mol Imaging. 2016;43(9):1611–20.
24. Sharma P, Watts A, Singh H. Comparison of internal dosimetry of ^{18}F-PSMA-1007 and ^{68}Ga-PSMA-11-HBED-CC. Clin Nucl Med. 2022;47(11):948–53.
25. Yoon JK, Park BN, Ryu EK, An YS, Lee SJ. Current perspectives on ^{89}Zr-PET imaging. Int J Mol Sci. 2020;21(12).
26. Pandit-Taskar N, O'Donoghue JA, Beylergil V, Lyashchenko S, Ruan S, Solomon SB, et al. Zr-huJ591 immuno-PET imaging in patients with advanced metastatic prostate cancer. Eur J Nucl Med Mol Imaging. 2014;89(11):2093–105.
27. Pandit-Taskar N, O'Donoghue JA, Durack JC, Lyashchenko SK, Cheal SM, Beylergil V, et al. A phase I/II study for analytic validation of ^{89}Zr-J591 ImmunoPET as a molecular imaging agent for metastatic prostate cancer. Clin Cancer Res. 2015;21(23):5277–85.
28. Pandit-Taskar N, Postow MA, Hellmann MD, Harding JJ, Barker CA, O'Donoghue JA, et al. First-in-humans imaging with ^{89}Zr-Df-IAB22M2C anti-CD8 minibody in patients with solid malignancies: preliminary pharmacokinetics, biodistribution, and lesion targeting. J Nucl Med. 2020;61(4):512–9.

Publisher's Note